

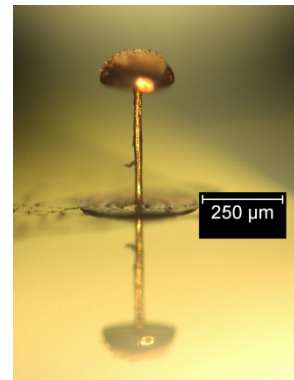
MEMS made in a Small Scale Research Lab – Opportunities for Functional Targets



F. Greiner, F. Dassinger, S. Quednau, H. F. Schlaak

Institute of Electromechanical Design
Institut für Elektromechanische Konstruktionen **EMK**

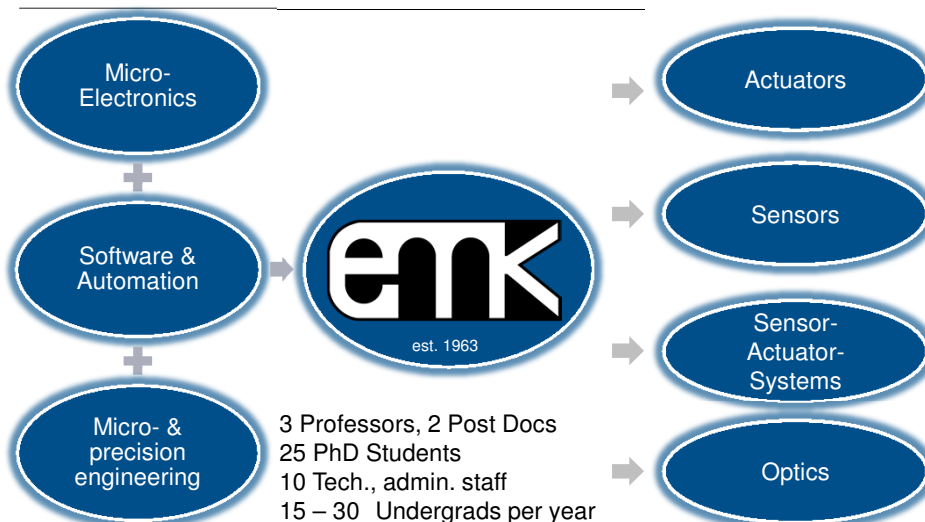
Merckstraße 25, D-64283 Darmstadt, Germany
www.institut-emk.de



21. Aug. 2012 | Institute of Electromechanical Design | Profes. Khanh, Schlaak, Werthschützky | 115



Institute for Electromechanical Design – EMK Institut für Elektromechanische Konstruktionen



21. Aug. 2012 | Institute of Electromechanical Design | Profes. Khanh, Schlaak, Werthschützky | 7



Cleanroom Laboratory for Microtechnology

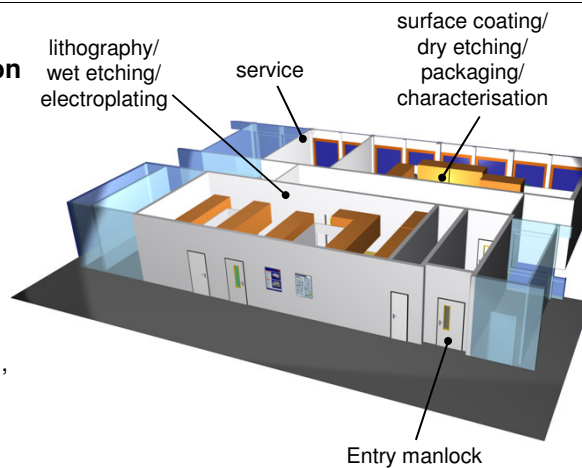


Clean room classification

1.000 - 100 within the laminar airflow boxes

Functionality

- about 60 m² for photolithography, wet etching, electroplating
- about 60 m² for packaging, surface coating, measurement



<http://www.emk.tu-darmstadt.de/en/institute/equipment/>

21. Aug. 2012 | Institute of Electromechanical Design | Profes. Khanh, Schlaak, Werthschützky | 13



Technology Overview Substrate Pretreatment



Sputtering



Alcatel

- DC/ HF Sputtering with RF-Bias
- 4 Cathodes
- Al, Cr, Cu, SiO₂
- Deposition Rates up to 1000 nm/min
- Vacuum Prechamber

Vapour Deposition



Balzers BAK 600

- Electron Beam and Resistance Evaporator
- Al, Cu, Cr, Ni, Ag, Ti, Au, Al₂O₃
- Thickness Control through Quartz Resonator

Polishing Machine



Logitech PM5

- Precision Polishing Jig with vacuum adapter
- Up to 4" wafer
- Plate Speed: 0-70 rpm
- Chemical Mechanical Polishing option

21. Aug. 2012 | Institute of Electromechanical Design | Profes. Khanh, Schlaak, Werthschützky | 83



Technology Overview UV-Lithography I



Spin Coater



SÜSS Delta 80 BM

- Rotating Lid
- Up to 4000 rpm

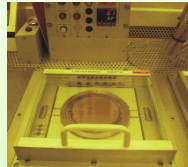
SÜSS LabSpin 6

- Up to 8000 rpm

Photo Resists

- SU-8 2000/3000
- AZ 9260
- AZ 15, 125 (n)XT

Hotplates



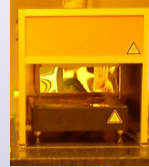
2x Hotplate 400

- Programmable Single Plate
- Up to 130 °C

3x GESTIGKEIT PR 5-3T

- Programmable Double Plate
- Up to 300 °C

IR Oven



FH Zwickau

- IR dry system for photoresist
- Up to 6" wafer
- Max. heat 130 °C
- Maximum substrate weight 150 g

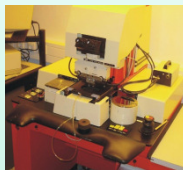
21. Aug. 2012 | Institute of Electromechanical Design | Profes. Khanh, Schlaak, Werthschützky | 84



Technology Overview UV-Lithography II



Mask Aligner



SÜSS MA 56 M

- 350 W UV-Lamp
- Up to 4" Masks
- Manual Alignment
- Up to 20 mW/cm²
- Process Monitoring

Filters

- g, h, i - Line
- g, h - Line
- i - Line

Developer



Sonosys 500

- Frequency 1 MHz
- Power 50 - 500 W

Multi-Bio-3D

- Orbital Shaker

Developer

- mr-Dev 600
- MIF 326, 826
- AZ 400k

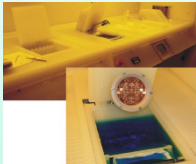
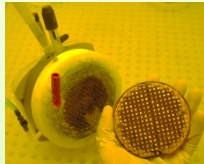
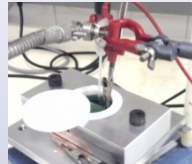
21. Aug. 2012 | Institute of Electromechanical Design | Profes. Khanh, Schlaak, Werthschützky | 85



Technology Overview

Micro- and Nano Electroplating



Micro Electroplating	Micro & Nano Electroplating	Nano Electroplating
 <p>M-O-T μGalv</p> <ul style="list-style-type: none"> Additive free Electrolytes Nickel (pH 4), Copper (acid) Currents up to 10 A Puls-Plating Option Plating rate up to 4 $\mu\text{m}/\text{min}$ 	 <p>silicet trio clip</p> <ul style="list-style-type: none"> 3 electrodes cell for 4" wafer Ion membrane for use with additives 1 μA - 3 A reverse pulse plating to extend to 100 kHz 2 l volume with particle filter 	 <p>Nano Electroplating Cell</p> <ul style="list-style-type: none"> Potentiostatic and Galvanostatic Plating Pulse- & Reverse-Puls-Plating up to 100 kHz Currents down to several nA





21. Aug. 2012 | Institute of Electromechanical Design | Profes. Khanh, Schlaak, Werthschützky | 86



Technology Overview

Plasma Activation & Etching



Isotrop Etching	Anisotrop Etching	Surface Activation	Wet Etching Machine
 <p>Muegge STP 2020</p> <ul style="list-style-type: none"> Remote Downstream Plasma Reactor for Polymer Etching (e.g. SU-8, BCB) O_2, CF_4, N_2 RF-Power: 3000 W at 13,56 MHz 	 <p>Plasma Technology RIE80</p> <ul style="list-style-type: none"> Parallel Plate Reactor for Substrate Cleaning and Polymer Etching O_2, CF_4, N_2 RF-Power: 300 W at 13,56 MHz 	 <p>Technics 300-E Plasma</p> <ul style="list-style-type: none"> Barrel Reactor for Substrate Cleaning and Surface Activation O_2, CF_4, N_2 RF-Power: 300 W at 13,56 MHz 	 <p>BUNGARD, Splash Center</p> <ul style="list-style-type: none"> Etching medium: Fe-III-Cl Line definition: 100 μm Max. board size: 210 x 300 mm

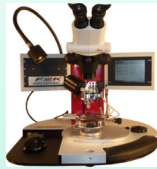
21. Aug. 2012 | Institute of Electromechanical Design | Profes. Khanh, Schlaak, Werthschützky | 87



Technology Overview Packaging Technologies



Wire Bonder



F&K Delvotek 53xx-BDA Bonder

- Ball Bonding down to 18 μm gold wire
- Deep access wedge bonding
- Automated y-axis for automated loops

Micro Assembly



Arteos TOMM 1

- Pic and placer
- Plate- and air-heater
- UV-curing
- Micro-dispenser
- Vacuum chuck

Pick and Place



Cooper Hand Tools WQB 4000SOPS

- Operating range 630 x 630 mm^2
- Soldering temperature 50 - 400 $^{\circ}\text{C}$
- Down to smallest package sizes

Vacuum Furnace



Heraeus, Nabertherm & Co

- Vacuum option
- Protective gas option e.g. N
- Temperature profile option
- High temperatures up to 1100 $^{\circ}\text{C}$

21. Aug. 2012 | Institute of Electromechanical Design | Profes. Khanh, Schlaak, Werthschützky | 89



Technology Overview Optical Inspection & Characterization



Thermography



FLIR SC655

- 640 x 480 Pixel
- -20 $^{\circ}\text{C}$ to +150 $^{\circ}\text{C}$
- 0 $^{\circ}\text{C}$ to 650 $^{\circ}\text{C}$
- Sensitivity: <0.05 $^{\circ}\text{C}$ @ +30 $^{\circ}\text{C}$

Optical Inspection



Keyence VHX-600

- 3CCD Camera
- 54 Mio Pixel
- Magnification up to 1000x
- 3D Measurement Option
- Measurements of Structural Widths

Laser Vibrometer



Polytec OFV 2502

- 2 sensor heads (OFV 534)
- Velocity demodulation
- 1.5 MHz
- Polytec OFV 3001
- Velocity demodulation
- 0.3 $\mu\text{m/s}$...10 m/s

High Speed Camera



Mikro GmbH

- 1280x1024 pixel
- 502 fps
- 55 min recordtime

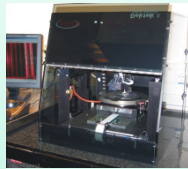
21. Aug. 2012 | Institute of Electromechanical Design | Profes. Khanh, Schlaak, Werthschützky | 92



Technology Overview Electro Mechanical Characterization I



Surface Profiler



DEKTAK 8 Profiler

- Measurement of Layer Thickness and Surface Profile
- Range from 10 nm up to 1 mm
- Stylus Force up to 0,09 mg

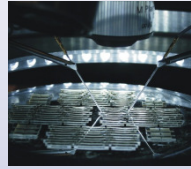
Bond Shear Tester



dage Microtester 22

- Testing strength of solder joints, wire bonds and more
- Stitch Test Failure Detection
- 20 gm & 10 kg Load
- Resolution +/- 0,5% of load

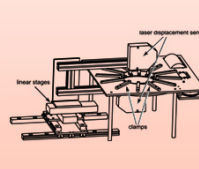
Motion-Analyzer



MEMS-Analyzer

- 2048 x 2048 Pixel
- 15 fps, 800 MBit/s
- Repeatability < 30 nm
- Force Measurements up to 1 N
- Field of View up to 11,7 x 11,7 mm²

EAP Characterization



EAP-Analyzer

- Static / dynamic deflection (line scan)
- Frequency response
- Preload simulation
- Sheet resistance
- Force-displacement

21. Aug. 2012 | Institute of Electromechanical Design | Profes. Khanh, Schlaak, Werthschützky | 90



Technology Overview Electro Mechanical Characterization II



High-Pressure Static Tester



COP-7000

- 500 MPa=5000 bar
- silicon oil
- Room temperature
- Pressure sensor**
 - P3MBP 5000 bar (HBM)
- Piston gauge**
 - 5ppm @ 5 000 bar
 - 1 kg / 50 bar

High-Pressure Dynamic Tester



MAXIMATOR

- up to 1000 bar
- Periodic load at 0.1 Hz to 20 Hz
- Curve shape rectangular, trapezoid or sinus
- 4 pressure connectors

21. Aug. 2012 | Institute of Electromechanical Design | Profes. Khanh, Schlaak, Werthschützky | 91



Technology Overview

Electrical Measurement Equipment



Signal Conditioning



Stanford Research SR 560

- low-noise preamplifier
- battery operating option

Krohn-Hite 3382

- programmable dual-channel filter
- 0.1 Hz – 200 kHz
- Butterworth or Bessel response

Impedance Analysis



Agilent 35670A

- dynamic signal analyzer
- 122 μ Hz - 102.4 kHz, 16-bit
- swept sine option
- GPIB

HP 4284 A

- Precision LCR-Meter
- 20Hz – 1 MHz
- GPIB

DAQ-Systems



Data Acquisition

- DMM, LCR-Meter
- Multi-Purpose DAQ (16 bit, 1,25 MSa)
- 8ch Bridge Input Module (24 bit, 25 kSa)

Universal Control

- PXI, cRIO
- AI, AO, DIO, SPI, Bridge

Peripherals



LeCroy

WaveRunner 44Xi-A

- 400 MHz, 5 GSa

Agilent DSOX3024A

- 200 MHz, 4GSa

Hameg HMP4040

- programmable power supply

Hameg HMF2525

- 25 MHz Arbitrary Signal generator

21. Aug. 2012 | Institute of Electromechanical Design | Prof. Khanh, Schlaak, Werthschützky | 93



High AR Metal Pillars

UV Direct LIGA Processing

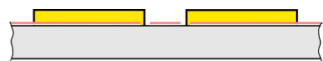
■ Si + SiO₂ ■ Cr ■ Al
 ■ Cu ■ SU-8 ■ AZ 125nXT



- Structured electrode layer: Cr + Cu 100 nm



- Sacrificial layer: SU-8 5 μ m

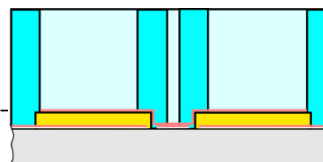


- Structured seed layer:
Cu 200 nm + Al 20 nm



- Exposed photoresist, undeveloped:
AZ125nXT 400 μ m

$$l_W = 400 \mu\text{m}, d_W = 30 \mu\text{m}$$



21. Aug. 2012 | Institute of Electromechanical Design | Prof. Khanh, Schlaak, Werthschützky | 116

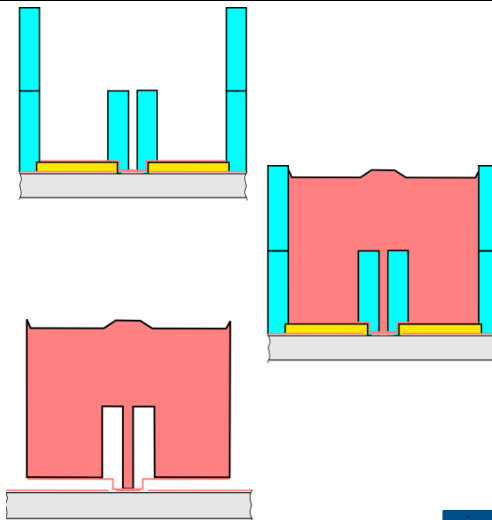


High AR Metal Pillars UV Direct LIGA Processing

■ Si + SiO₂ ■ Cr ■ Al
 ■ Cu ■ SU-8 ■ AZ 125nXT



- Structured mold for electroforming:
AZ125nXT 2 x 400 μ m
- Filled mold: 700 μ m Cu
 - Current: DC, pulse, pulse reverse
 - Contacting: pillars and blocks grown simultaneously
- Stripping
 - Dry etching with reactive oxygen radicals (muegge/R3T)



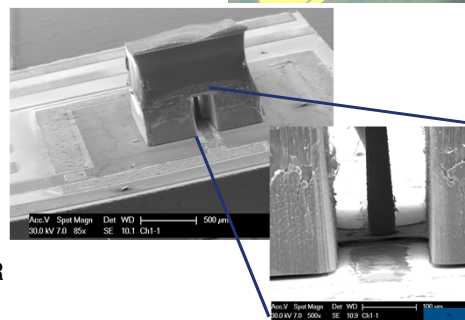
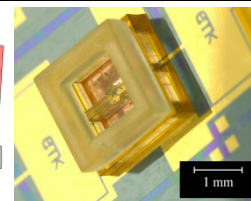
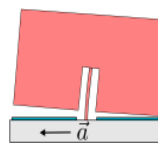
21. Aug. 2012 | Institute of Electromechanical Design | Profes. Khanh, Schlaak, Werthschützky | 117



High Aspect Ratio (AR) Metal Pillars for Minimal Footprint MEMS Suspension



- Inertial sensor
 - 1 device: 2 axes acceleration sensor and 1 axis gear rate sensor
 - Acceleration: seesaw
 - Gear rate: crosstalk due to Coriolis force
- Scale-bridging: wire diameter (d)
 - UV lithography: $d = 40 \mu\text{m}$, AR 10:1
 - XR lithography: $d = 4 \mu\text{m}$, AR 25:1
 - IT lithography: $d = 400 \text{ nm}$, AR 75:1
- Focus on technology
 - Galvanoform with high Aspect Ratio and multiple layers
 - Electroplating with heterogenous AR



21. Aug. 2012 | Institute of Electromechanical Design | Profes. Khanh, Schlaak, Werthschützky | 36

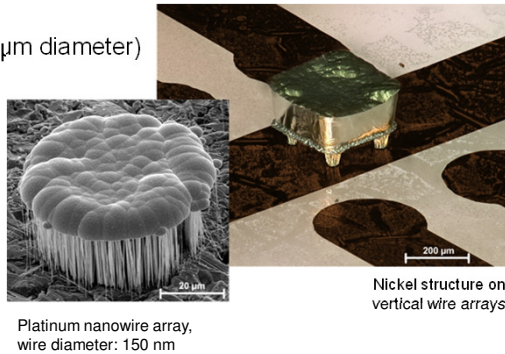


ELEMENT - Electromechanical Sensors Based on One-Dimensional Nanostructures



Development of an inertial sensor

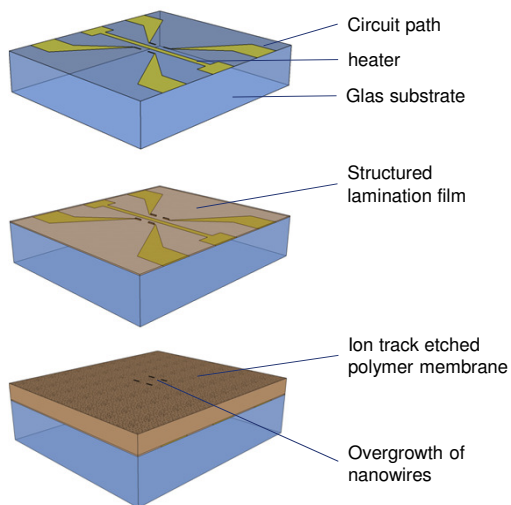
- Use of high elastic nanowires with very high aspect ratio (500:1)
- Assembling nanowire-arrays (50 μm diameter) as spring elements
- Nanoscale enables the use of noble metals with excellent physical properties
- Detection of the inertial mass displacement using a magnetoresistive sensor principle



21. Aug. 2012 | Institute of Electromechanical Design | Profes. Khanh, Schlaak, Werthschützky | 37



Process for batch nanowire integration in micro systems



- Structuring of heater and circuit paths for the nanowire arrays

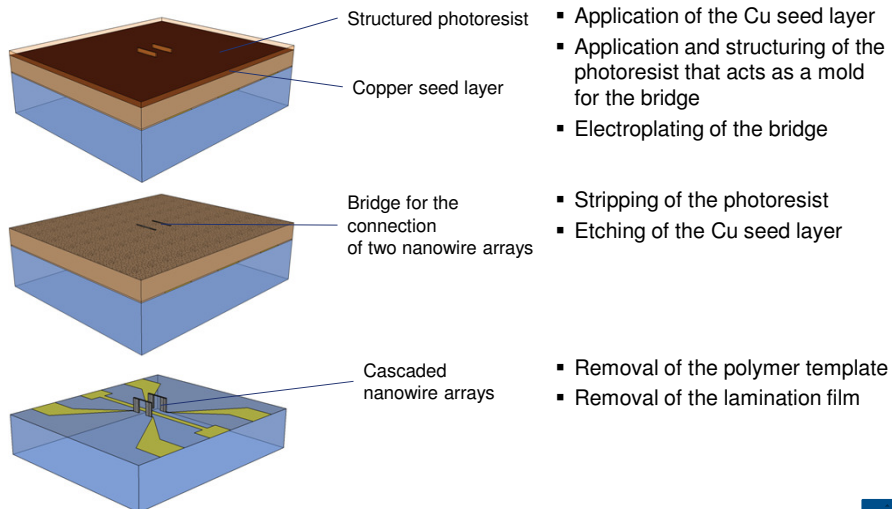
- Application of a lamination film
- Structuring of holes for uncovering the seed layer

- Lamination of the ion track etched polymer template
- Electrodeposition into the pores until overgrowth

21. Aug. 2012 | Institute of Electromechanical Design | Profes. Khanh, Schlaak, Werthschützky | 118



Process for batch nanowire integration in micro systems



- Application of the Cu seed layer
- Application and structuring of the photoresist that acts as a mold for the bridge
- Electroplating of the bridge
- Stripping of the photoresist
- Etching of the Cu seed layer
- Removal of the polymer template
- Removal of the lamination film

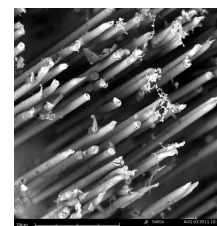
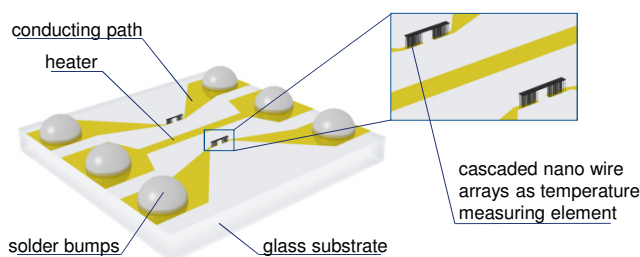
21. Aug. 2012 | Institute of Electromechanical Design | Profes. Khanh, Schlaak, Werthschützky | 119



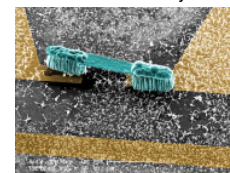
3-DOING – 3-Dimensionale Mikro-Nano-Integration für die Gasflusssensorik



- Funded Project by BMBF, VDI/VDE-IT
- Duration: 01/2011 – 12/2013
- Development of a gas flow sensor which uses metallic nano wires as sensitive elements
- Improvement of the measurement performance, especially for photoacoustic devices



Integration of metallic nano wires in micro systems

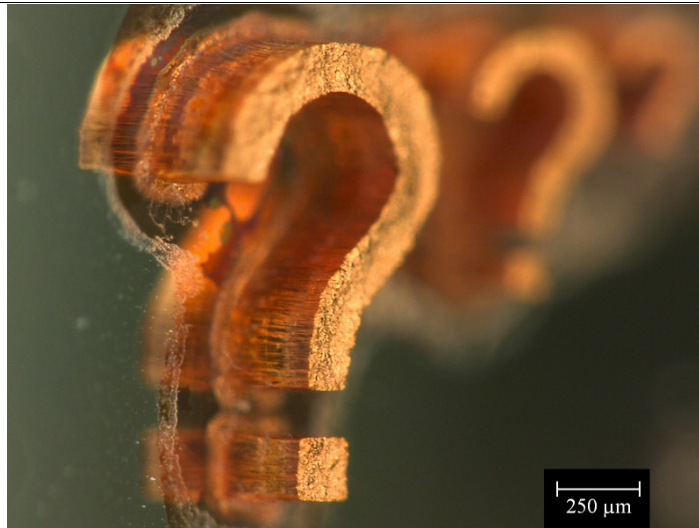


cascaded nano wire arrays

21. Aug. 2012 | Institute of Electromechanical Design | Profes. Khanh, Schlaak, Werthschützky | 40



Questions?



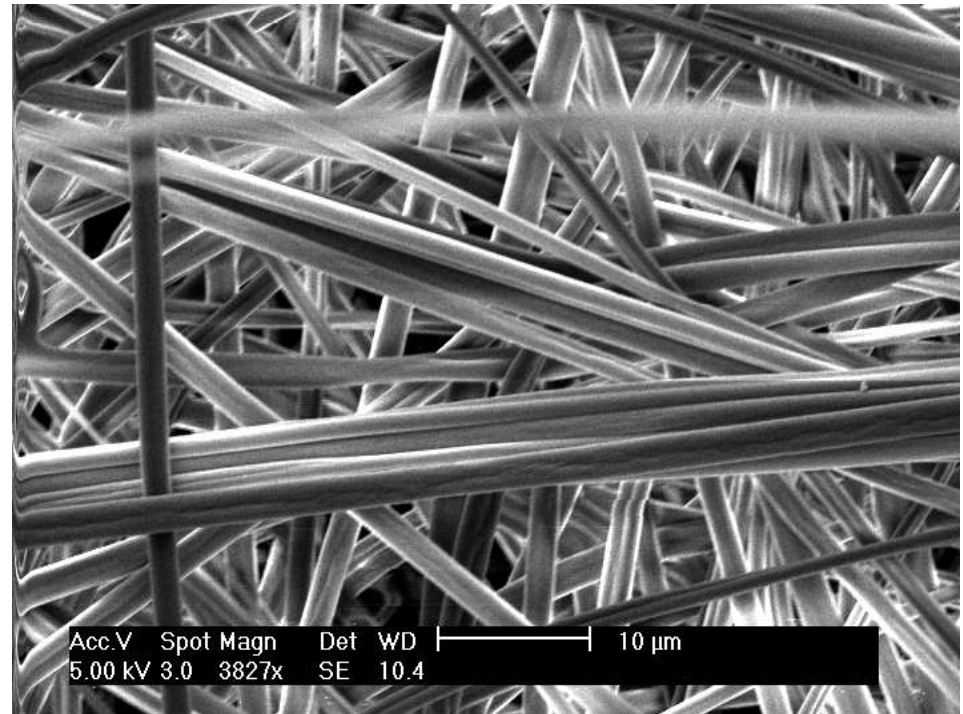
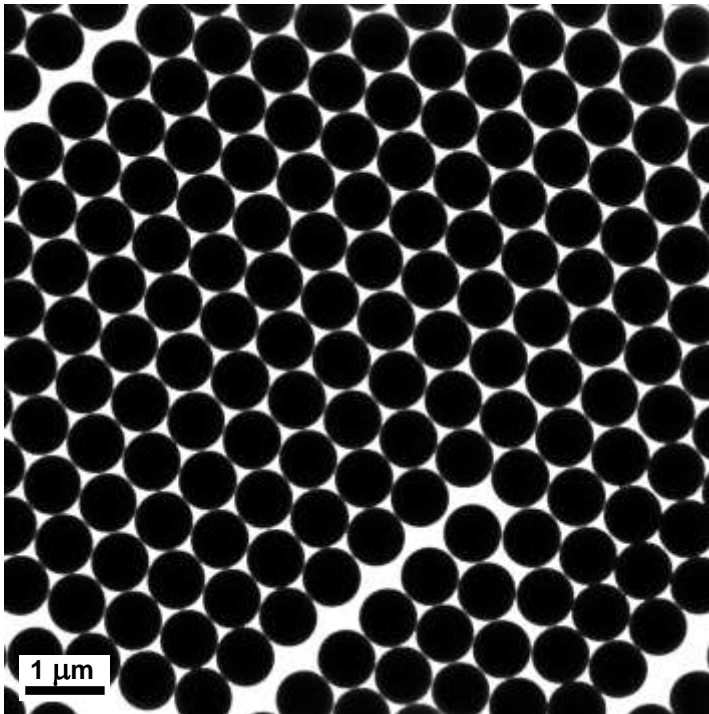
21. Aug. 2012 | Institute of Electromechanical Design | Profes. Khanh, Schlaak, Werthschützky | 120



FROM MONODISPERSE BEADS & FIBRES TO MICRO & NANO STRUCTURES

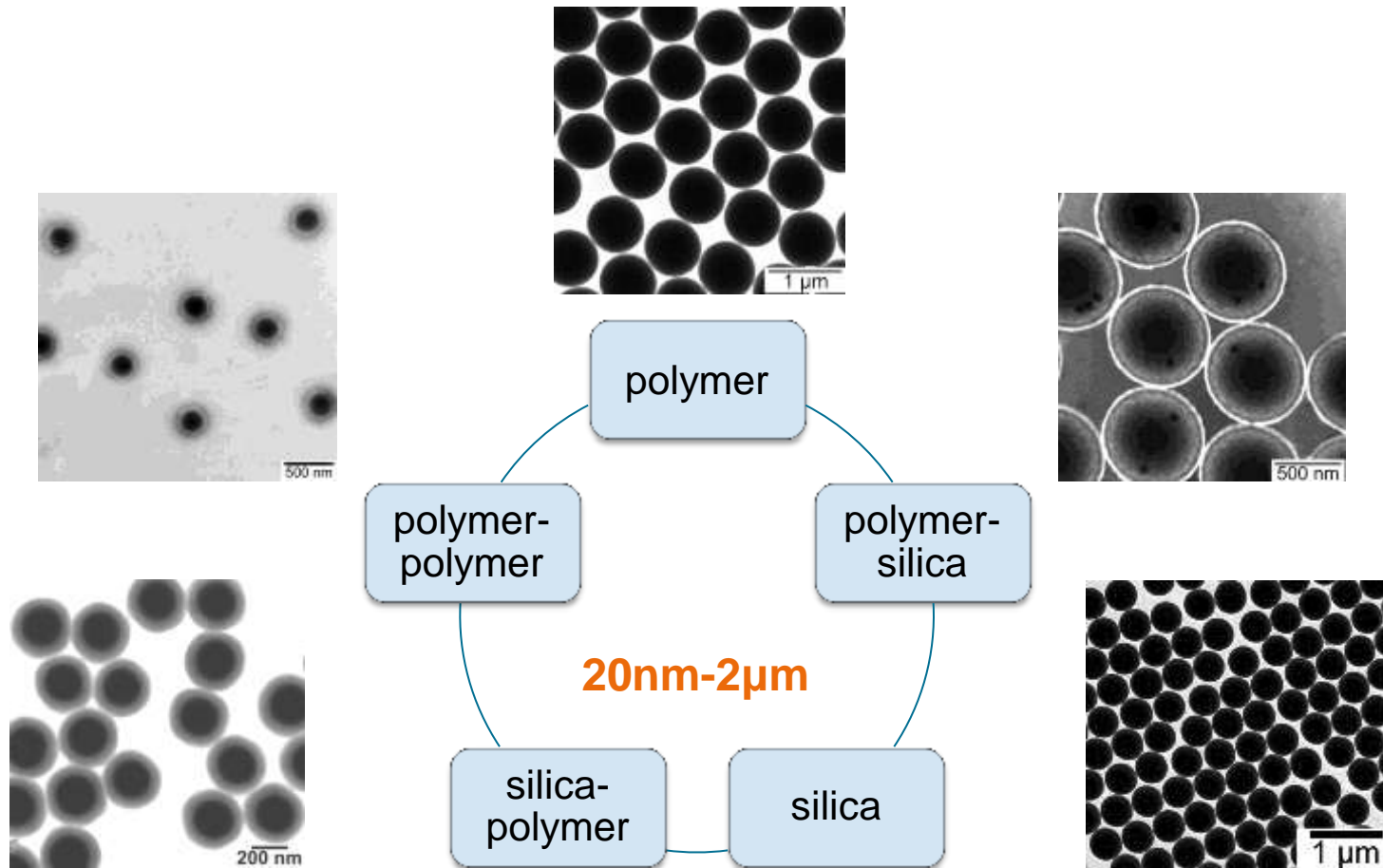
C.G. Schäfer and G.P. Hellmann

4th Target Fabrication Workshop 2012



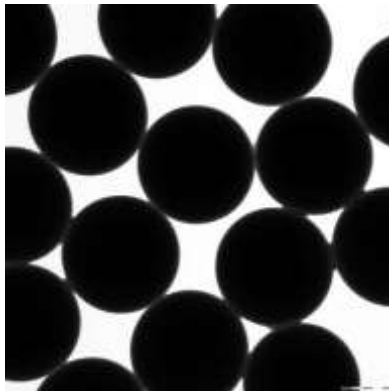
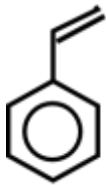
Seite 1

MONODISPERSE BEADS



Polymer Beads Synthesis

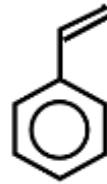
emulsion polymerisation



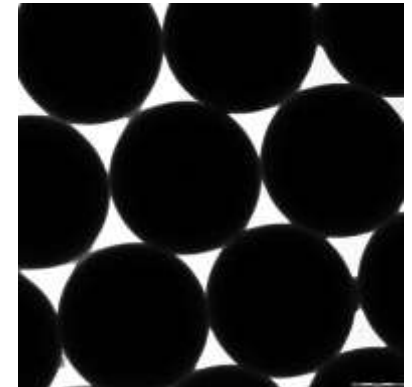
beads
50-500nm

beads from acrylates+styrenes
by various techniques:
emulsion, emulsifierfree,
mini-/microemulsion and swelling
polymerisation

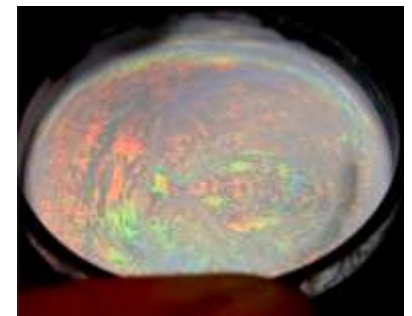
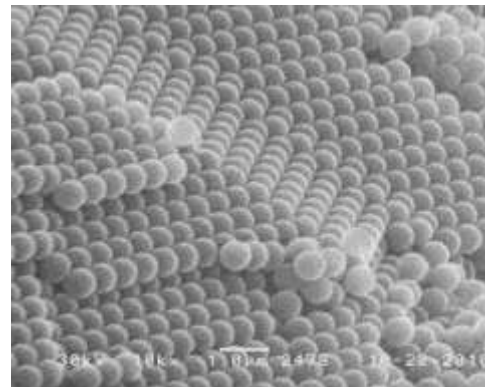
growing/swelling



+ functional
comonomer

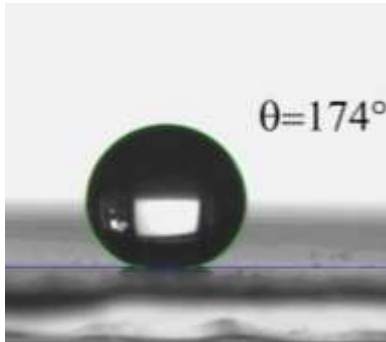


beads
100-2000nm

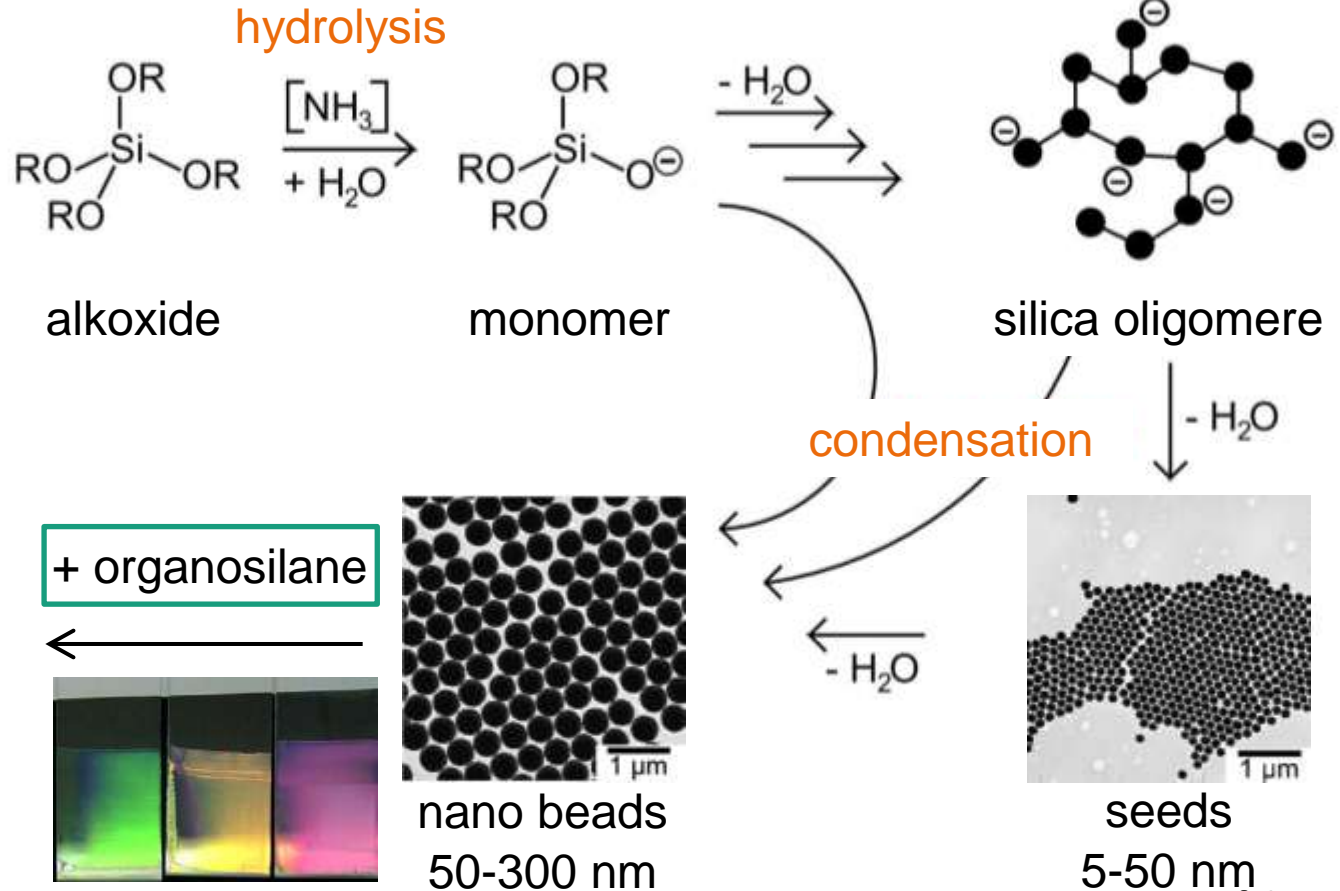


Silica Beads

Stöber Process



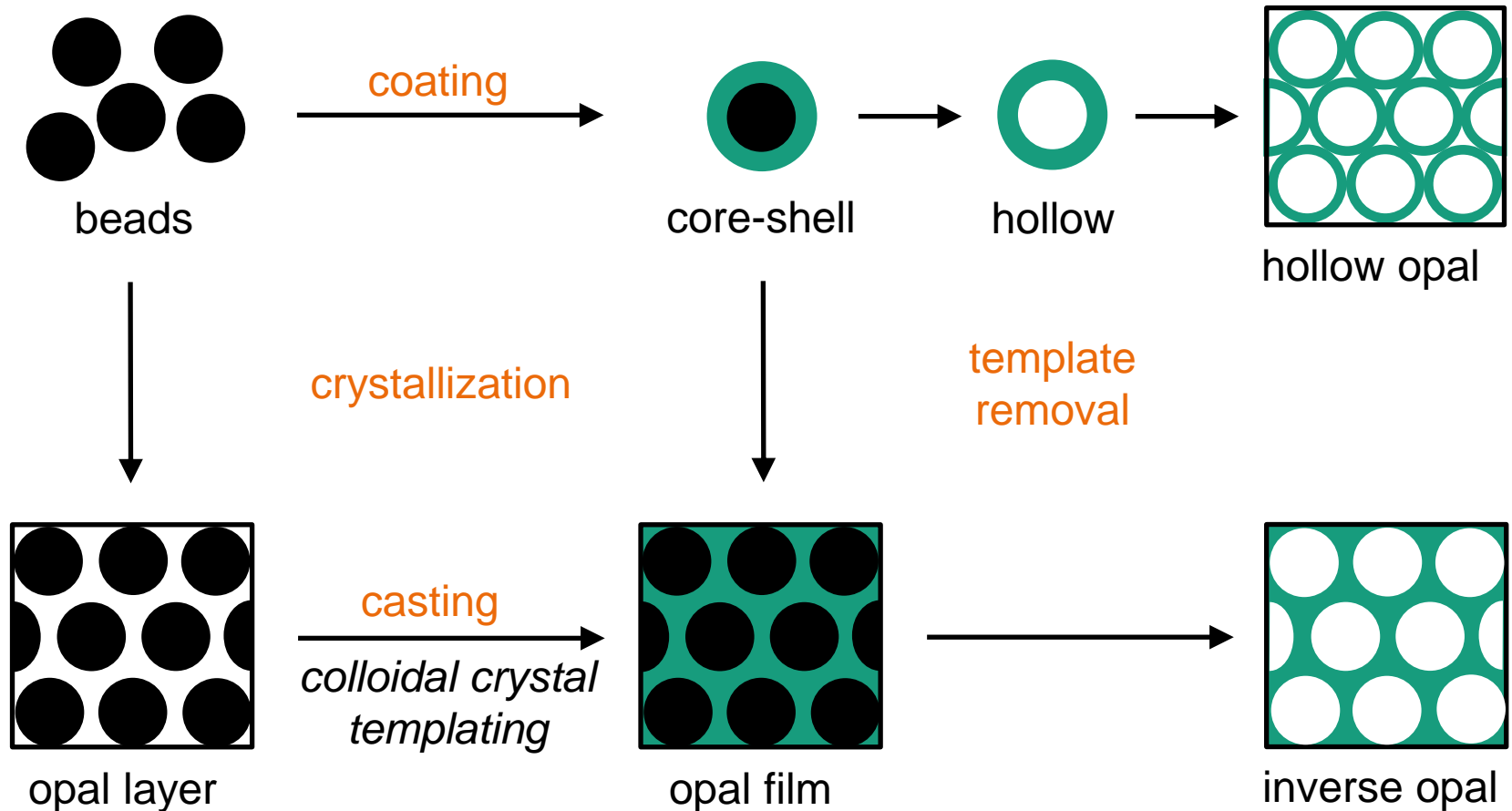
epoxy+amine



Seite 4

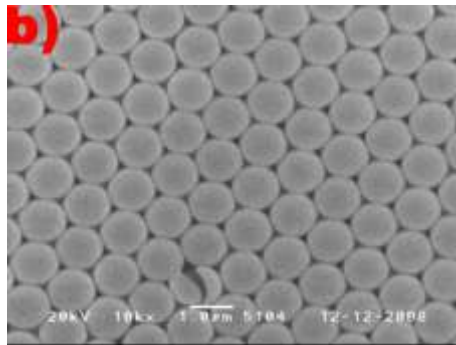
Strategies to Structured Materials

Coating, Casting, Colloidal Crystal Templating

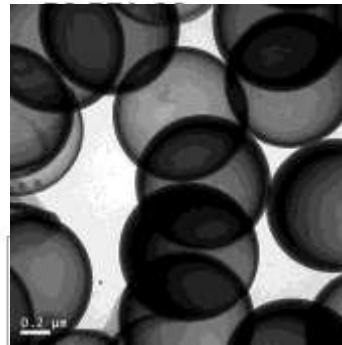
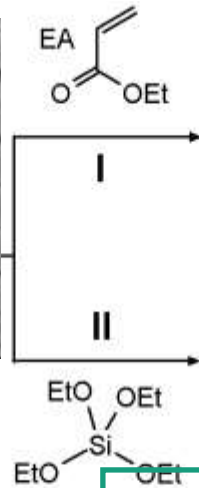


Coating

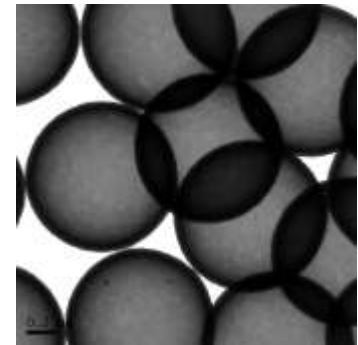
Hybrid Particles and Hollow Spheres



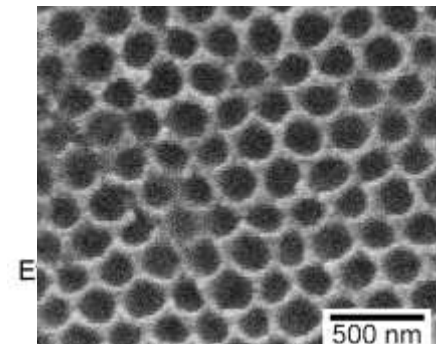
hollow opal



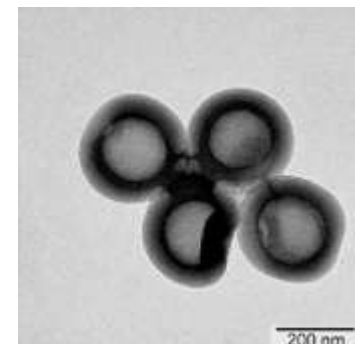
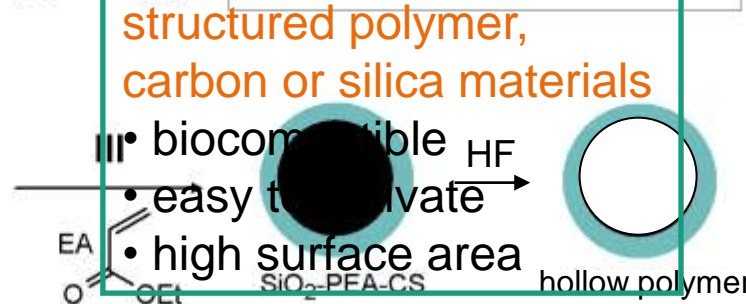
hollow carbon



hollow silica



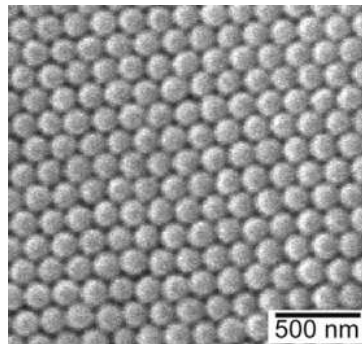
polymer inverse opal



hollow polymer

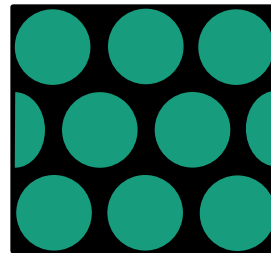
Casting and Colloidal Crystal Templating

Inverse Opals and Double Opals



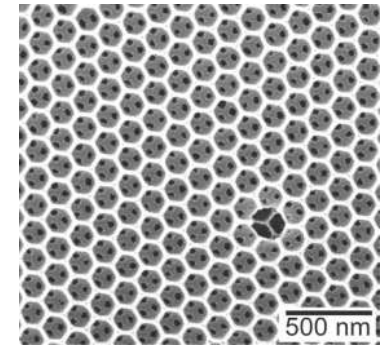
polymer opal

infiltration
sol-gel
solution

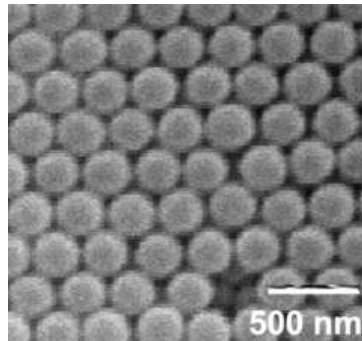


opal film

calcination

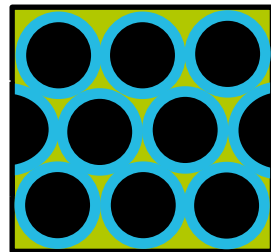


inverse opal



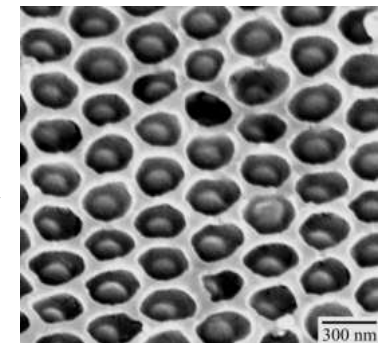
silica-polymer

infiltration
sol-gel
solution



opal film

calcination



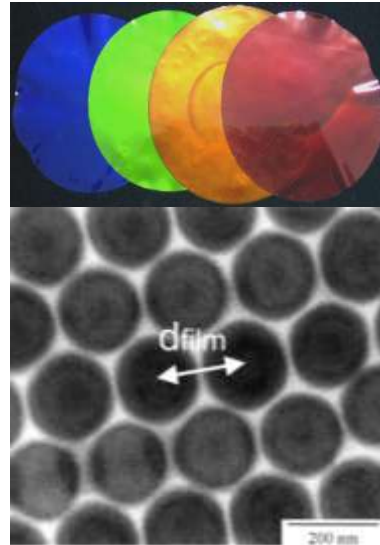
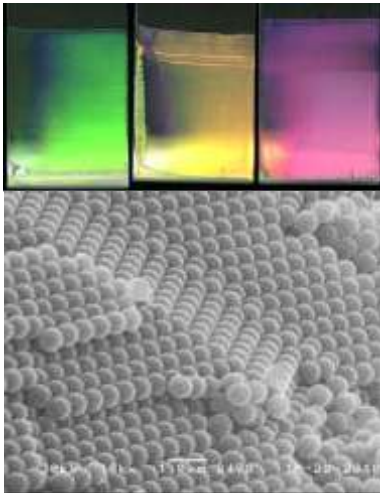
double opal

Structured Materials

Colloidal Crystals

opal layers:

- silica
- polymer
- polymer-silica
- silica-polymer
- hollow silica

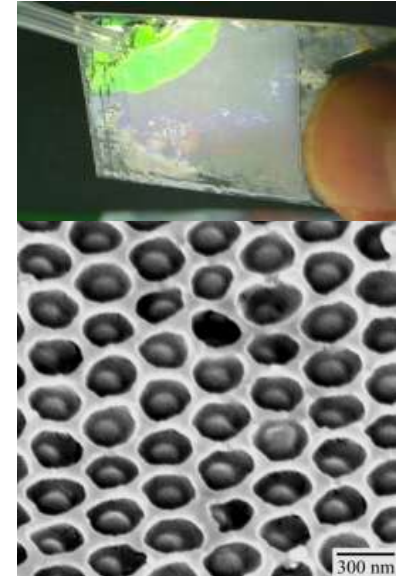
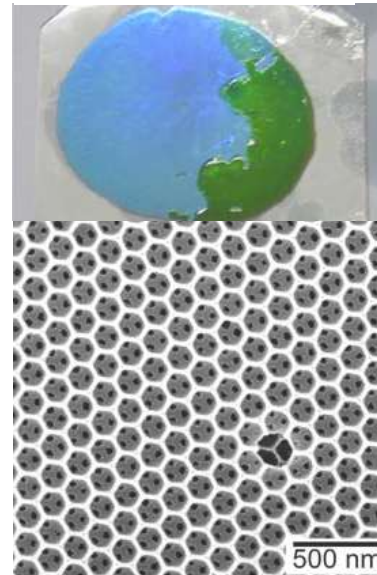


opal films:

- silica-polymer
- polymer CS

inverse opals:

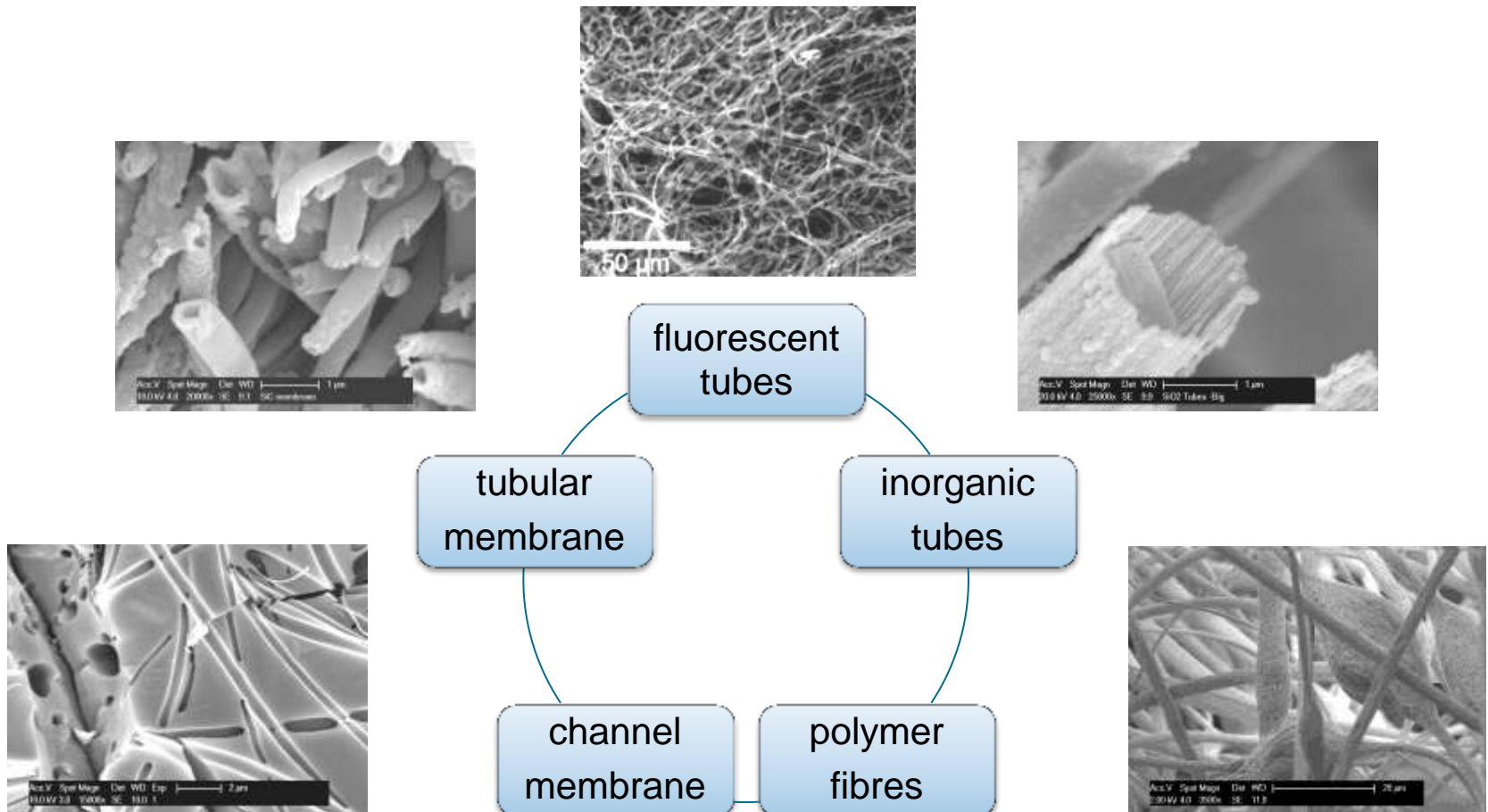
- polymer
- silica
- TiO_2
- SnS_2



double opals:

- silica- TiO_2
- silica- SnS_2

FIBRES AND POROUS MATERIALS



Polymer Fibres

Electrospinning

setup



macroscopic

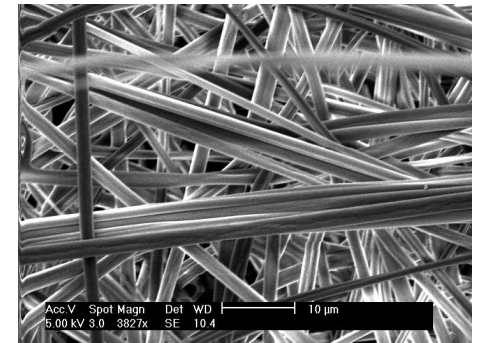


polymer fibre mat

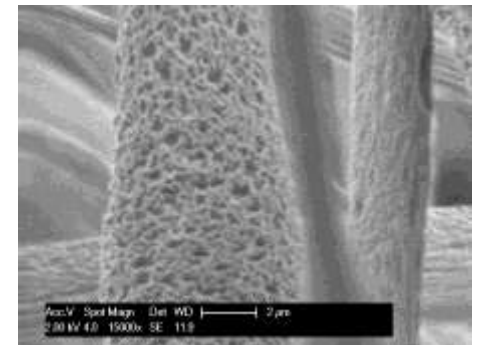
fibres from PMMA or PS,
uniform in size and shape,
variation of the diameter
by the spinning parameters

structured materials???

SEM

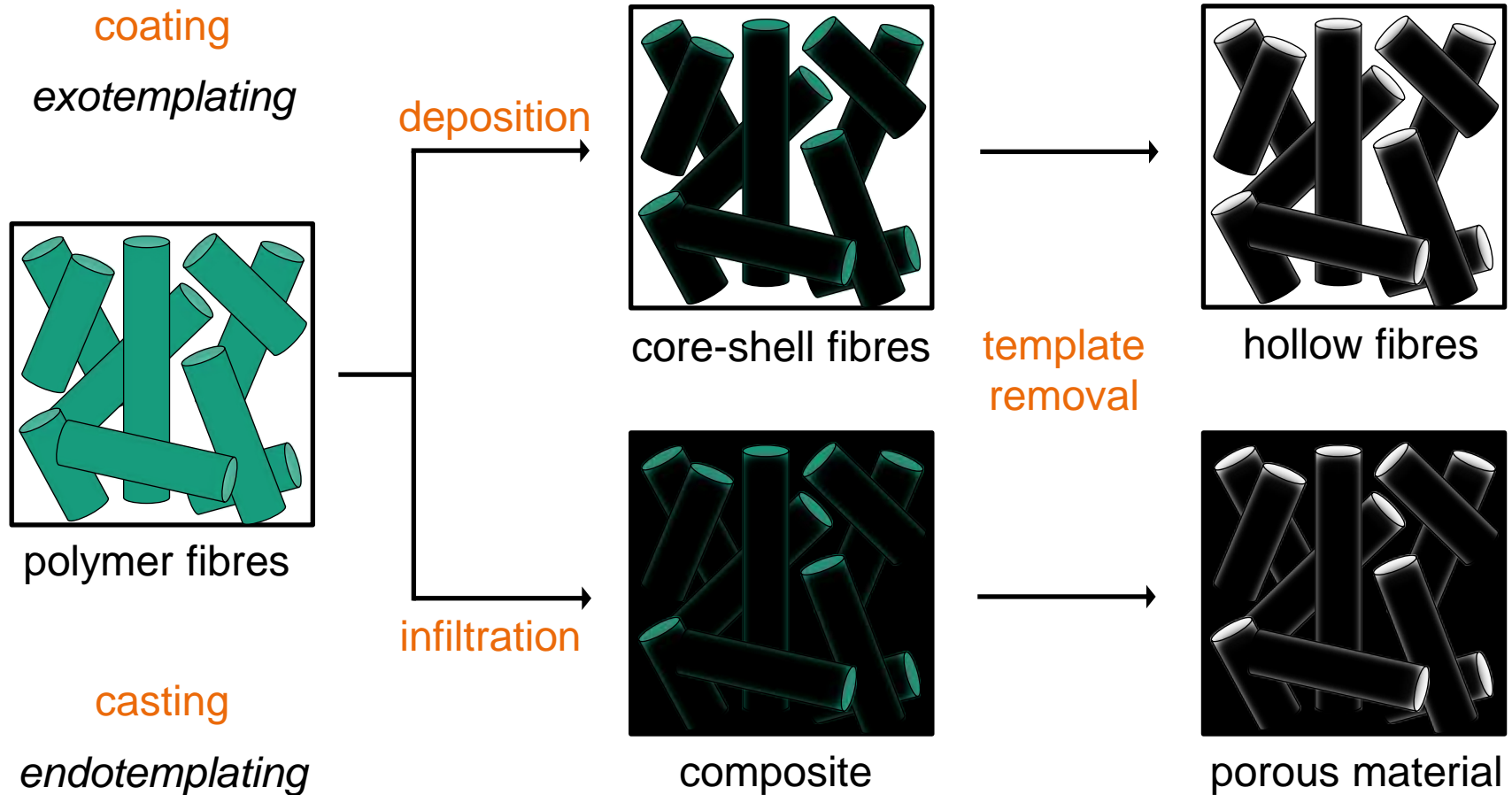


porous fibres



Strategies to Structured Materials

Coating, Casting and Membrane Templating



Coating Hollow Fibres



polymer fibres

Stöber
process
→

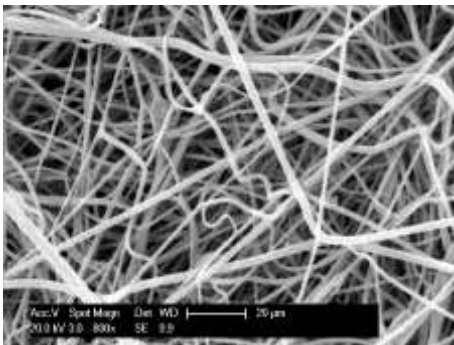


core-shell fibres

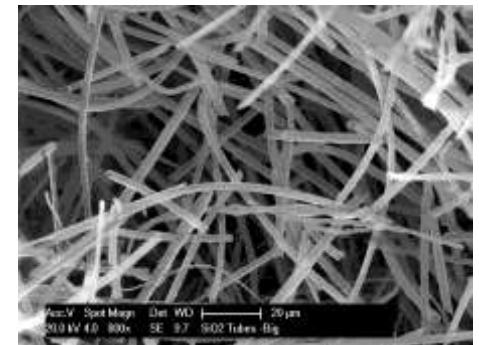
calcination
→



hollow fibres

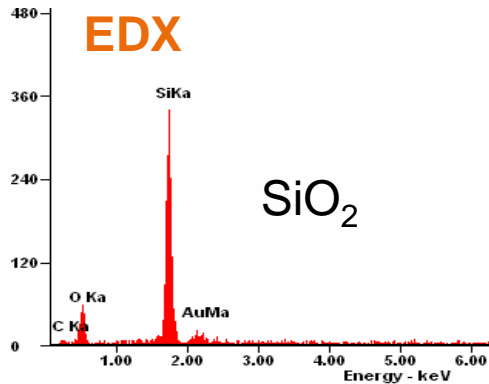


production of **inorganic tubes** from silica or ceria
by **sol-gel coating**:
tuning of the interface

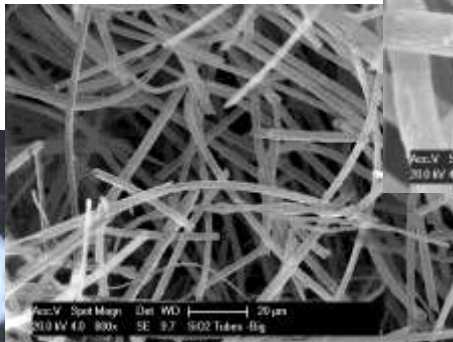


Hollow Silica Fibres

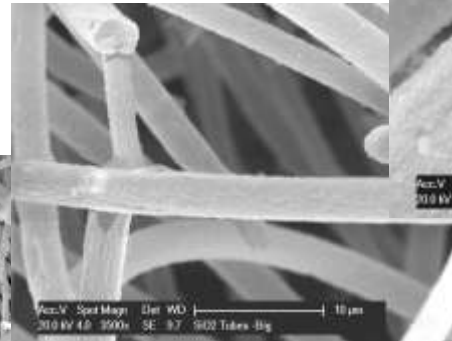
Structure Hierarchy



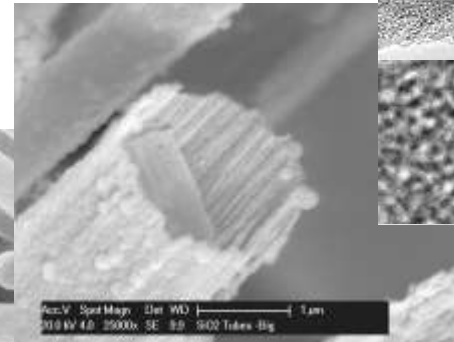
mat



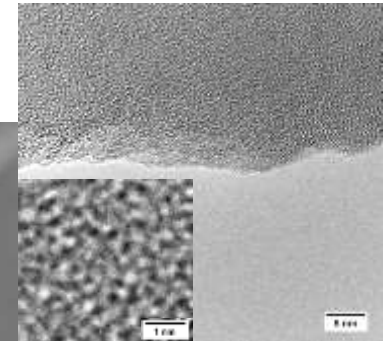
fibrous



hollow



particles

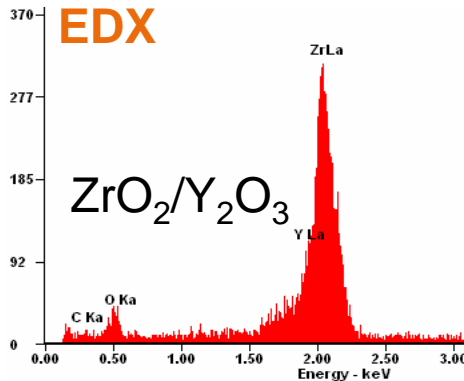


amorphous

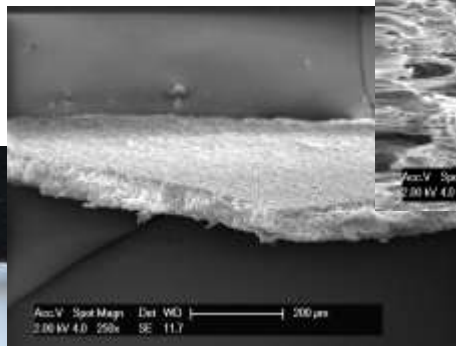
hierarchical structured
hollow silica fibre mat,
composed of amorphous
silica nanoparticles

Casting

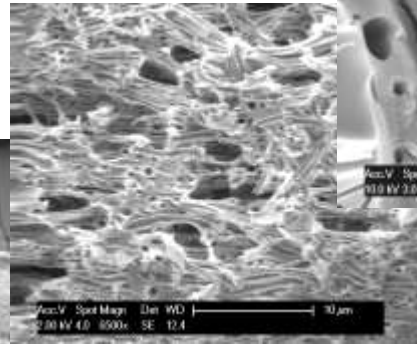
Hierarchical Structured Channel Membranes



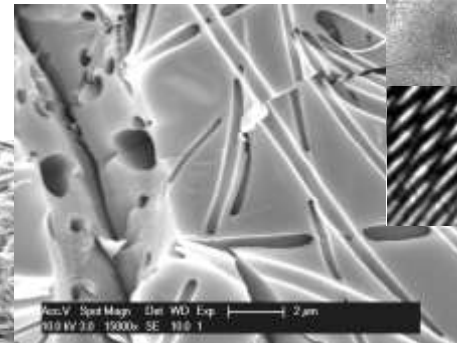
film



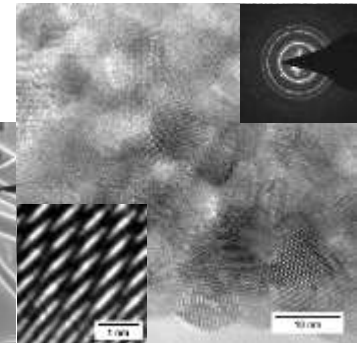
layer



porous



channels

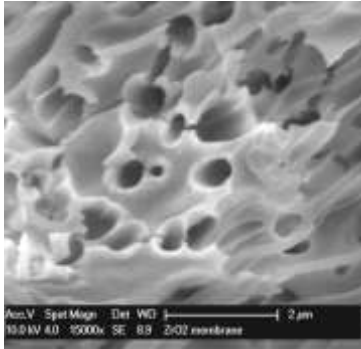


crystalline

hierarchical structured Y_2O_3
doped ZrO_2 solid electrolyte
channel membrane composed
of crystalline domains

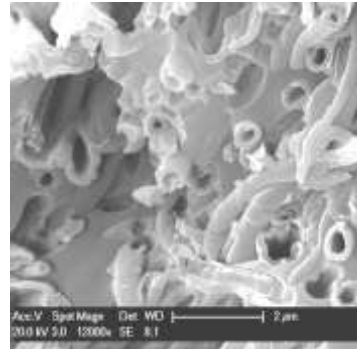
Membrane Templating

Tubular Structured Membranes

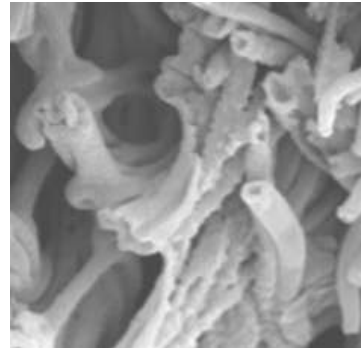


channel
membrane

coating
→
propene
700°C

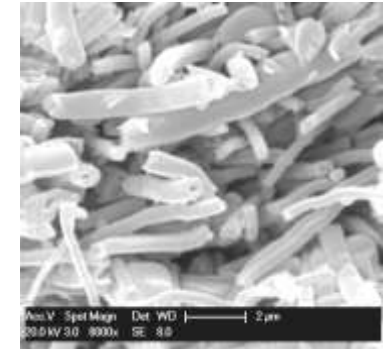


conversion
↓
1600°C

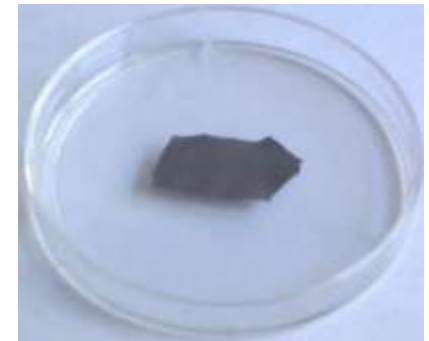


SiC hollow fibres

template
removal
→
HF
+ 1600°C



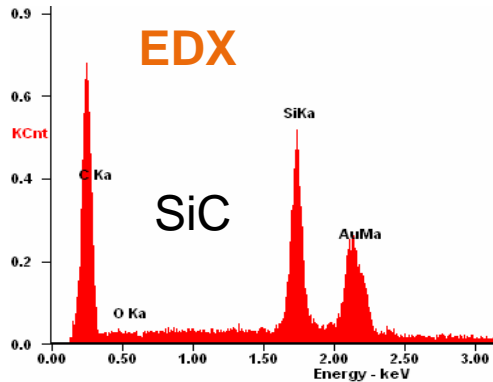
graphite
hollow fibres



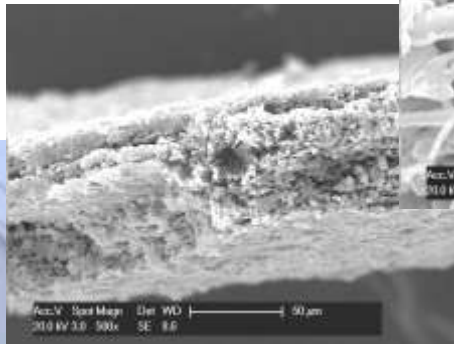
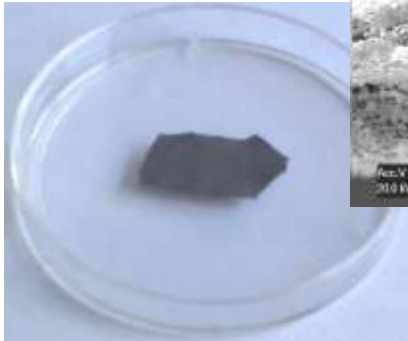
conservation of
the superstructure:
tubular structured
membranes composed
of submicron tubes

Tubular Structured SiC Membrane

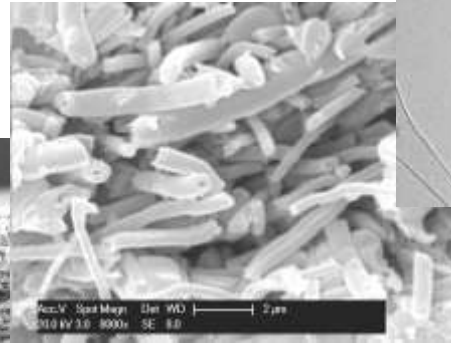
Structure Hierarchy



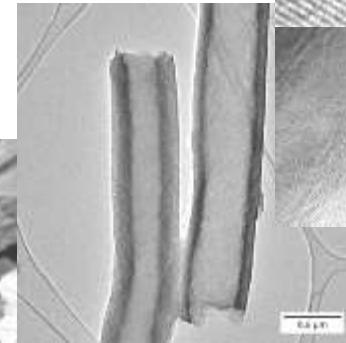
film



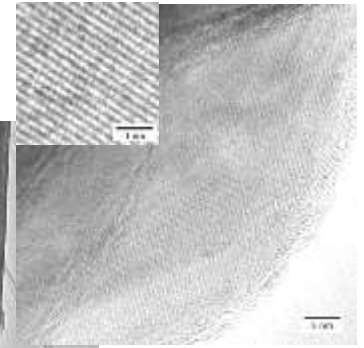
porous



fibrous



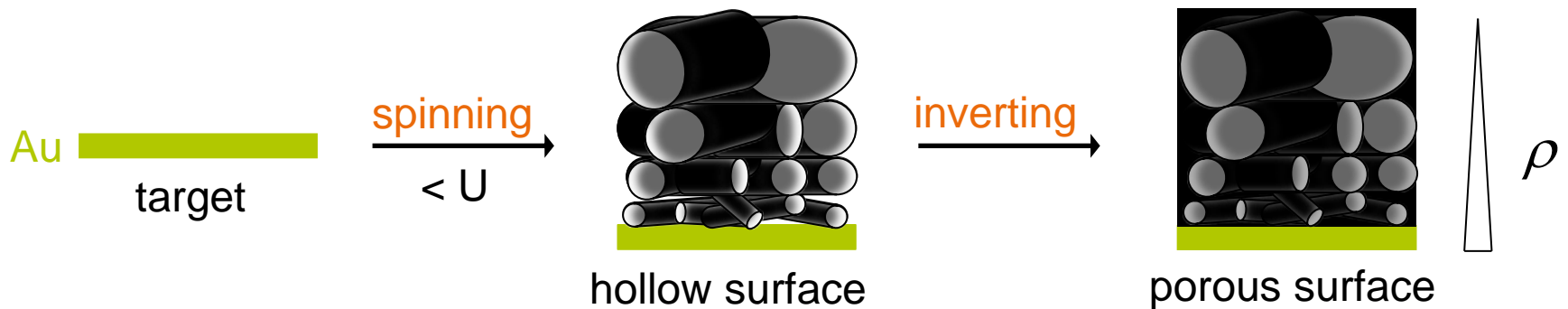
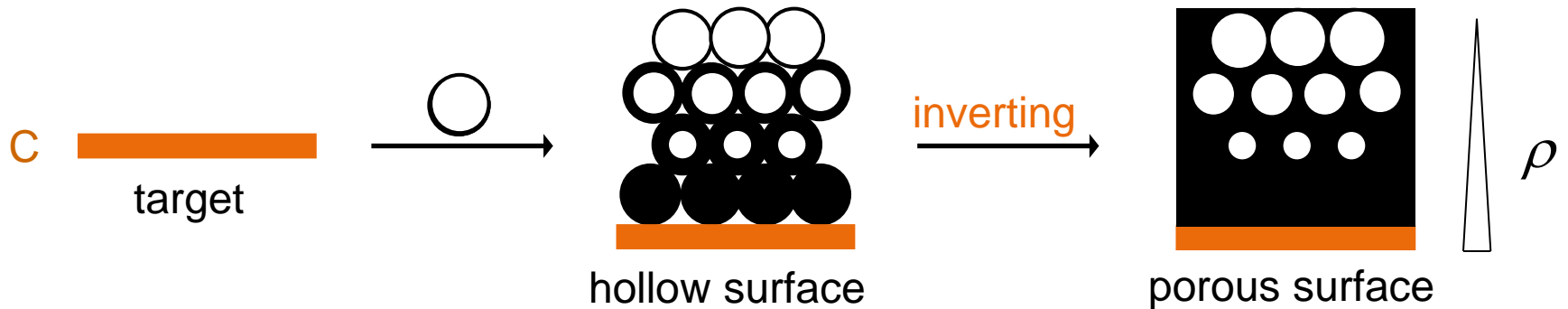
hollow



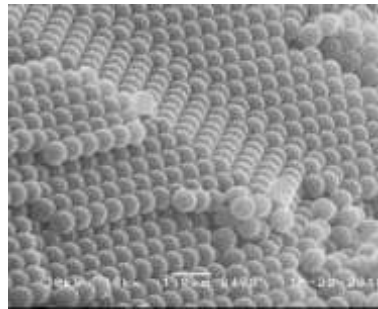
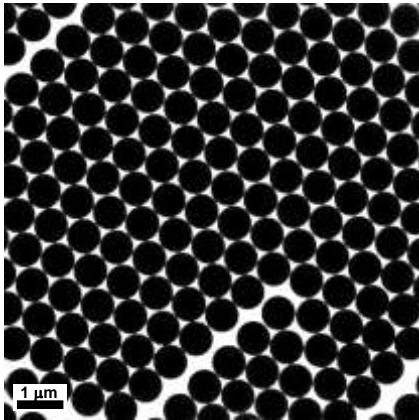
crystalline

hierarchical structured
SiC membrane composed
of crystalline tubes

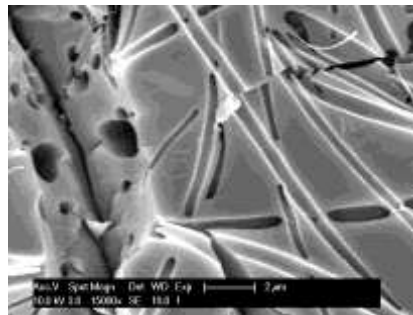
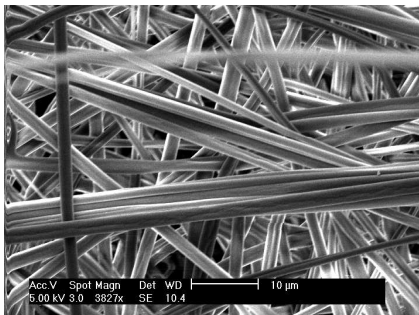
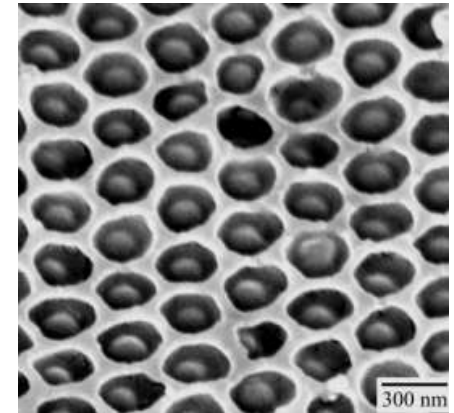
STRUCTURED TARGETS



SUMMARY



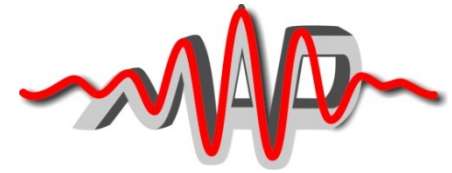
production of **hierarchic**
macro-, micro- and nano-
structured materials



Target Production and Characterization for High Intensity Laser Plasma Experiments

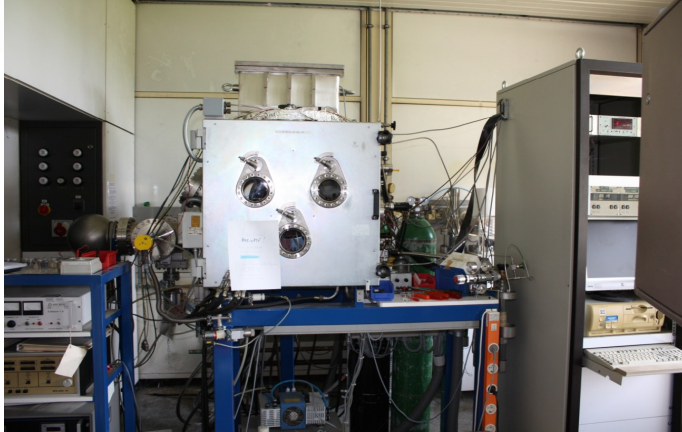
Christian Kreuzer

Ulrich Friebe, Hans Jörg Meier, Dagmar Frischke, Tobias Ostermayer, Florian Stehr, Wenjun Ma, Peter Hiltz, Christian Kreuzer, Jerzy Szerypo, Jörg Schreiber

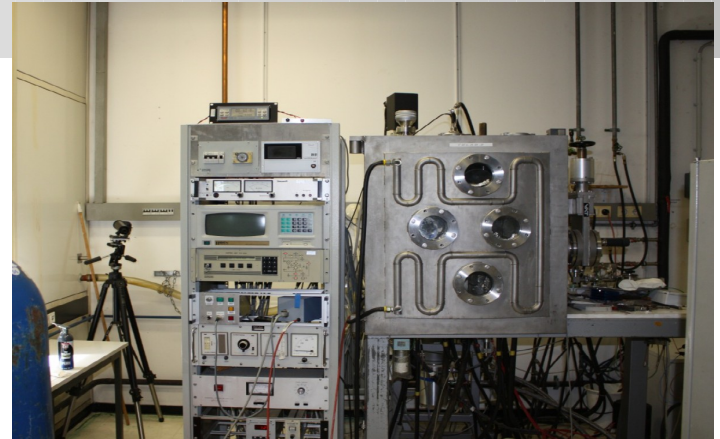


Introduction of the (small) target lab in Munich:

- Vacuum deposition methods for thin metal and other element foils
- Ultra thin DLC foils
- Low density nanotube targets
- High proton content plastic foils
- FIB targets
- Levitated MLT-targets
- Characterization of thin films



Sputter deposition



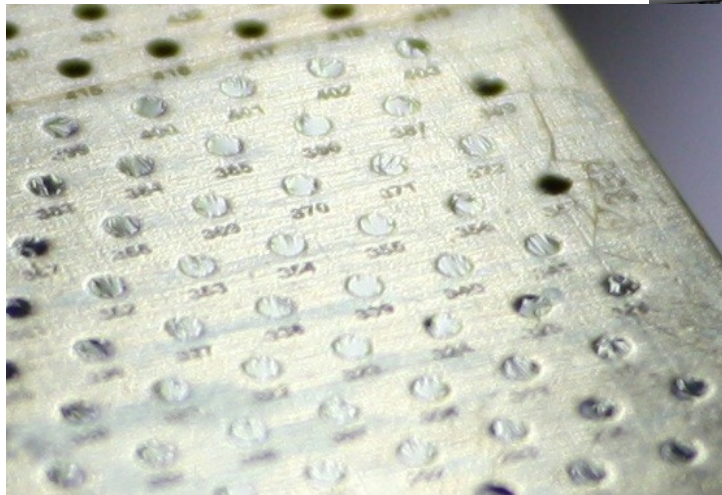
Thermal and electron gun evaporation

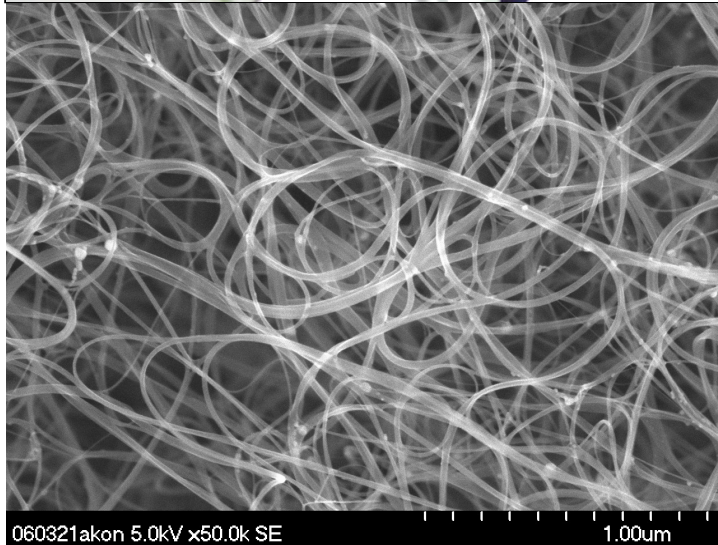
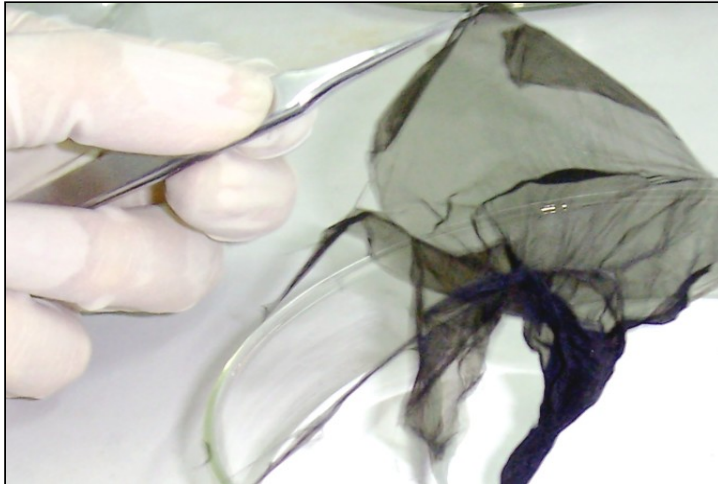


Filtered Argon storage box for oxygen
and water free storage of sensitive targets

-FCVA system

- DLC foils in the range
of 3 to 40 nm

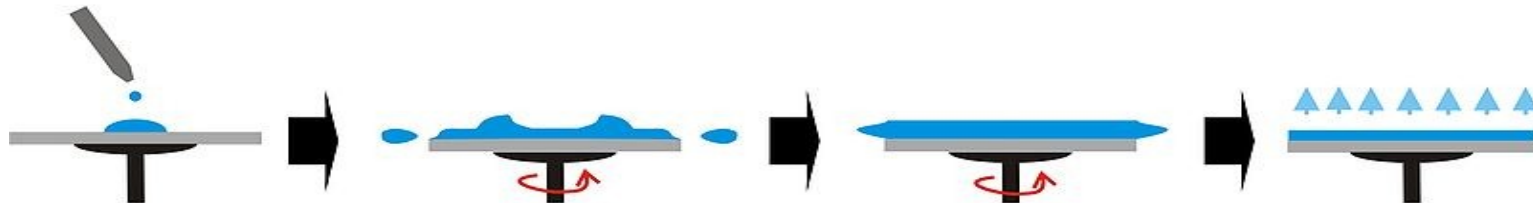
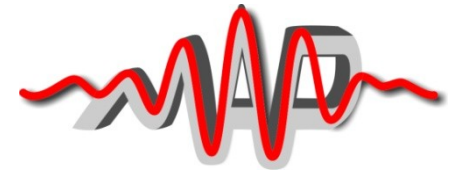




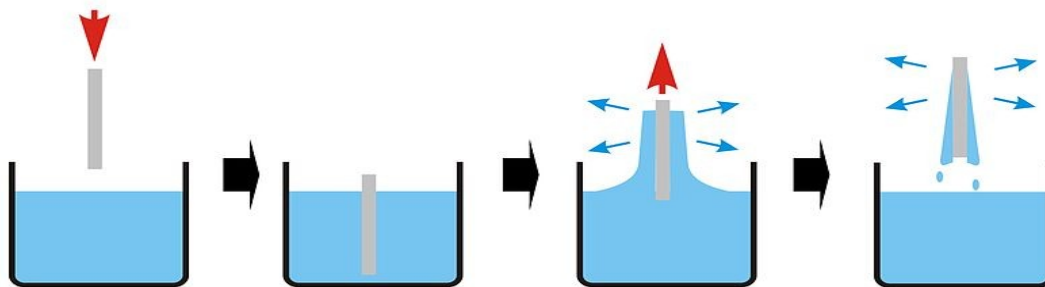
CVD system capable for temperatures up to 1500 °C

Ideal for producing low density CNT nets

For more details Wenjun Ma will give a special talk to this topic



Spin Coating

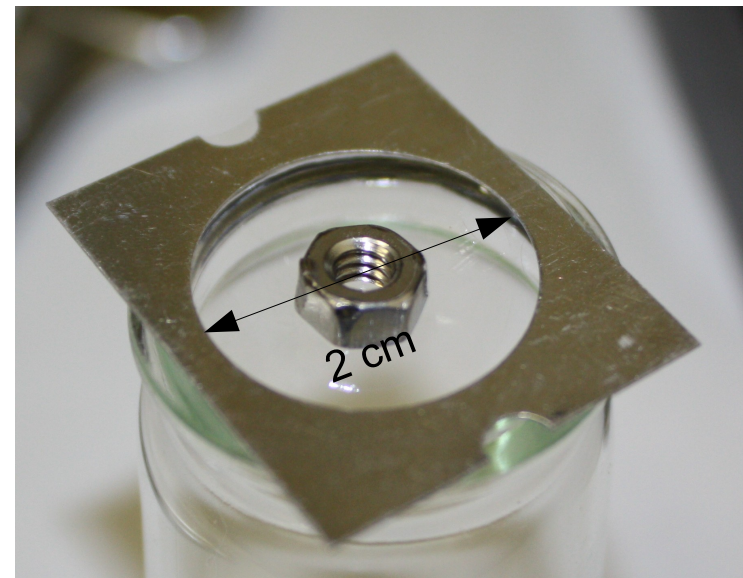
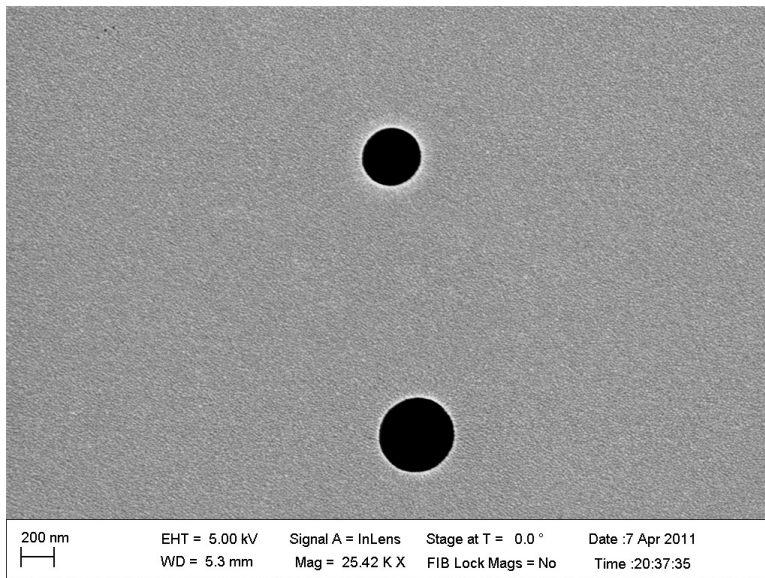


Dip Coating

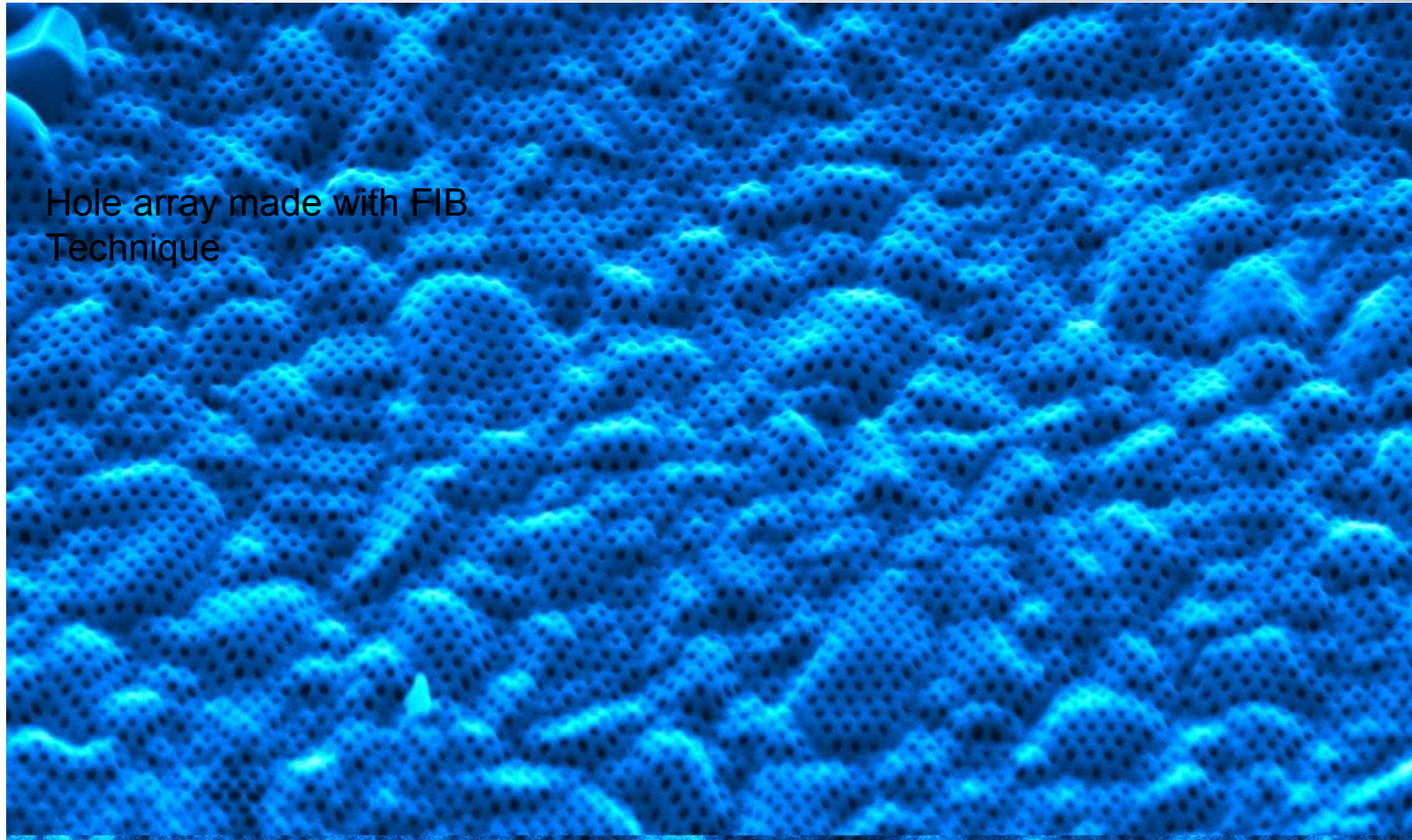
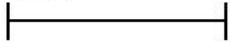


Small portable spin coater
With rotating speed up to
300 rps

- Method for easy to handle high proton content targets
- Thinnest foils down to 5 nm possible
- Strong and flexible foils can be spun over large areas
- Very flat surfaces possible



Hole array made with FIB
Technique

1 μm 

EHT = 5.00 kV

WD = 5.0 mm

Signal A = SE2

Mag = 16.02 K X

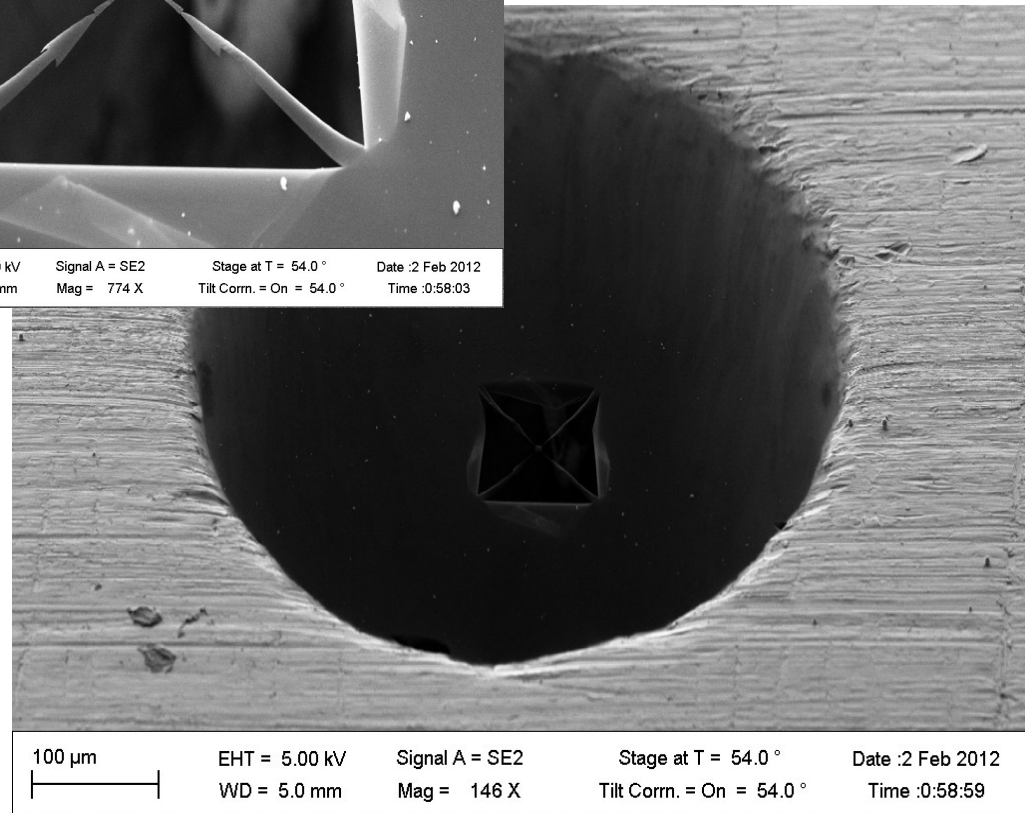
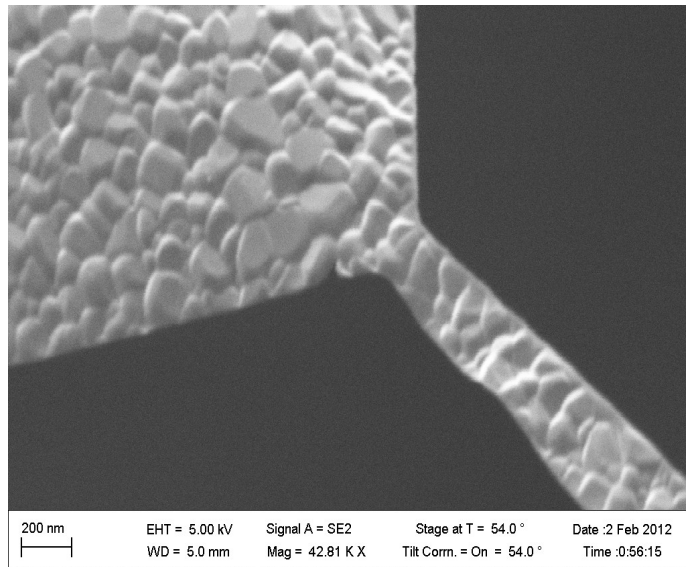
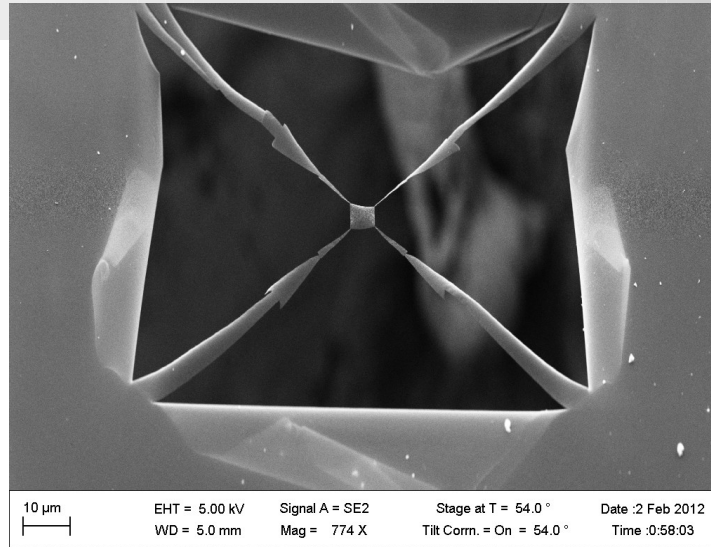
Stage at T = 54.0 °

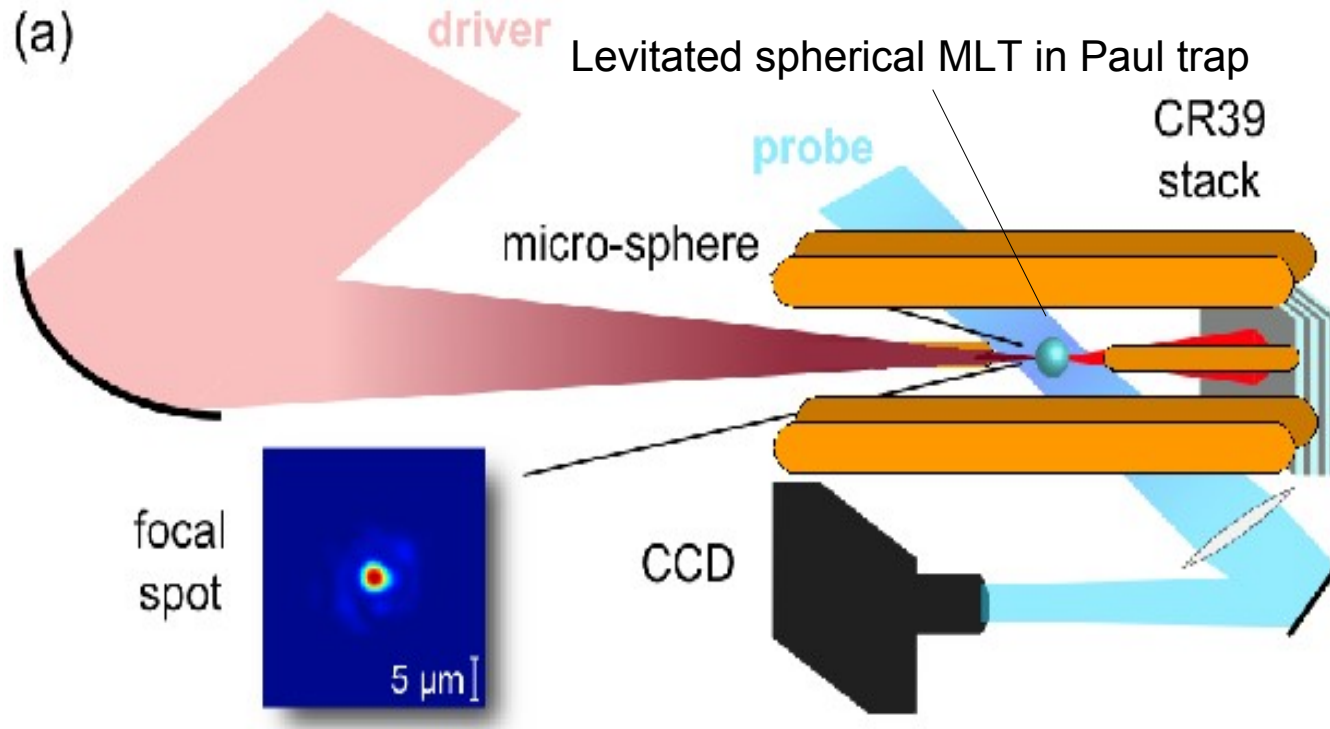
Tilt Corr. = On = 54.0 °

Date :17 May 2011

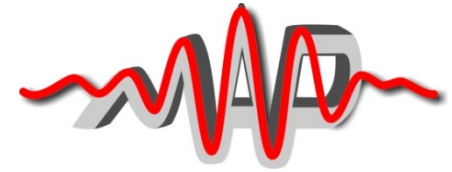
Time :10:19:10

FIB cut out MLT from DLC foil





Peter Hilz will give a special talk about this topic



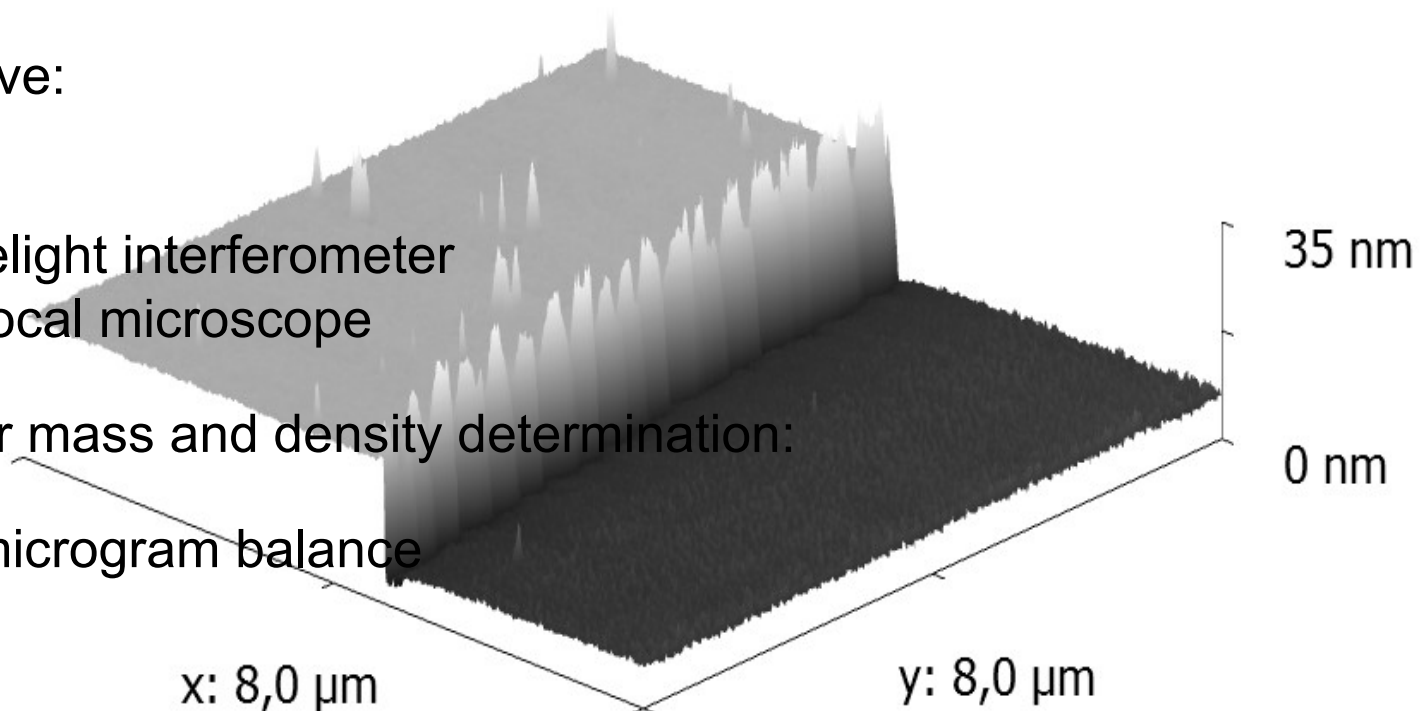
Mainly thickness determination:

We have:

- AFM
- Whitelight interferometer
- Confocal microscope

And for mass and density determination:

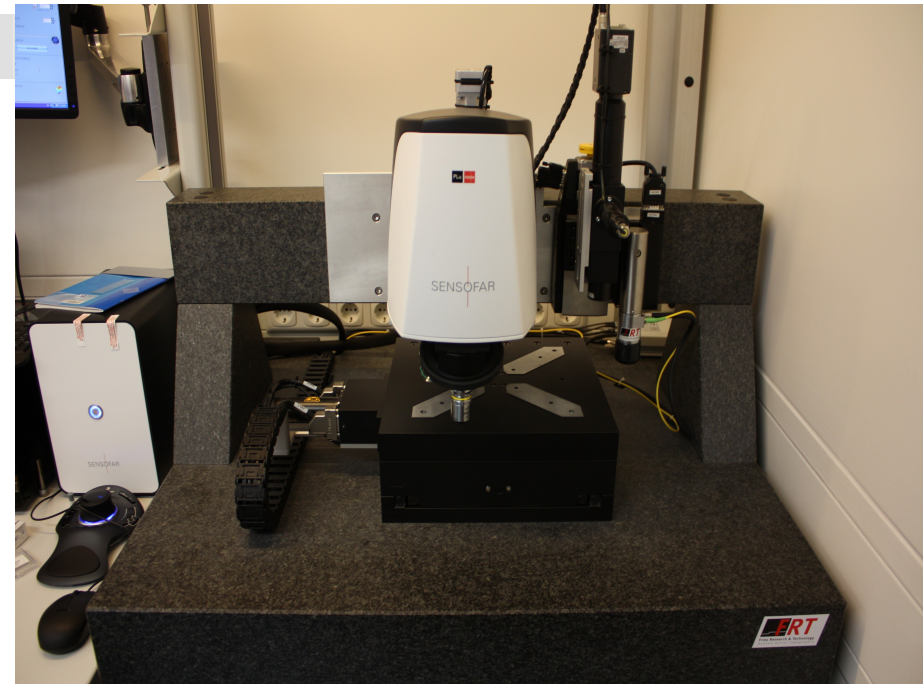
- Sub microgram balance





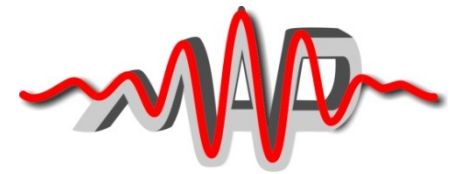
Sub microgram Balance

- Resolution 100 ng
- max load 5 g

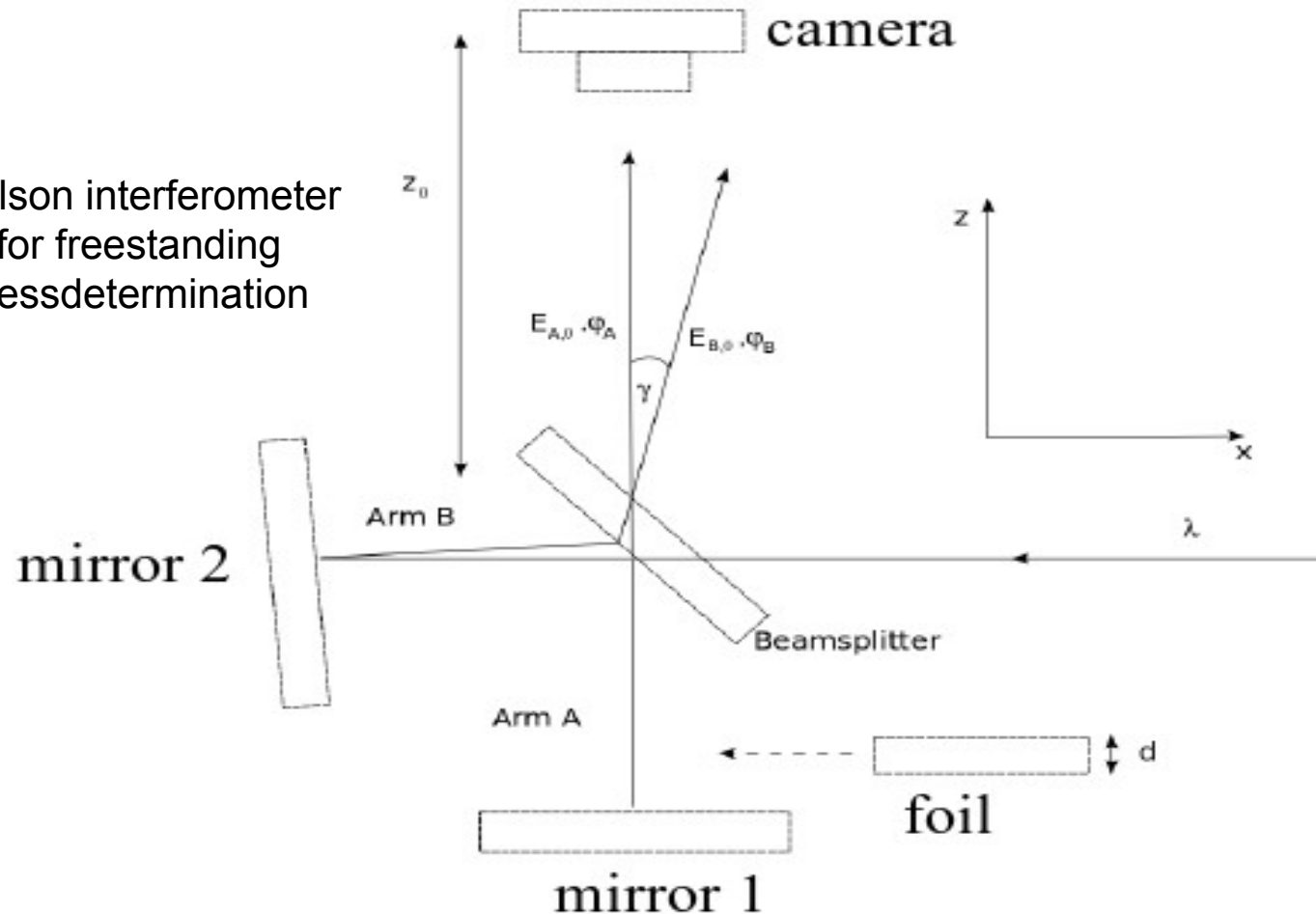


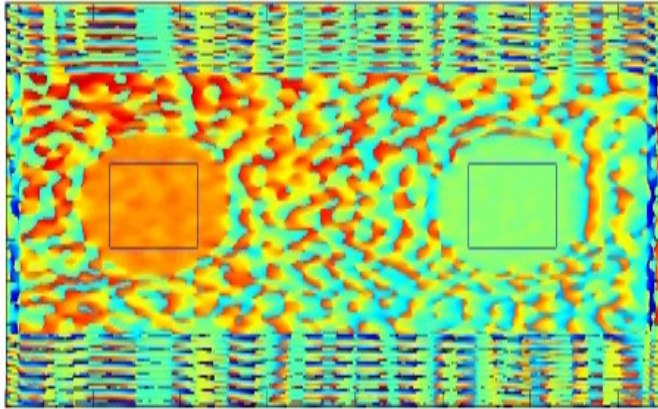
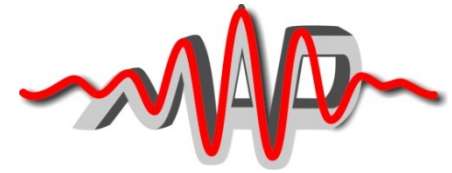
AFM, whitelight interferometer and Confocal Mikroskop

- Resolution down to 0.1 nm possible (for AFM)
- Covering all thickness ranges of interest from ultra thin (nm range) to thin (several μm range)

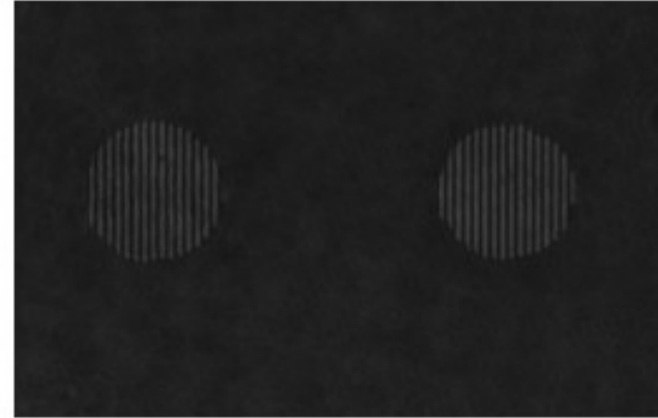


Michelson interferometer
Used for freestanding
thicknessdetermination

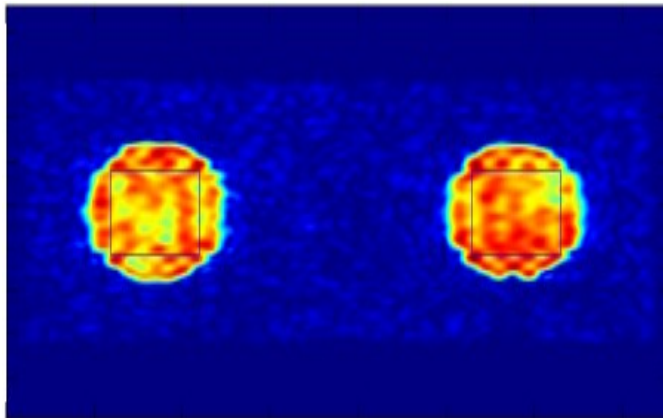




Phase difference with and without foil



Raw image before conversion



Amplitude measurement

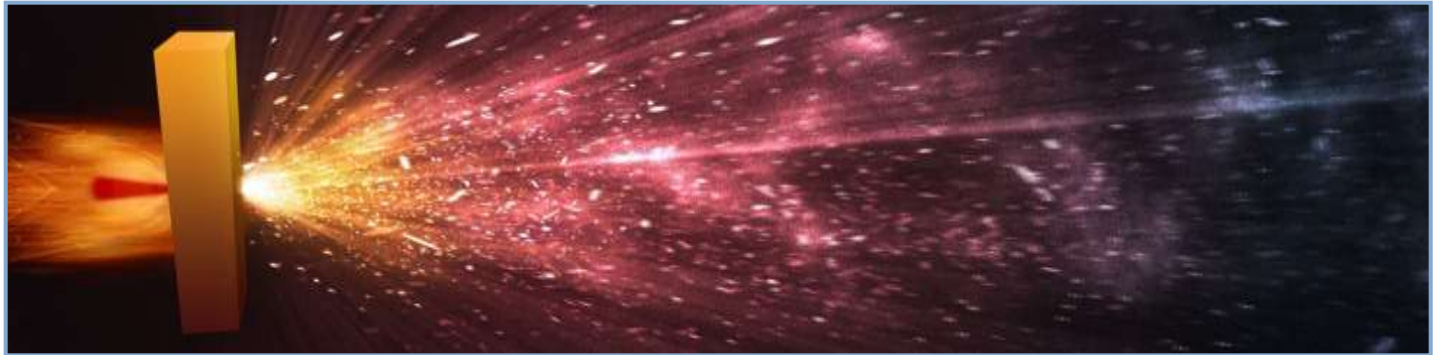
But:

Not just simple phase measurements possible

Also absorption has to be taken into account

Thank you for your
attention

Novel multi-layered foam-attached targets for advanced ultraintense laser-driven proton acceleration



Alessandro Zani

Department of Energy - Politecnico di Milano

4^o Target Fabrication Workshop 2012

Mainz, August 21st 2012

Contents

1. Ultraintense laser-driven ion acceleration

Interaction in the near-critical regime

Road towards enhanced TNSA

2. Target production and characterization

3. First preliminary experimental results

4. Conclusions



Contents

POLITECNICO DI MILANO



A. Zani

Mainz,
August 21st 2012

1. Ultraintense laser-driven ion acceleration

Interaction in the near-critical regime

Road towards enhanced TNSA

2. Target production and characterization

3. First preliminary experimental results

4. Conclusions

Interaction in the near-critical regime

Key role played by **PLASMA DENSITY** n_e

$$\text{Critical density: } n_c(\text{cm}^{-3}) \simeq \frac{1.1 \times 10^{21}}{(\lambda/\mu\text{m})^2}$$

Underdense plasmas: $n_e < n_c$

- Gas targets: interaction volume = entire plasma
- Collisionless absorption of laser energy: electron acceleration:

$$E_{\text{max}} \sim \sqrt{\frac{n_e}{10^{18}}} f\left(\frac{\omega}{k}\right) \text{ GV/cm} \quad [\text{A. Modena et al. } \textit{Nature} \textbf{377}, 606 (1995)]$$

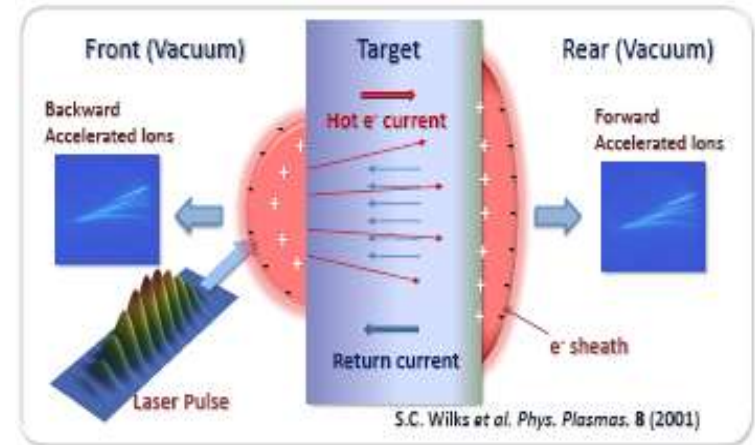
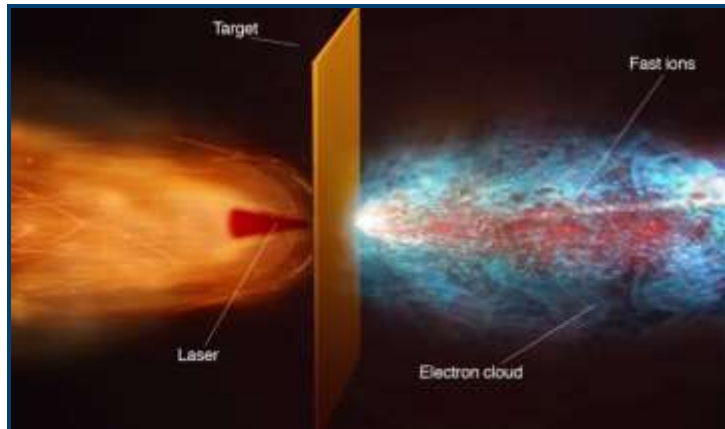
Overdense plasmas: $n_e > n_c$

- Solid targets: interaction volume = skin depth $d_s \simeq \left(\frac{\lambda}{2\pi}\right) \sqrt{\frac{n_c}{n_e}}$
- Collisionless absorption of laser energy: fast electrons generation

[P.Mulser,D.Bauer "High Power Laser-Matter Interaction", Springer (2010)]



Laser-driven ion acceleration



Target Normal Sheath Acceleration (TNSA):

- Relativistic electron expansion into a solid target leads to high charge separation at solid-vacuum interfaces



High electric fields ($\text{MV}/\mu\text{m}$) and proton acceleration (MeV)

- Maximum proton energy is limited by laser absorption

H. Daido et al. *Rep. Prog. Phys.* **75**(5), 056401 (2012)

A. Macchi et al. *Rev. Mod. Phys.* (to be published)

Road towards enhanced TNSA (I)

Evident interest in "intermediate" conditions $n_e \sim n_c$

Scalings predicting **more efficient absorption** and **fast electron generation**

[L.Willingale et al. *Phys. Rev. Lett* **96**, 245002 (2006); **102**, 125002 (2009)]

[S.S.Bulanov et al. *Phys. Plasmas* **17**, 044105 (2010)]

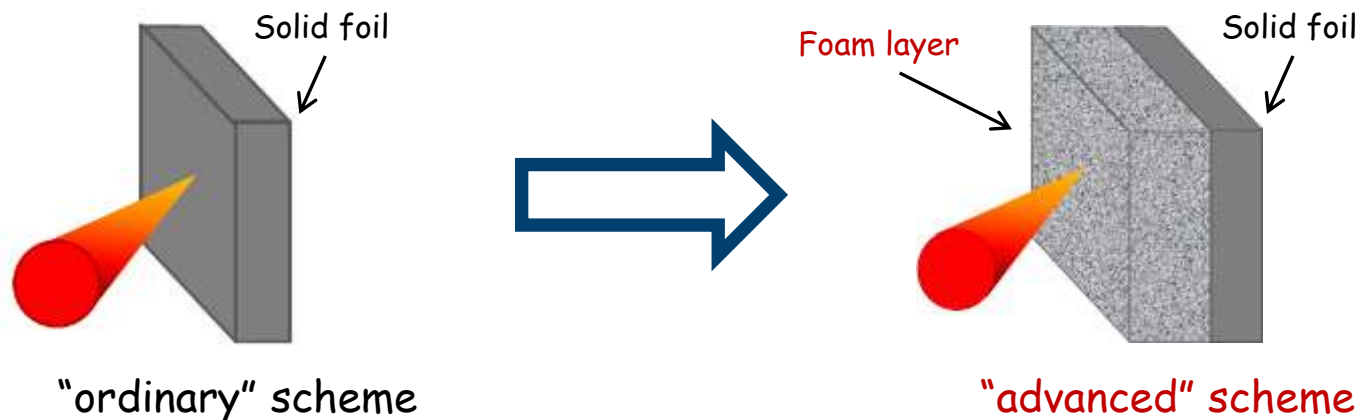
[T. Nakamura et al. *Phys. Plasmas* **17**, 113107 (2010)]

A. Zani

Mainz,
August 21st 2012

"Advanced" TNSA regime

Multi-layered targets: low-density layer + solid foil



Road towards enhanced TNSA (II)

2D/3D Particle-In-Cell numerical simulation results:

[A.Sgattoni et al. *Phys. Rev. E* **85**, 036405 (2012)]

- enhanced TNSA, gain factor in excess of 2 for maximum proton energy
- optimal foam thickness depends on laser intensity and foam density
- high energy absorption by the target

Experimental part of the work

- Multilayered target manufacturing
 - A proper control of foam physical properties (density, adhesion to solid..) is NOT straightforward
- First experimental investigation of proton acceleration



Contents

POLITECNICO DI MILANO



A. Zani

Mainz,
August 21st 2012

1. Ultraintense laser-driven ion acceleration

Interaction in the near-critical regime

Road towards enhanced TNSA

2. Target production and characterization

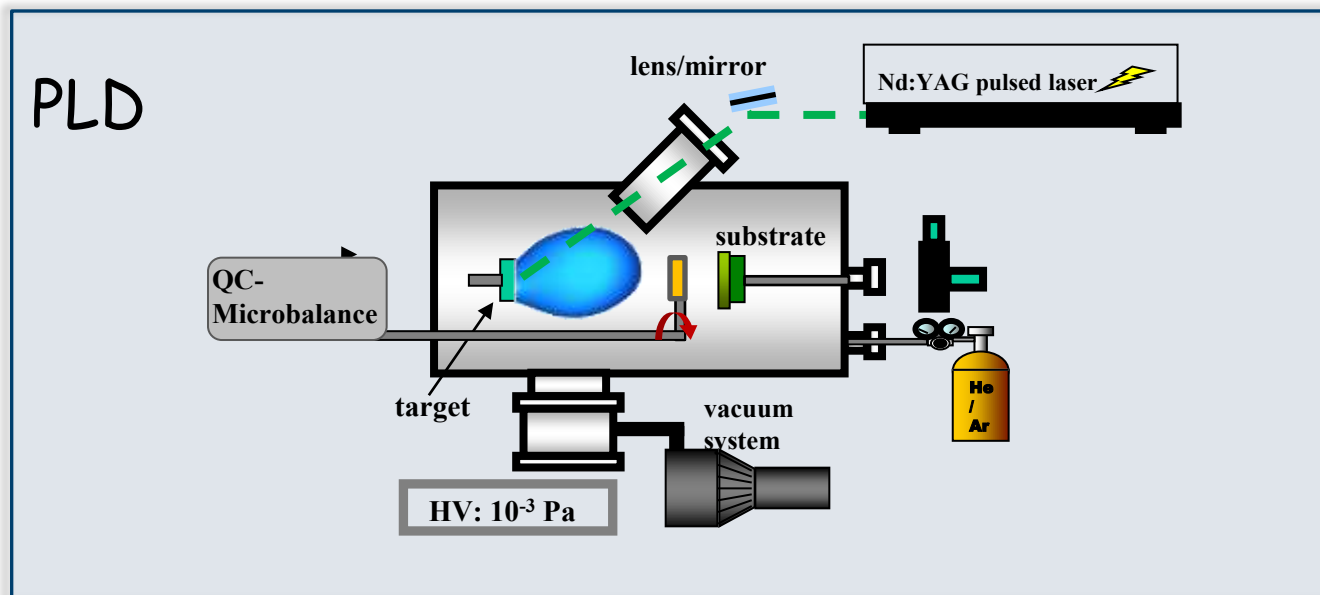
3. First preliminary experimental results

4. Conclusions

Multi-layered target production (I)

Goal: Near-critical carbon foam attached onto a solid substrate

- Why carbon? Low Z and volatile oxides
- densities around mg/cm^3 for laser wavelength $\sim 1 \mu\text{m}$
- Production technique: **Pulsed Laser Deposition (PLD)**
 - ✓ Large choice of materials and substrates
 - ✓ good adhesion properties
 - ✓ possibility to obtain controlled nanostructures



Multi-layered target production (II)

Deposition parameters:

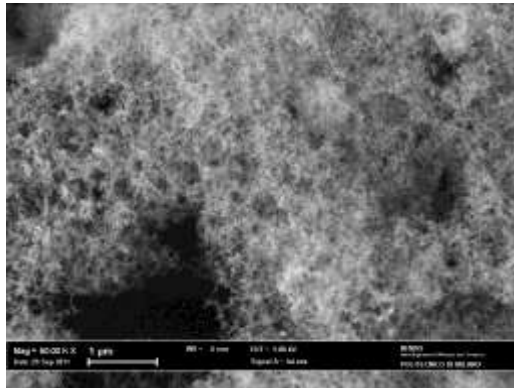
- Wavelength: 532 nm
- Gas pressure: 0 - 1000 Pa
- Target-substrate distance: 8,5 cm
- Fluence: 0,8 J/cm²

Substrates:

- Si<100> -> test depositions for characterization
- Al (10-1.5-0.7 μm) -> target fabrication

Target: Pyrolitic graphite

Carbon foam morphology: SEM analysis



Structure at high magnification is clearly very open and porous
(Pore size is tens of nm)

On a mesoscale structures arrange differently by varying one process parameter:
gas pressure / gas type / inlet gas flow

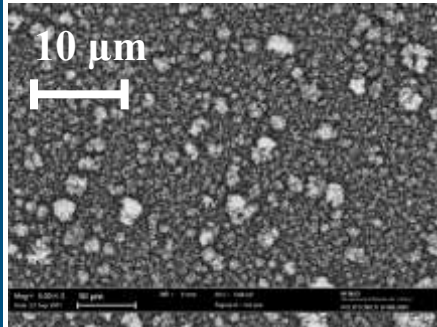
morphology

structure

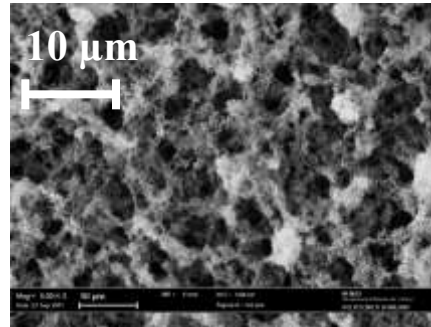
density

Process parameters: morphological characterization

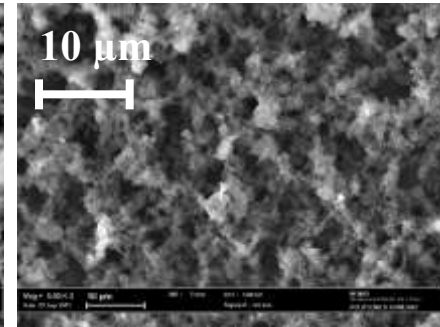
A. Zani et al,
*Ultra-low density carbon foams produced
by pulsed laser deposition, in preparation*



30 Pa



100 Pa

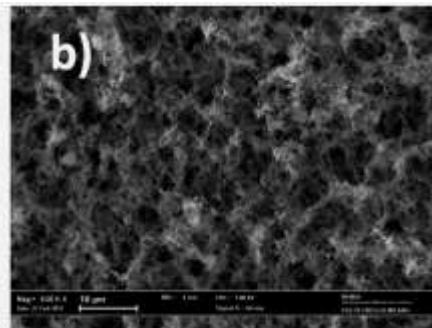
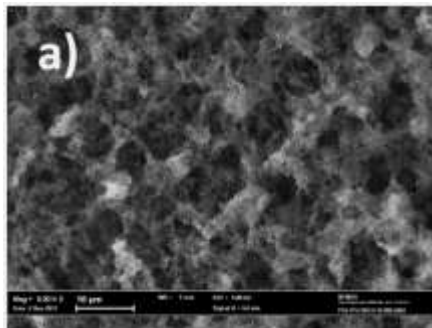
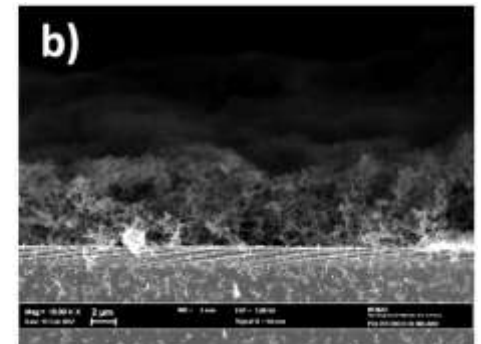
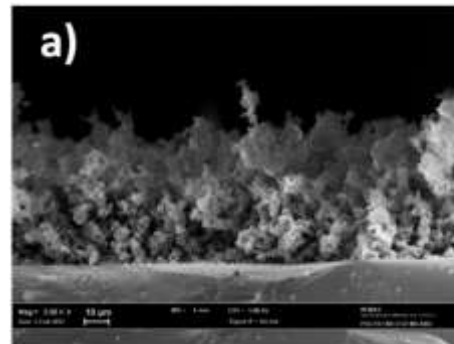


300 Pa

**Ar
pressure**

Ambient gas type:

- He (500 Pa) a)
- Ar (100 Pa) b)



Ambient gas flow (Ar):

- 1 sccm + transverse dir.: a)
- 100 sccm & || dir.: b)

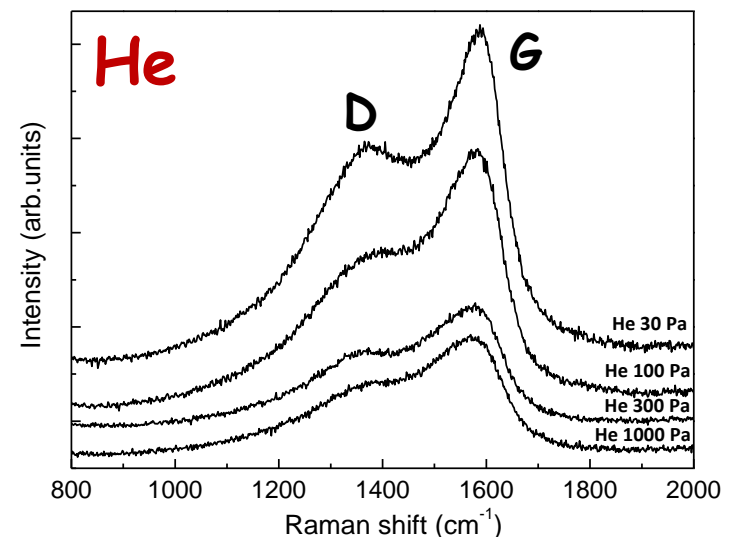
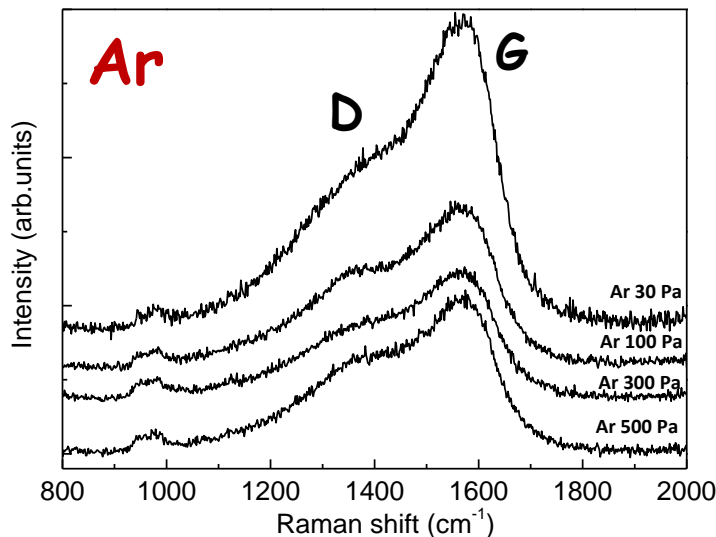
Process parameters: structural characterization

A. Zani et al,
*Ultra-low density carbon foams produced
by pulsed laser deposition, in preparation*

- Raman spectroscopy is a very common technique for structural characterization of carbon materials
- I_D/I_G gives information about the amount and type of sp^2 bonds and about the typical dimensions of crystalline domains

Results (following the procedure in Ferrari et al. *PRB* 61 14195 (2000))

- Prevalence of sp^2 bonds
- All deposition conditions show the same nanostructure

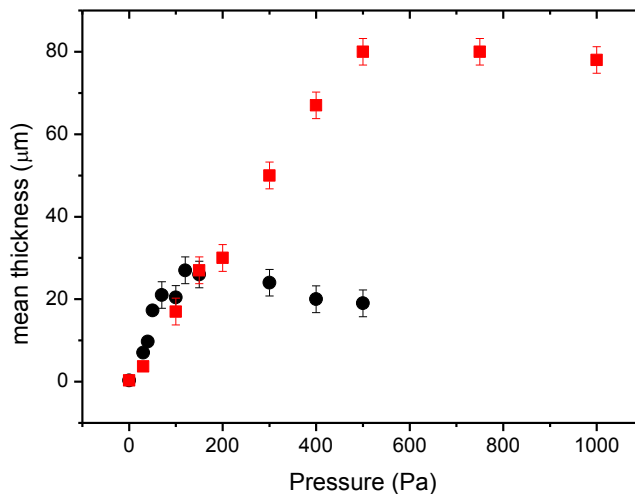
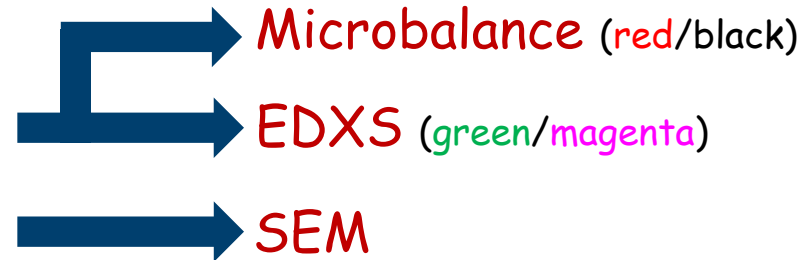


Density measurement (I)

Performed combining:

- Areal density measurement

- Thickness measurement

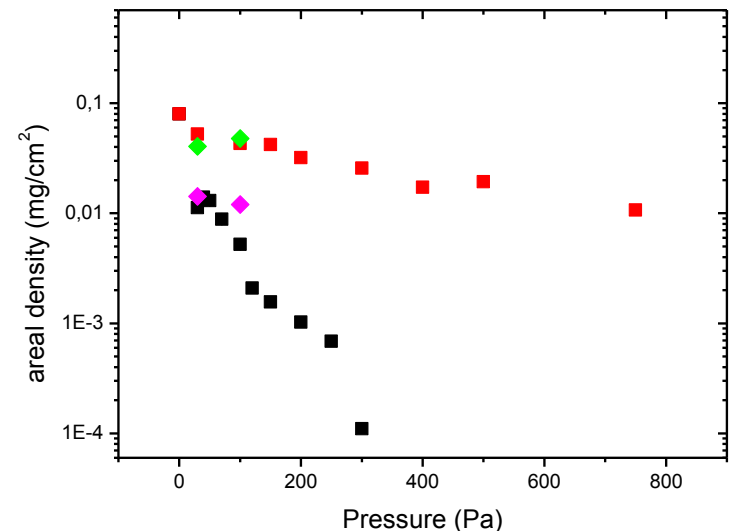


He (red): saturation at $80\mu\text{m}$ and good coverage till 1000Pa

Ar (black): saturation at $20\mu\text{m}$ and scarce coverage after 400Pa

He (red): almost constant in the whole pressure range

Ar (black): nearly 1 order of magnitude lower due to relevant scattering between C and Ar



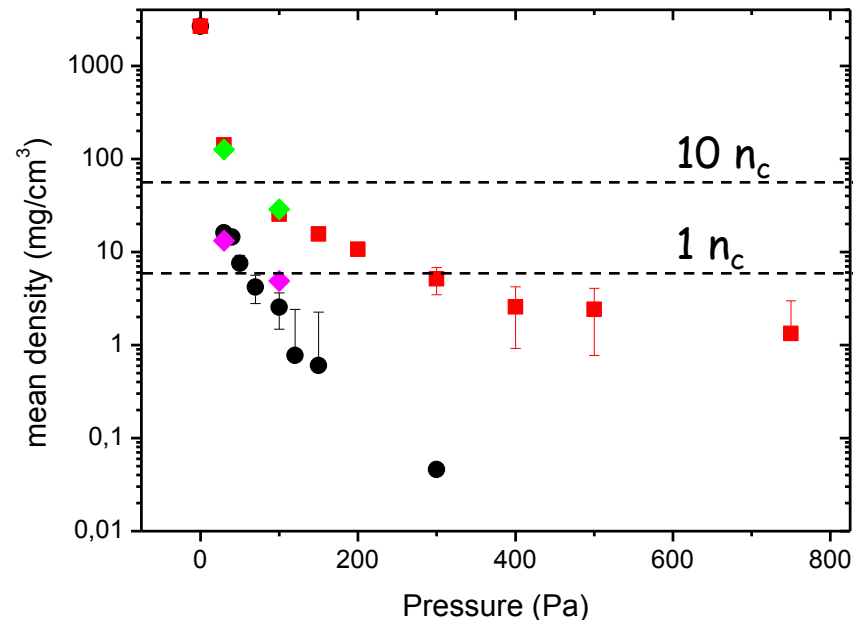
Density measurement (II)

A. Zani et al,
*Ultra-low density carbon foams produced
by pulsed laser deposition, in preparation*

✓ Assuming:

- fully ionized carbon
 - $\lambda = 0.8 \mu\text{m}$ incident laser
- ➡ $\rho_{\text{cr}}(\text{C}) \approx 5.7 \text{ mg/cm}^3$

✓ Able to reach in a controlled way near-critical densities!



Noteworthy:

- Inlet gas flow does not affect any physical properties but the surface uniformity
- EDXS density measurements are still work in progress BUT evidence that microbalance becomes scarcely reliable above 100-200 Pa in Ar

Contents

1. Ultraintense laser-driven ion acceleration

Interaction in the near-critical regime

Road towards enhanced TNSA

2. Target production and characterization

3. First preliminary experimental results

4. Conclusions



First preliminary experimental results (I)

Test of foam-attached targets on UHI100 facility at CEA-Saclay

- broad intensity range (5×10^{16} - 5×10^{19} W/cm²)
varying individually: **focal spot**, **energy** and **duration**
- examined several different experimental conditions

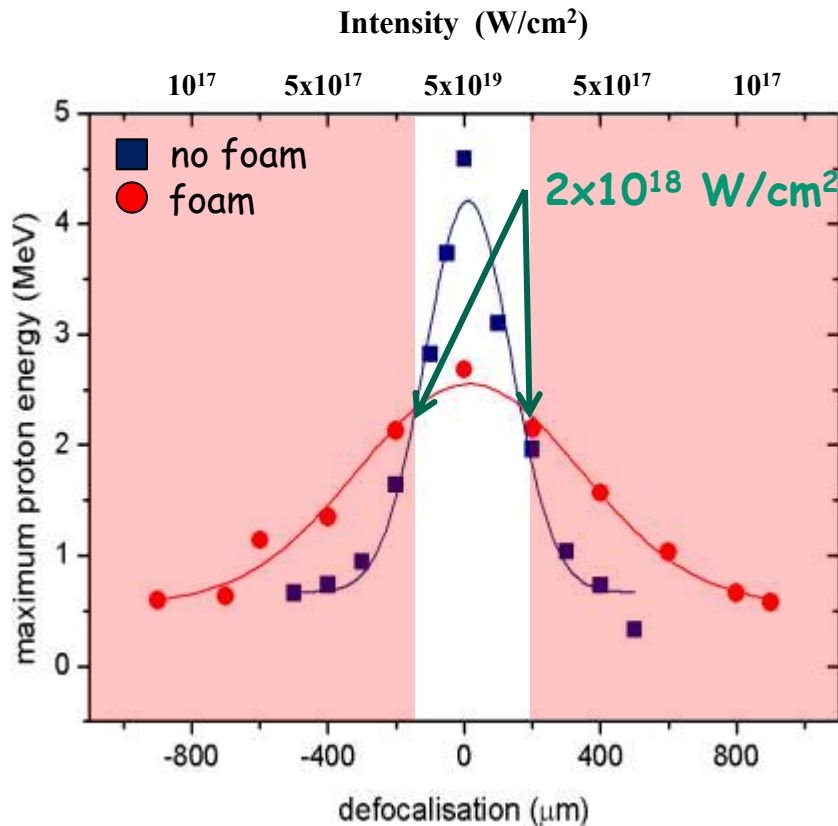
- High (10^{12}) and low (10^7) contrast shots
- "Bare" target (Al) thicknesses: 0.7 - 1.5 - 2 - 6 - 10 - 20 - 30 - 100 μm
- "Foam-attached" targets
 - foam thickness: from 9 to 22 μm
 - foam density: 0.5 - 1 - 2 n_c
 - Al substrate thickness: 0.7 - 1.5 - 10 μm

➔ Very reliable set of data



First preliminary experimental results (II)

→ Different interaction conditions seem to appear when a foam is present



At sufficiently low intensity ($<10^{18} \text{ W}/\text{cm}^2$) proton response with foam targets appears to be definitely higher.



In this region maximum proton energy gain factor using a foam is between $2 \div 4$



Contents

1. Ultraintense laser-driven ion acceleration

Interaction in the near-critical regime

Road towards enhanced TNSA

2. Target production and characterization

3. First preliminary experimental results

4. Conclusions



Conclusions

- In the near-critical regime it is possible to enhance ultraintense laser absorption as well as TNSA process:
"foam-attached targets"
- Potential in producing:
 - ✓ foam materials having controlled density-composition in the near critical regime
 - ✓ foam layers directly grown on solid surfaces (solving adhesion problems)
 - ✓ materials with controlled density profile

Next...

- ✓ achievement of independent control of foam parameters (density, uniformity, thickness)
- ✓ Deeper physical comprehension of first experimental results
- ✓ Other forthcoming experiments ($>10^{20}$ W/cm²)



Acknowledgments

M. Passoni, D. Dellasega
D. Rizzo, V. Russo



POLITECNICO
DI MILANO

T. Ceccotti, V. Floquet
P. D'Oliveira, Ph. Martin



A. Macchi, A. Sgattoni



www.nanolab.polimi.it

www.suldis.org

POLITECNICO DI MILANO



A. Zani

Mainz,
August 21st 2012

Cryogenic Targets for Laser and Particle Beams

4th Target Fabrication Workshop | Mainz | August 21, 2012



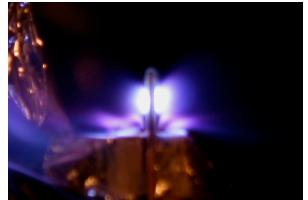
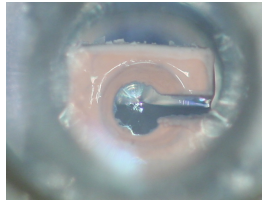
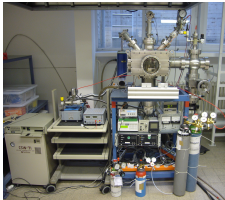
TECHNISCHE
UNIVERSITÄT
DARMSTADT

Stefan Bedacht

Technische Universität Darmstadt

Institut für Kernphysik

AG Hoffmann





Cryogenics

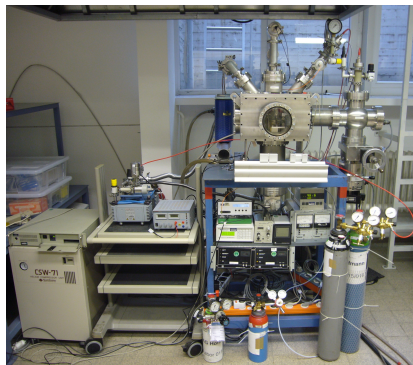
Cryogenics is the branch of physics dealing with the production and effects of very low temperatures, *i.e.*, temperatures below 100 K.

Goals

1. fabrication of thin solid hydrogen targets
2. characterization of the surface quality of the targets
3. using the targets for laser and particle beam experiments

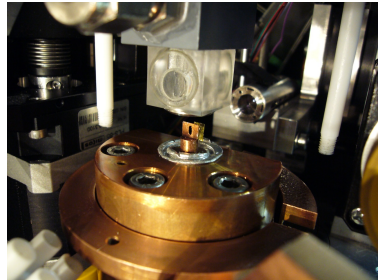
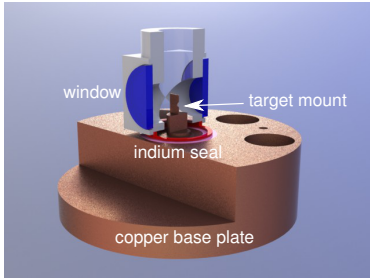
Requirements

- ▶ vacuum chamber
- ▶ cooling device
- ▶ pure gases
- ▶ pressure control
- ▶ temperature control
- ▶ target diagnostics

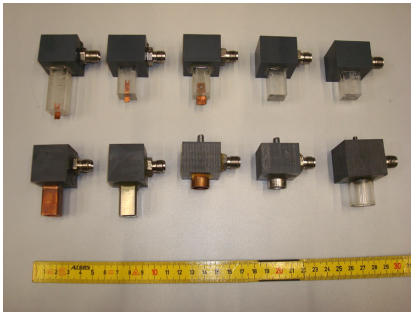


Cryogenic test rig at TU Darmstadt.

Growing Chamber



- ▶ copper base plate features good heat conduction
- ▶ high tightness due to indium seal
- ▶ windows for real time optical diagnostics
- ▶ motorized polycarbonate growing chamber



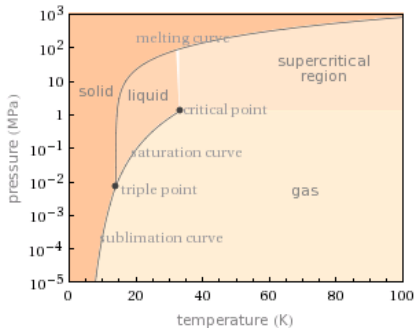
Different growing chambers. [J. Menzel]

- ▶ target geometry is determined by the geometry of the growing chamber and the target mount
 - ▶ thickness: μm to cm
 - ▶ diameter: mm to cm
- ▶ growing process takes about 1 min to 30 min
- ▶ thickness can be reduced by thermal evaporation

Growing Procedure



TECHNISCHE
UNIVERSITÄT
DARMSTADT



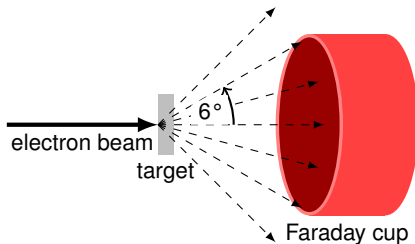
Phase diagram of hydrogen. [Wolfram/Alpha]

1. ensure vacuum better than 10^{-5} mbar
2. cool copper base plate down to less than 10 K
3. attach growing chamber to base plate
4. adjust gas pressure and temperature
5. fill growing chamber with target gas
6. wait for target to solidify

Target Thickness Measurement – Electron Gun

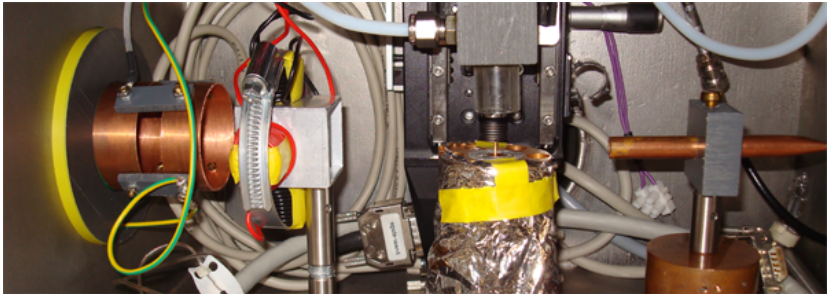


TECHNISCHE
UNIVERSITÄT
DARMSTADT



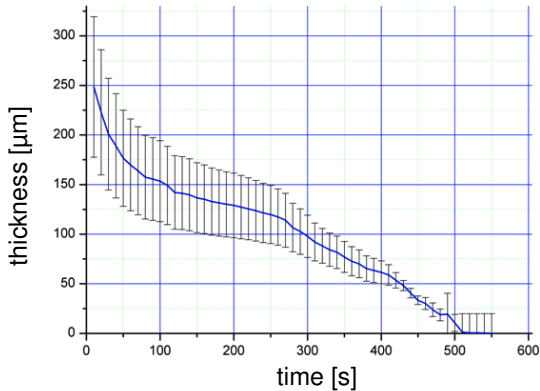
- ▶ electron beam: 14 kV, 5 μ A, 2 mm in diameter
- ▶ current detected by the Faraday cup is correlated with target geometry
- ▶ experimental results are compared with results of *Geant4* simulations

Target Thickness Measurement – Electron Gun



Electron gun setup. [J. Menzel]

Target Thickness Measurement – Electron Gun



Deuterium target thickness vs. time. [J. Menzel]

Target Thickness Measurement – Interferometry



Commercial chromatic confocal sensor and interferometer. [*Precitec Optonics*]

Capabilities

- ▶ measuring range $3\text{ }\mu\text{m}$ to $250\text{ }\mu\text{m}$
- ▶ sampling rate 32 Hz to 2000 Hz
- ▶ chromatic confocal and interferometric mode
- ▶ lateral resolution $20\text{ }\mu\text{m}$ to $2\text{ }\mu\text{m}$
- ▶ vertical resolution 14 nm to 10 nm

Difficulties

- ▶ reflective geometry
- ▶ geometric constraints



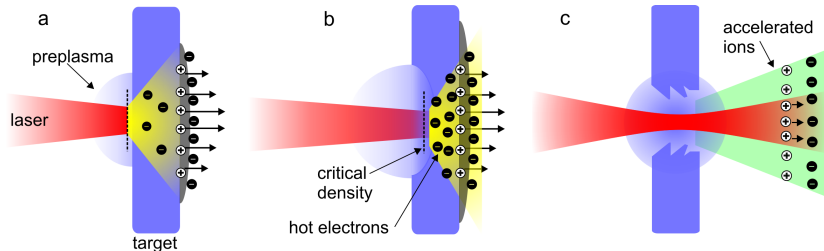
Advantages

- ▶ pure targets
- ▶ free standing
- ▶ adjustable thickness (μm to cm)
- ▶ large diameter (few mm^2 to cm^2)
- ▶ medium repetition rate (2 to 3 targets per hour)
- ▶ solid state density (e.g. 0.09 g cm^{-3} for solid hydrogen)

Disadvantages

- ▶ immobility
- ▶ complex setup & alignment

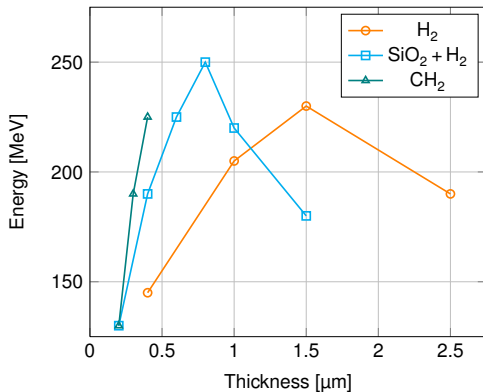
Laser Breakout Afterburner (BOA)



Target Normal Sheath
Acceleration (TNSA)

Intermediate phase

Laser Breakout
Afterburner (BOA)

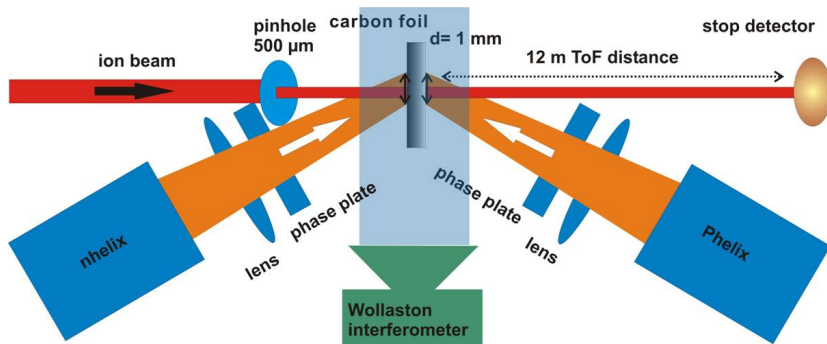


Laser Parameters

- ▶ 120 Joule in 500 fs
- ▶ intensity of $10^{21} \text{ W cm}^{-2}$
- ▶ contrast greater than 10^9
- ▶ linear polarization

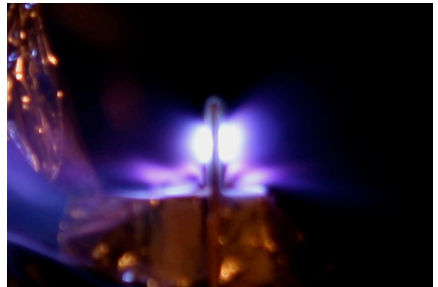
Simulation by Lin Yin, Los Alamos National Laboratory

Energy Loss in Plasma



Laser setup at Z6 target area at GSI, Darmstadt.

Energy Loss in Plasma – Deuterium Target



Cryogenic deuterium target irradiated by two high energy laser pulses. [J. Menzel]



Summary

- ▶ pure targets
- ▶ homogenous solid state density
- ▶ growing process takes about 1 min to 30 min
- ▶ initial target thickness adjustable between μm and cm
- ▶ targets made from hydrogen, deuterium, nitrogen, argon, and neon
- ▶ setup can be implemented at target areas like *Z6*, *GSI*
- ▶ preliminary experiments with cryogenic nitrogen and deuterium targets were performed at *GSI*



Future Goals

- ▶ precise surface/topology characterization
- ▶ cryogenic layer on ultra thin plastic substrates
- ▶ use cryogenic targets in laser accelerated ion experiments
- ▶ use cryogenic targets to measure the energy loss of heavy-ion beams in a fully ionized plasma



Collaborators

- ▶ Prof. Dr. Dr. h.c./RUS Dieter Hoffmann
- ▶ Prof. Dr. Markus Roth
- ▶ Dr. Gabriel Schaumann
- ▶ Dr. Jurij Menzel
- ▶ Alexandra Tebartz
- ▶ GSI Plasma Physics Group

Financial Support

- ▶ *Federal Ministry of Education and Research, Germany*
- ▶ *HiPER Project*

The End



TECHNISCHE
UNIVERSITÄT
DARMSTADT



Thank you for your attention!

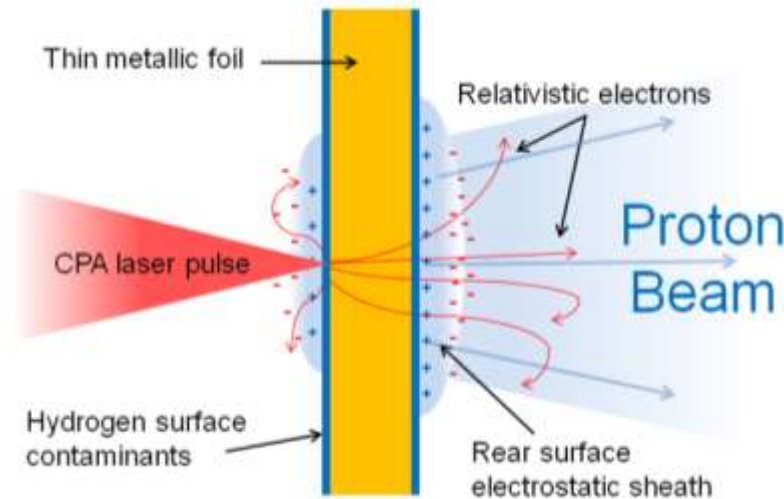


Development of Cryogenic Windowless Targets

Stephanie Tomlinson

Martin Tolley, Chris Spindloe, David Neely, Paul Holligan, Tom Bradshaw,
Mike Courthold, Chris Pulker , Marco Bourghesi

Introduction



- Potential applications include tumor therapy, radiography and laser driven fusion
- Light Sail Radiation Pressure Acceleration (LSRPA).
- Maximum energy available scales favourably with decreasing target density



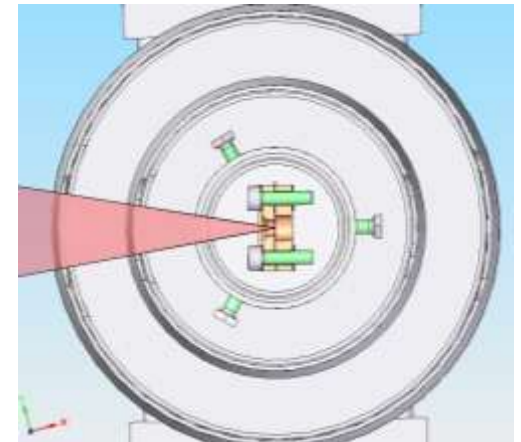
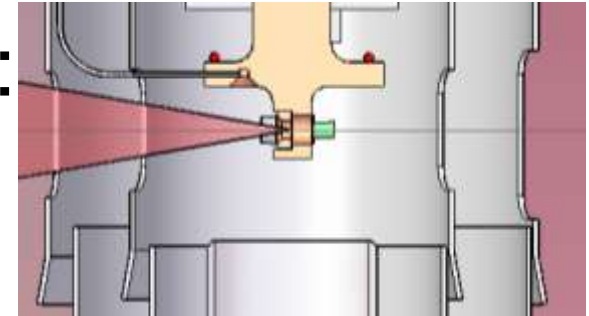
Parameters

Target parameters defined by:

- Laser
- Blast region
- Alignment tolerance
- Thickness for light sail regime
- Material & purity

Aim:

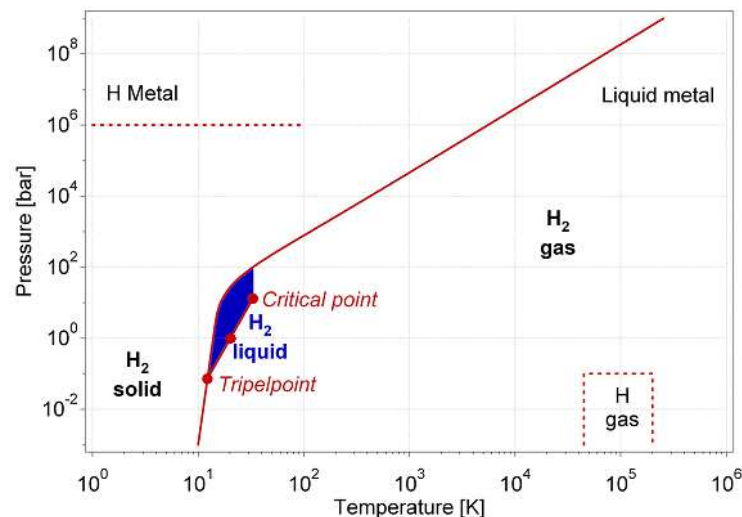
- 2-5mm diameter
- 50 micron thickness
- Windowless



Proposed Method

- Condensation method

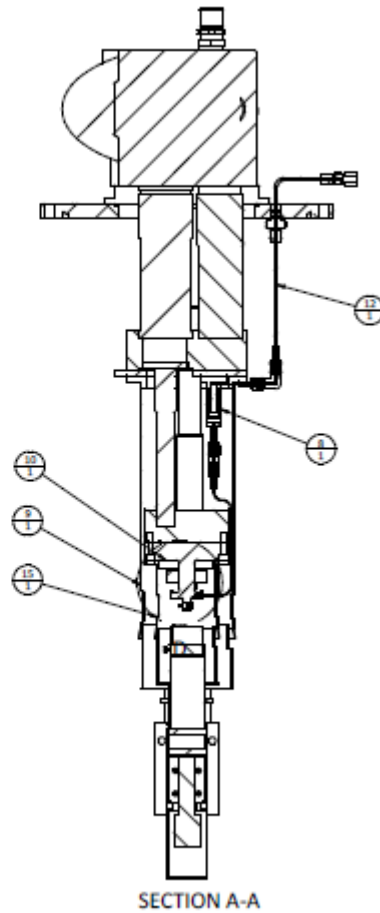
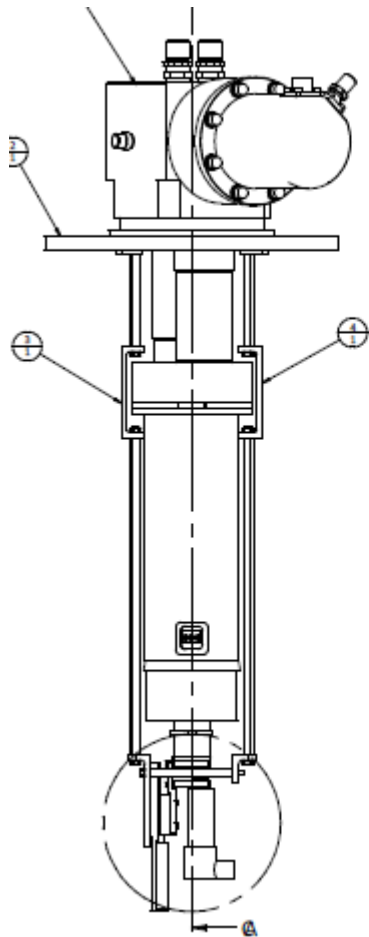
- Local wet vapour
- Condense onto substrate
- Flow & surface tension
- Solidify
- Vacuum



	Hydrogen	Deuterium
Pressure at Critical Point (bar)	13	16.6
Temperature at Critical Point (K)	33.5	38.4
Pressure at Triple Point (bar)	0.07	0.17
Temperature at Triple Point (K)	13.8	18.7



Design - Overview

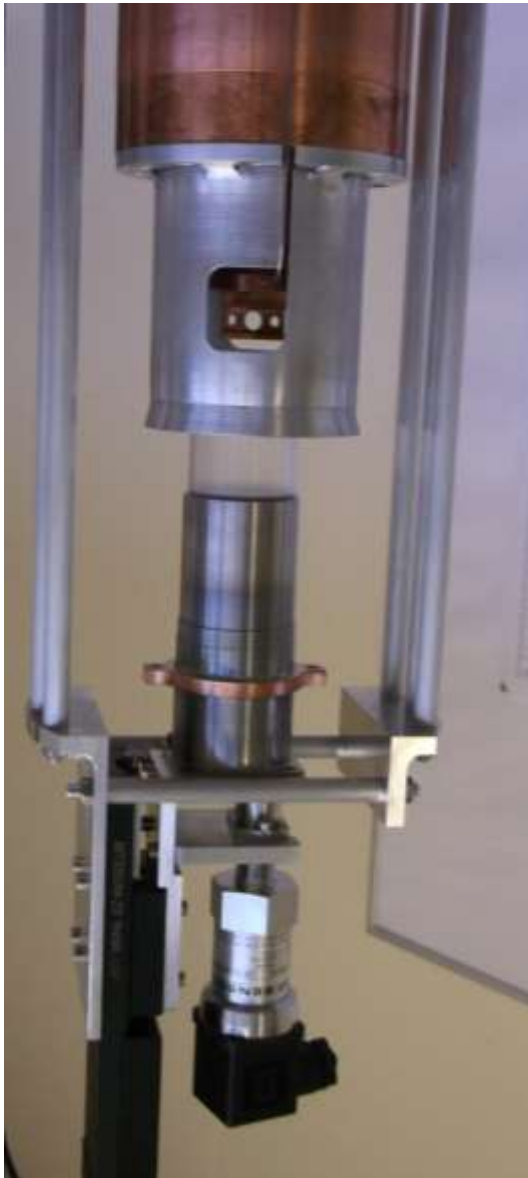


Cryocooling

- Pulse Tube
 - Cryogen free
 - No moving parts in coldhead

1 st Stage Capacity		40W @ 65K	
2 nd Stage Capacity		1.0W @ 4.2K	
Lowest Temperature 2 nd Stage			<3K
Cooldown Time 2 nd Stage			<80min.
1 st Stage Vibration (x,y,z)	±3µm	±2µm	±6.3µm





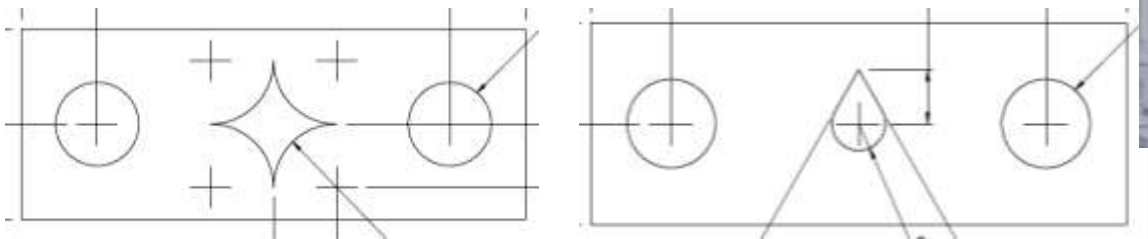
Design

- Local Hydrogen Boundary
 - Small volume
 - Seal
 - Transparent
 - Removable
 - Low conductivity



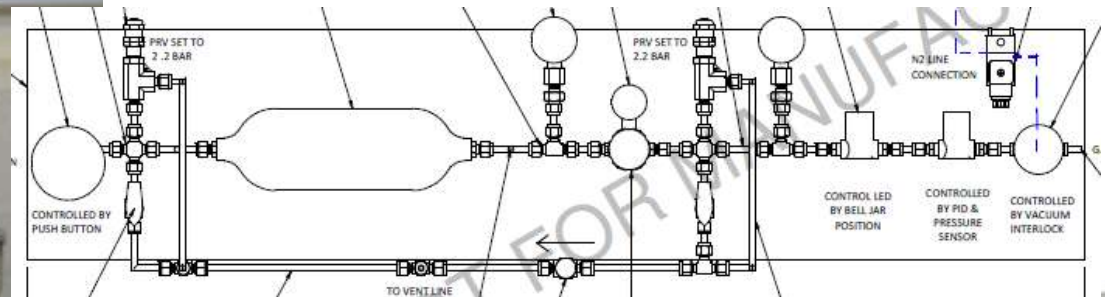
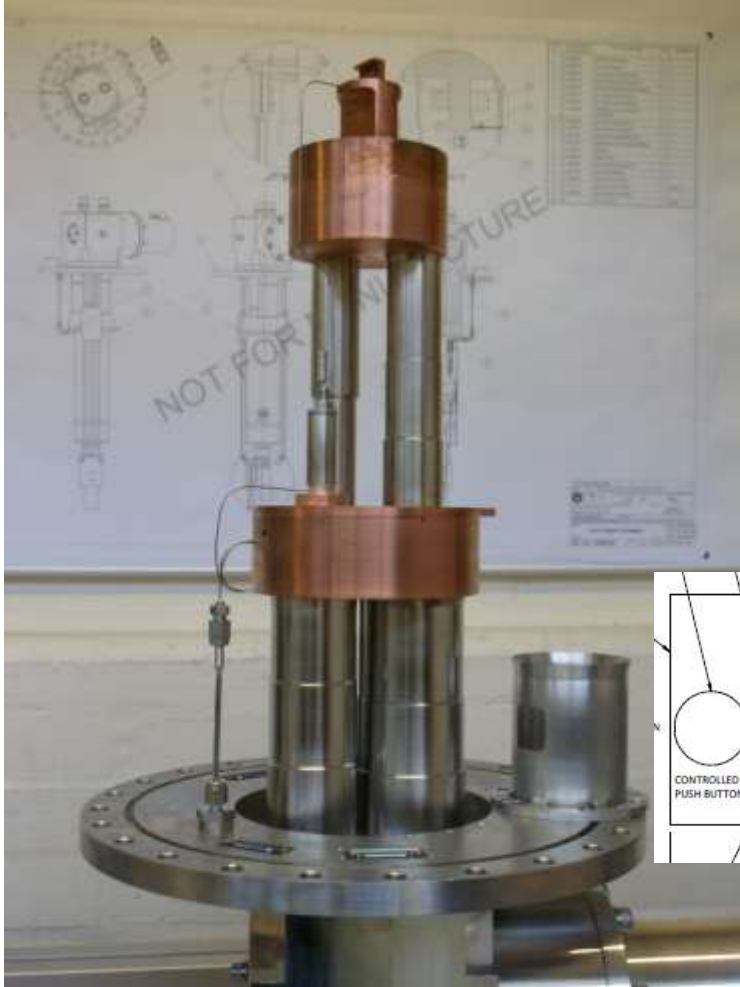
Design

- Target mount and foils
 - photo-etched in copper
 - smallest feature accuracy of $\pm 25\mu\text{m}$
 - Range of diameters



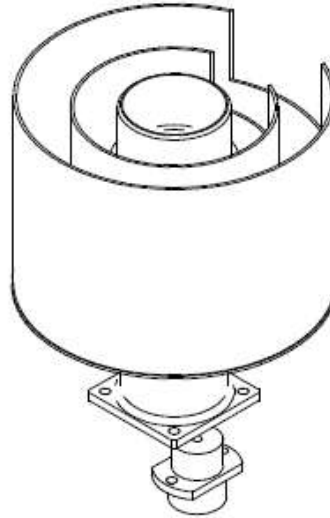
Design

- Gas Feed
 - Capillaries
 - Heat Exchanger
 - Pressure & Valves



Design

- Heat Loads
 - Warm Gas
 - Pre-cooled
 - Room Radiation
 - Shields
 - Apertures
 - Move with boundary
 - Fixed to cold stages
 - Latent Heat



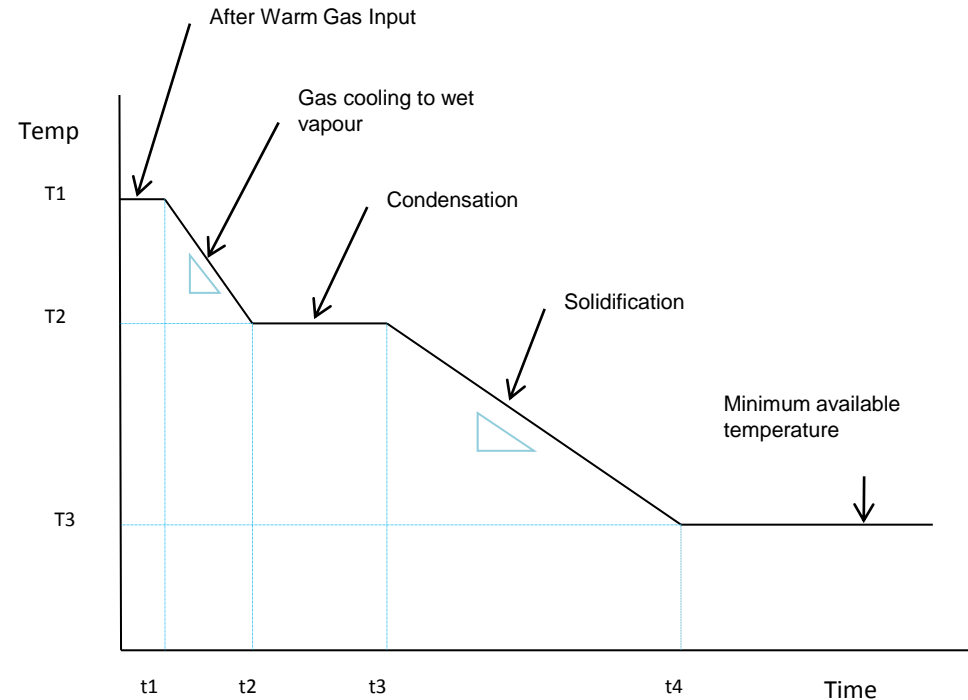
Design

- Pressure and Temperature Control
- Omega CYC325 Temperature Controller, 2 diode/RTD inputs
- Omega CY7-SD3 Cryogenic Temperature Sensor
- RS Components Heaters (Resistors)
- Impress Sensors DMP331P Flush Diaphragm
- Impress Sensors CMC-99 Indicator and PID Controller



Testing

- Current Status
 - Fully assembled
- Engineering Tests
 - Pressure systems functioning
 - Pressure and temperature controllable
 - Temperature and pressure profiles



Characterisation

- Target parameters
 - Thickness
 - Foil design, surface roughness, feature accuracy
 - Time to produce targets
 - Sublimation rate
 - Repeatability
- Laser Testing
 - Alignment
 - Blast region
 - Surface Contamination



Thank you for listening.
Any questions?



Science & Technology
Facilities Council

Design - Cooling

- Pulse Tube Principle

- Adiabatic Compression

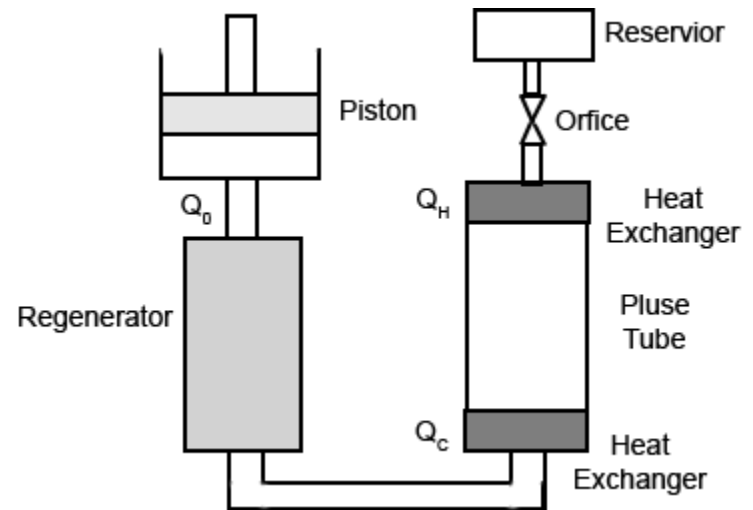
- Regenerator absorbs heat
 - Gas in pulse tube is heated
 - Rejects heat

- Adiabatic Expansion

- Gas in pulse tube cools
 - Absorbs heat as it flows through cold heat exchanger
 - Regenerator heats gas

- Net effect of cycle

- Average enthalpy flow from cold to hot end
 - Constant temperature gradient in regenerator



Fabrication of Ultrathin Near Critical Density Targets

Wenjun Ma

Department of Physics , LMU , Garching, Germany

Group members

J. Bin, K. Aligner, P. Hilz, D. Kiefer, C. Kreuzer, H. Wang, T. Ostermayr, J. Szerypo, H.J. Maier, D. Habs, J. Schreiber

Team goal: laser-driven ion acceleration and its biomedical applications



Ludwig-Maximilians-Universität München:

K. Allinger, J. Bin, P. Hilz, D. Kiefer, W. Ma, Sebastian Raith, T. Ostermayr, Joerg Schreiber

K. Khrennikov, S. Karsch et al.

H. Wang, J. Szerypo, T. Tajima, X.Q. Yan, D. Habs, F. Krausz

W. Assmann, S. Reinhardt, W. Draxinger

S. Rykovanov, H. Ruhl

Technische Universität München

J. Wilkens , Nicole Humble, et al.

Why Near Critical Density Targets?

Group velocity of plane EM waves in plasma

$$v_g = c \left(1 - \frac{n}{n_c} \right)^{1/2} \rightarrow 0$$

Very high absorption efficiency:

- soft X-ray source
- ablation layer for ICF targets
- hot electron source for ion acceleration

Strong coupling between laser and plasma:

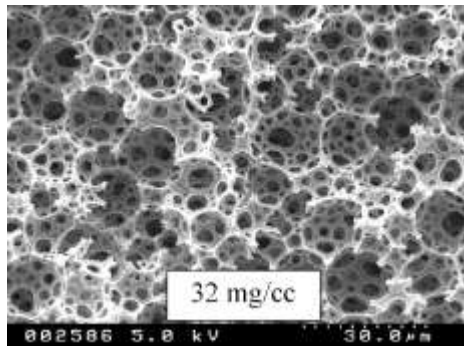
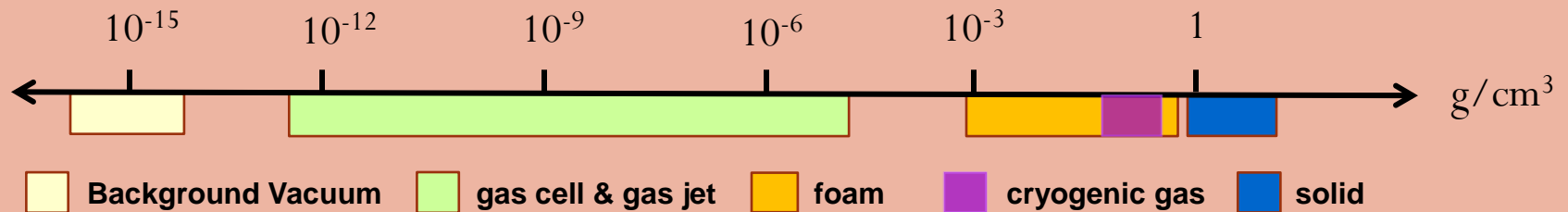
- pulse shaping
- relativistic plasma shutter

Critical density

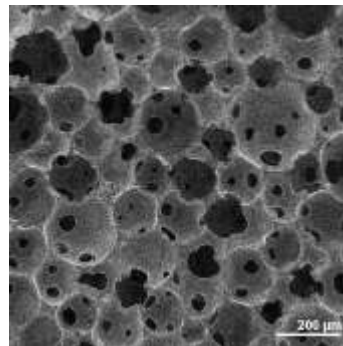
$$n_c = \frac{m_e \omega}{4\pi e^2} = 1.1 \times 10^{21} / (\lambda / \mu m)^2 cm^{-3}$$

For $\lambda=800$ nm, fully ionized light atoms (C,N,O)

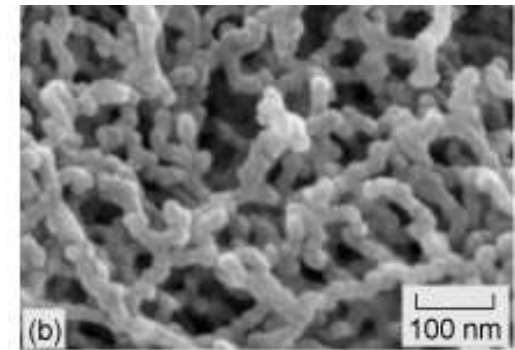
$$\rho \sim 6 \text{ mg/cm}^3$$



PolyHIPE foam



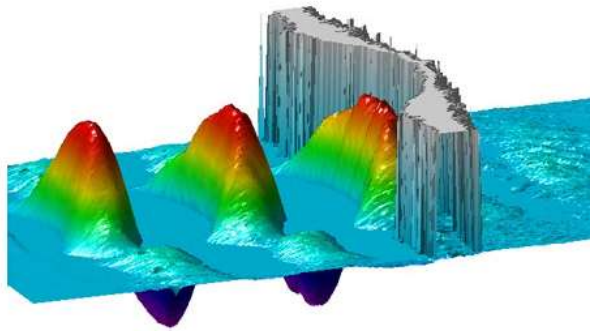
Polystyrene foam



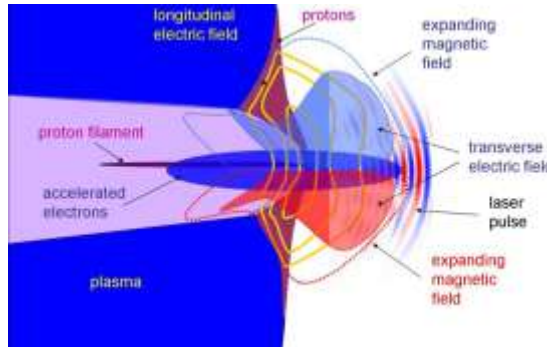
Silica aerogel

Near Critical Density Targets for Laser-driven Ion Acceleration

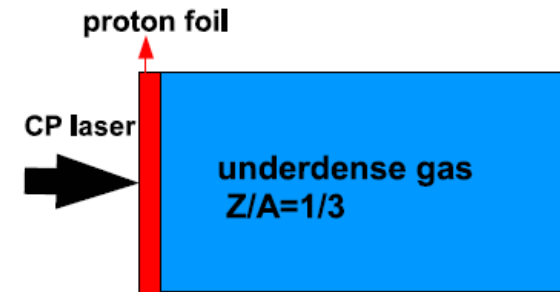
Enhanced TNSA & RPA



Magnetic vortex acceleration



Two-stage acceleration



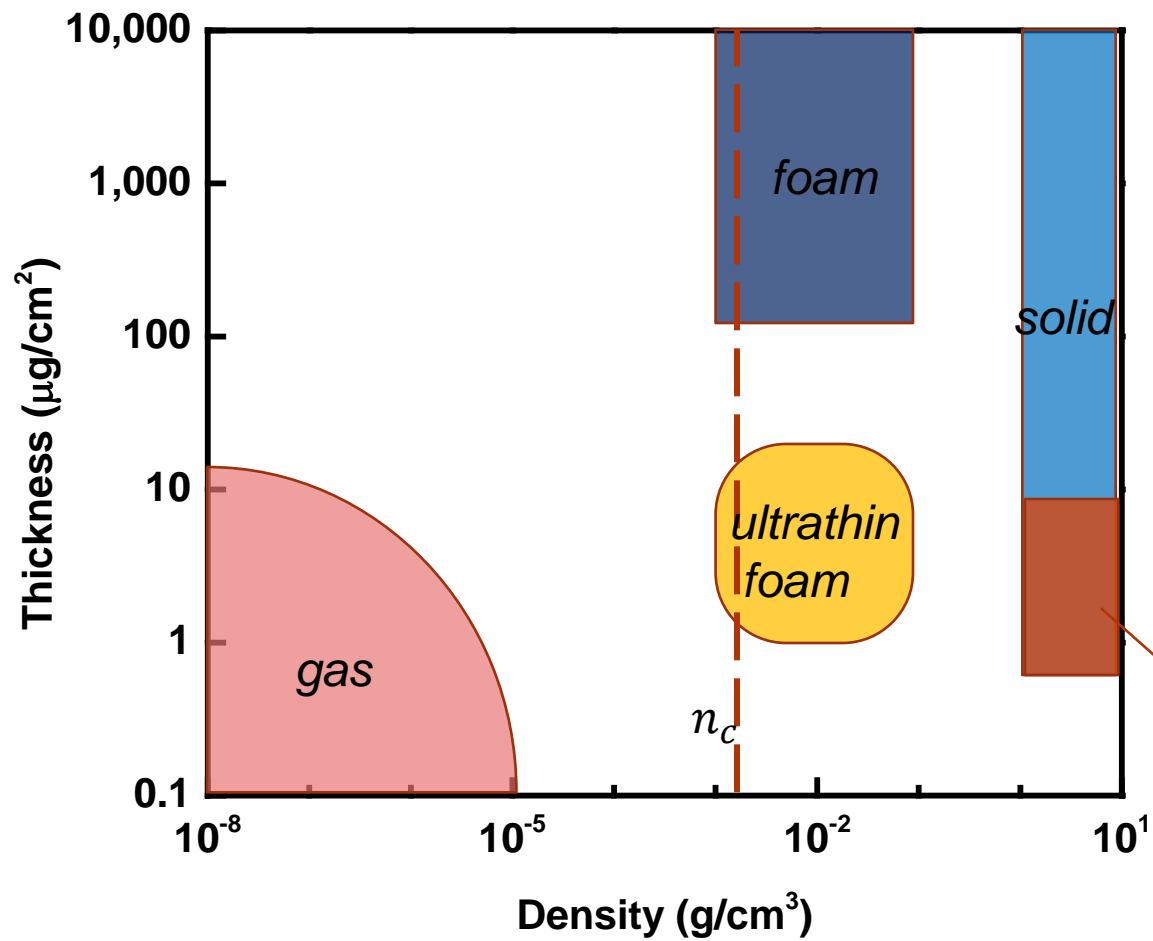
Requirements

- ❑ high homogeneity

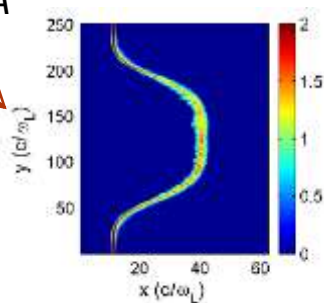
focus spot $3\sim 5\ \mu\text{m}$, pore size $< 200\ \text{nm}$

- ❑ ultrathin

depletion length of high-power femtosecond laser: $2\sim 10\ \mu\text{m}$

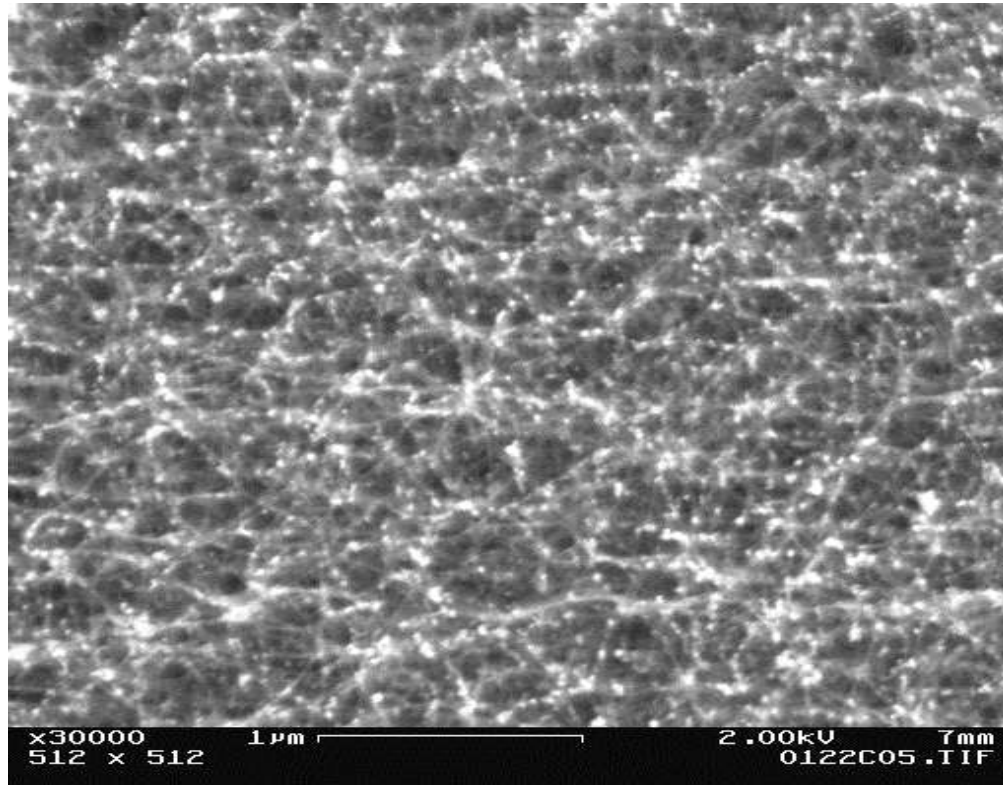


RPA



A. Henig et al. Phys. Rev. Lett. **103**, 245009 (2009).

Ultra-low density, ultra-thin carbon nanotube films

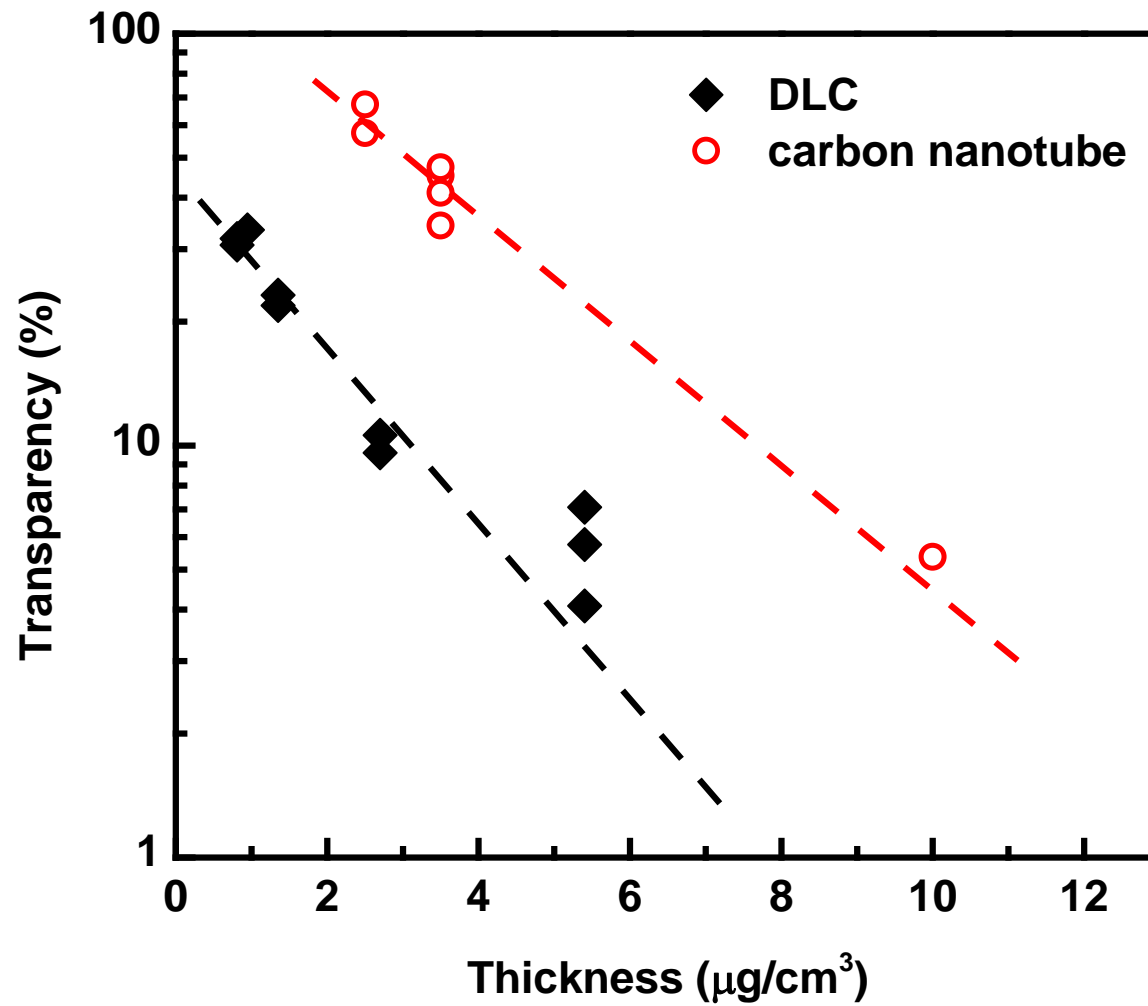


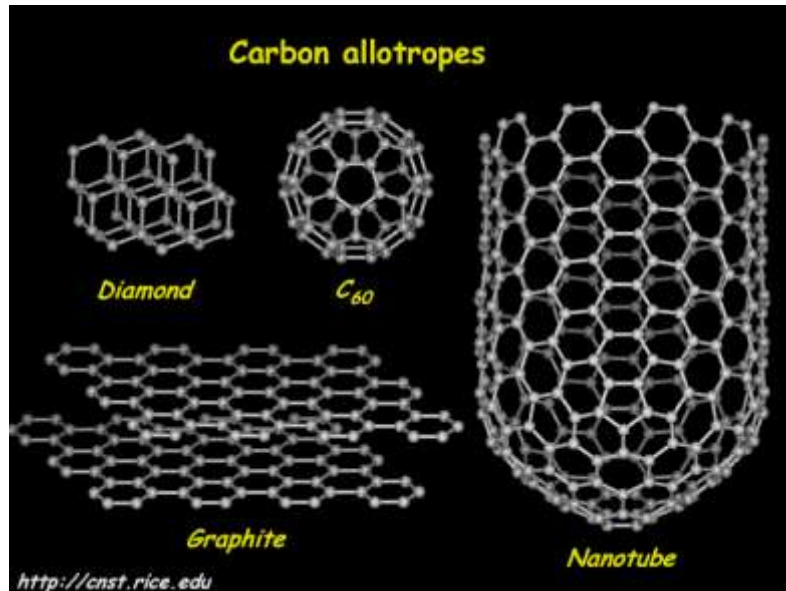
$$\rho = 25 \sim 50 \text{ mg/cm}^3$$

$$d = 2.5 \sim 100 \text{ ug/cm}^2$$

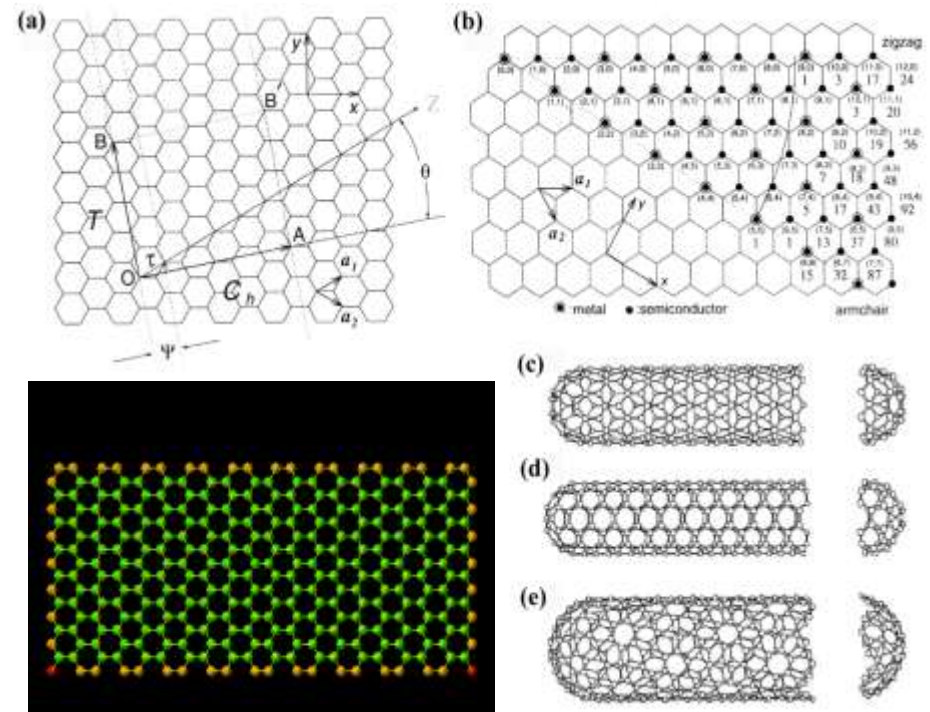
$$n_e/n_c = 5 \sim 10$$

Transparency vs targets thickness (from Astra Gemini 500TW laser)





allotropes of carbon

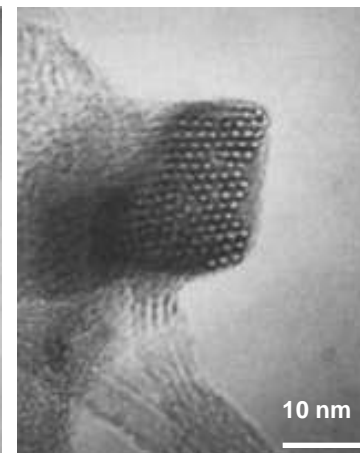
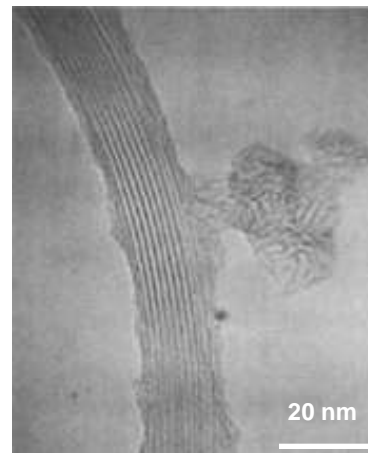
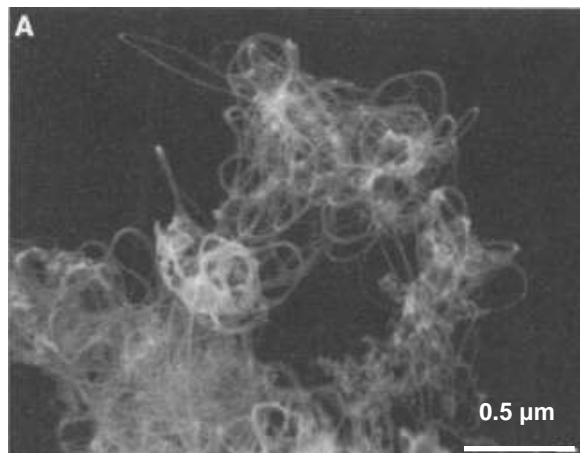


α SWNT can be viewed as scrolled from a single lay of graphite

Individual SWNT



SWNT bundle



➤ Diameter

0.4~2 nm

2~40 nm

➤ Length

1μm~1cm

1μm~1cm

➤ Metallicity

Metallic or Semiconducting

Metallic

➤ Conductivity

/

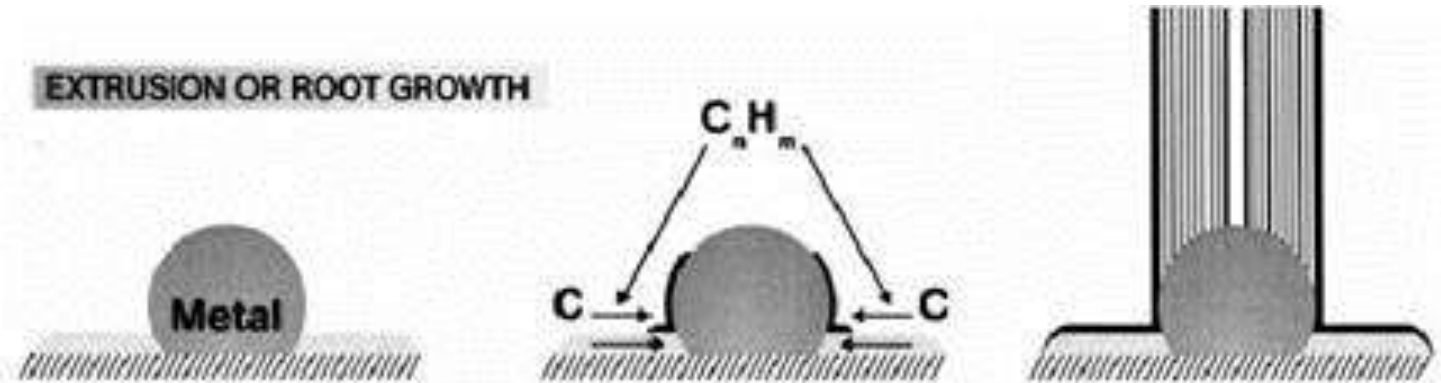
~20,000 Scm⁻¹

➤ Tensile Strength

30~40 GPa

<20 GPa

Growth mechanism of Carbon Nanotubes



nanoparticle
formation

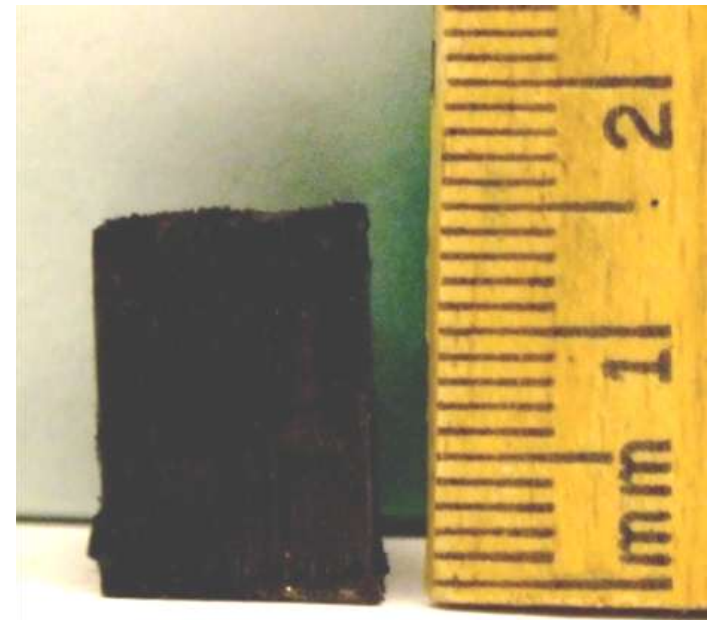
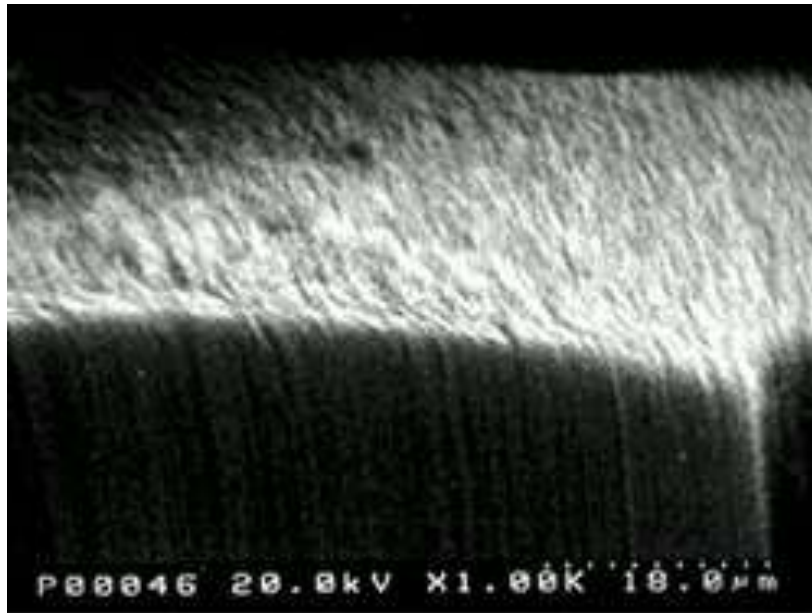
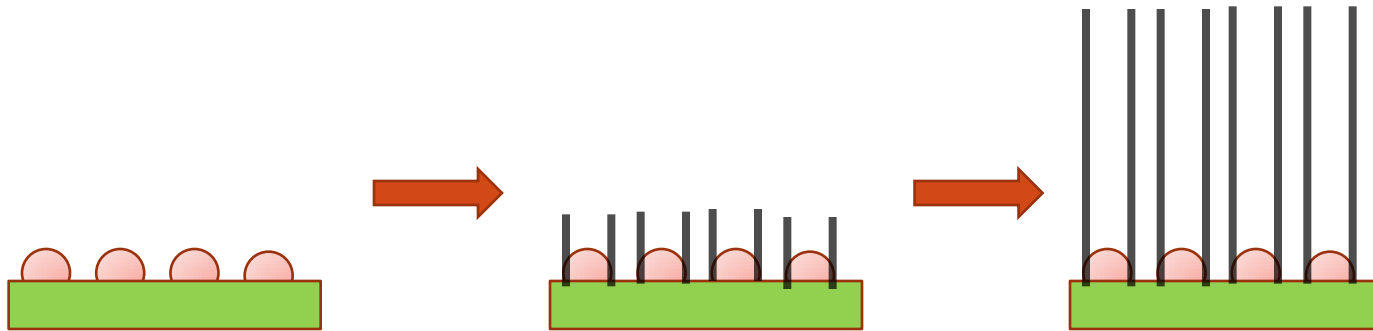


carbon
aggregation

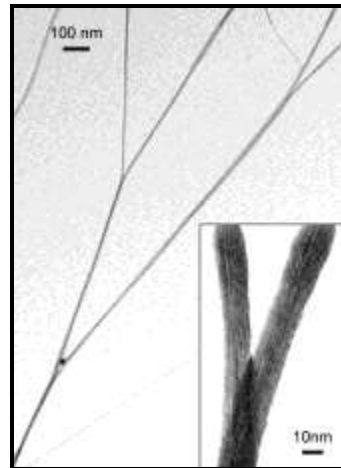
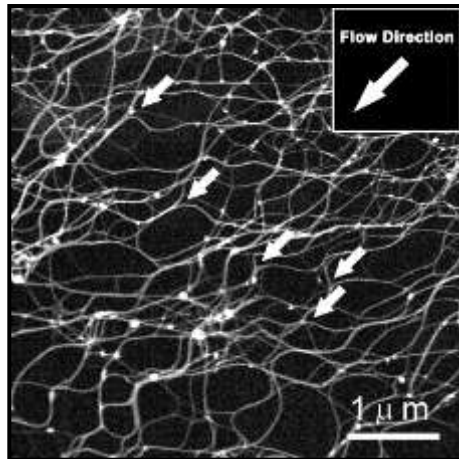
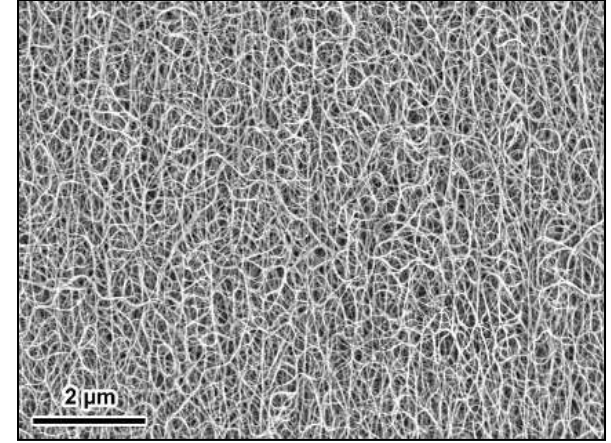
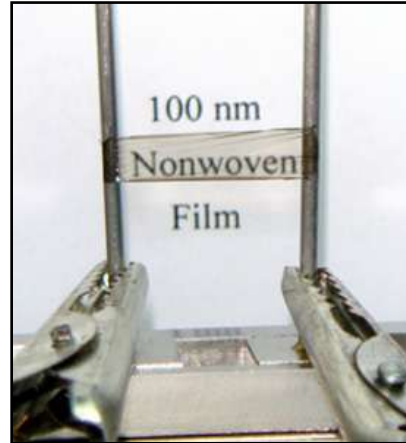


nanotube
growth

Carbon Nanotube Arrays



Strong, Highly Conducting, Transparent SWNT Films



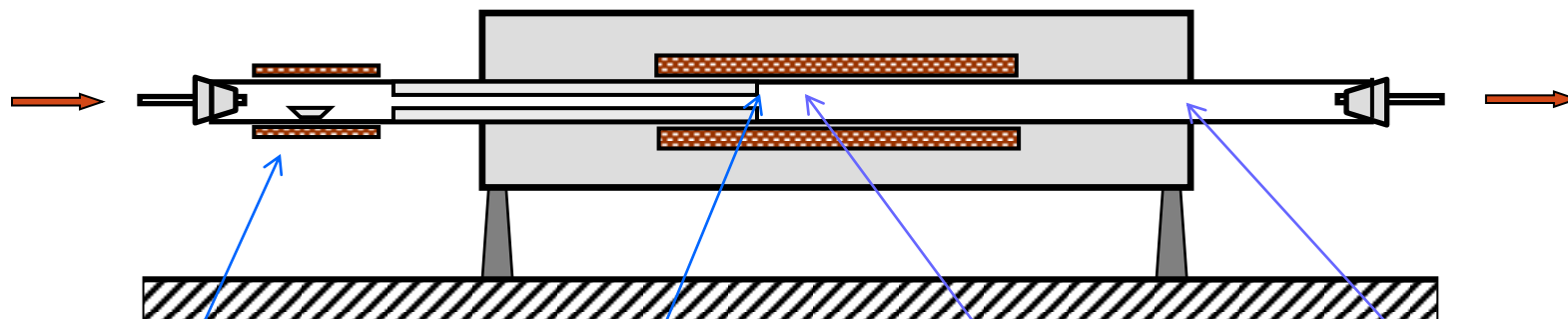
block inter-bundle slippage under load

➡ tensile strength > aluminum sheet

lower tunneling barriers & higher electron transition efficiency between SWNT bundles

➡ $\sigma \sim 2000 \text{ S/cm}$

Floating Catalyst Synthesis Method



Step 1

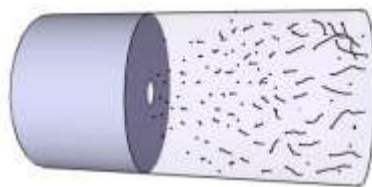
Catalysts Sublimation

Ar & CH₄



Step 2

Nanosized Catalysts
Sprayed out



Step 3

Short Tubes Form in
the Air and Grow



Step 3

Deposition

Chemical Vapor Deposition System



High Temperature Tube Furnace

Heated Length: 1 m

Highest Working Temperature: 1300°C



Gas Flow System

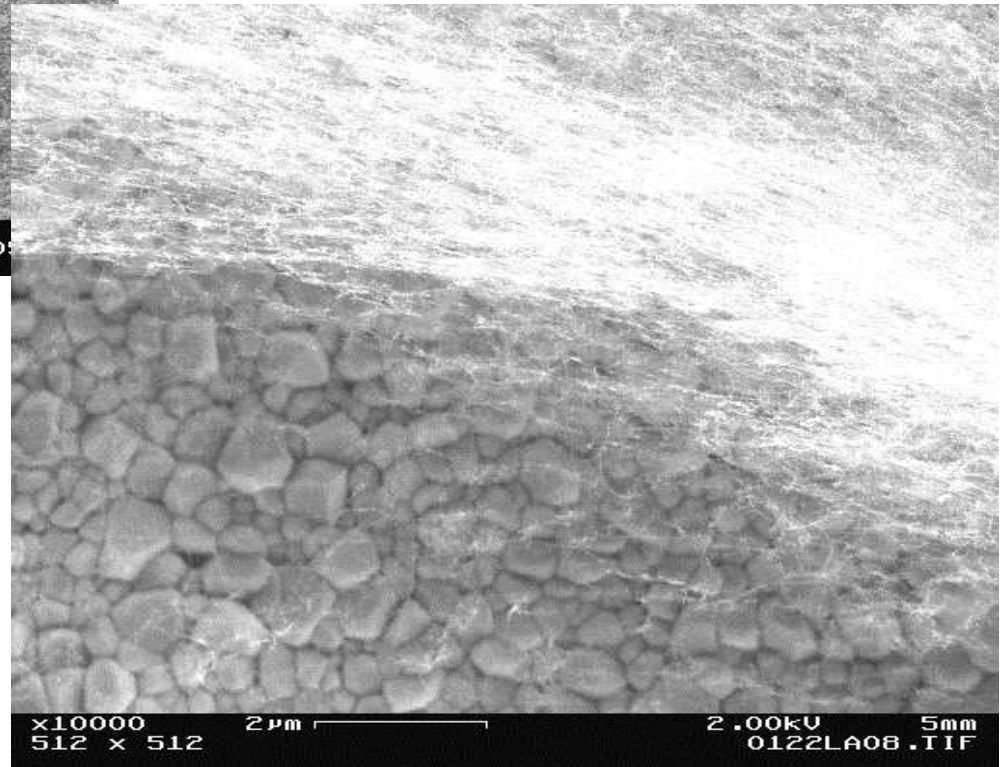
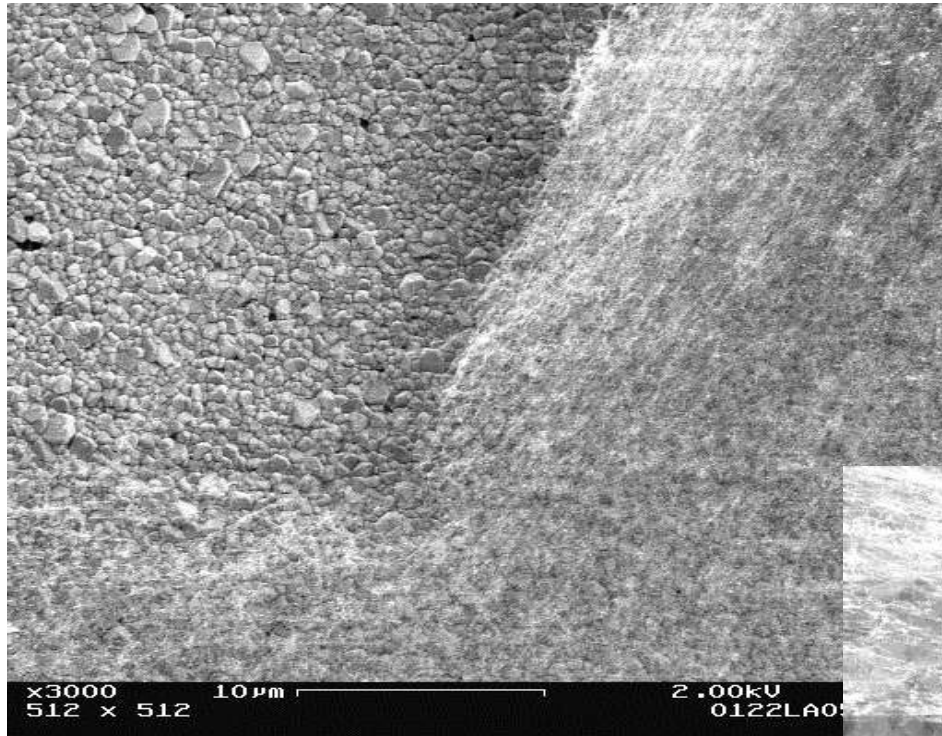
Gas type: Ar, CH₄, O₂, H₂

Maximum Flow rate: 10,000 sccm

CH₄ Flow Precision: 0.01 sccm

System sealing: HV standard

DLC & CNT double-layer targets



THANK YOU



Novel Micro-Focusing Cone Indent Target Fabrication

D.Haddock¹, C Spindloe¹, M. Tolley¹, M Beardsley², E Barber², G Scott³, and
D Neely¹

*¹Central Laser Facility, Rutherford Appleton Laboratory, Science and
Technology Facilities Council, Harwell Oxford, Didcot, Oxon, OX11 0QX.*

*²RAL Space, Rutherford Appleton Laboratory, Science and Technology
Facilities Council, Harwell Oxford, Didcot, Oxon, OX11 0QX.*

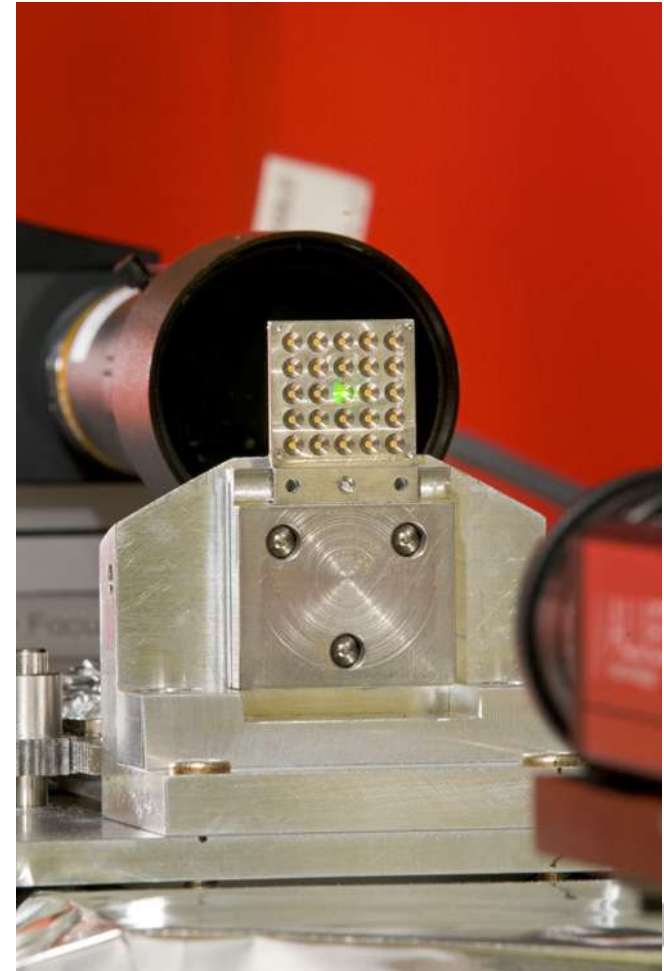
³Department of Physics, University of Strathclyde, Glasgow UK.

High-repetition rate targetry



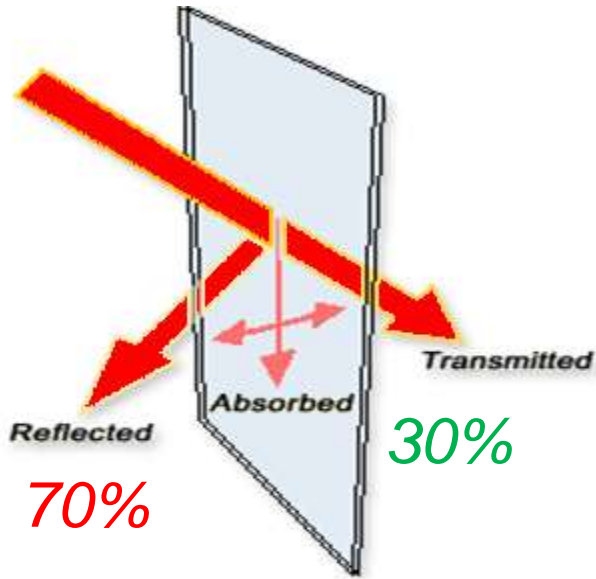
~2m

- World's first high repetition rate, dual beam Petawatt user facility
- Medium energy (15J per beam) but ultra-short pulses (30 fs), 1 shot every 20 seconds



Science & Technology
Facilities Council

Background



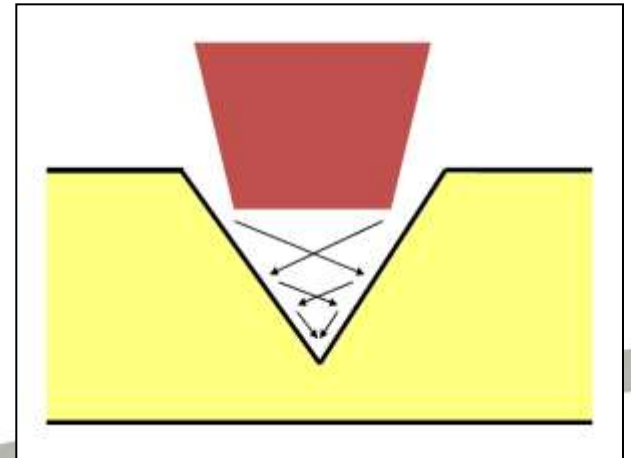
Increase in laser power is expensive and tricky

- Approximately 70% laser light is specularly reflected from flat targets
- This energy is usually lost from the system!

“Light trap” Proposed

Multiple internal reflections increase chance of absorption

Estimates at an increase to 60-70% laser absorption; double the energy previously available.

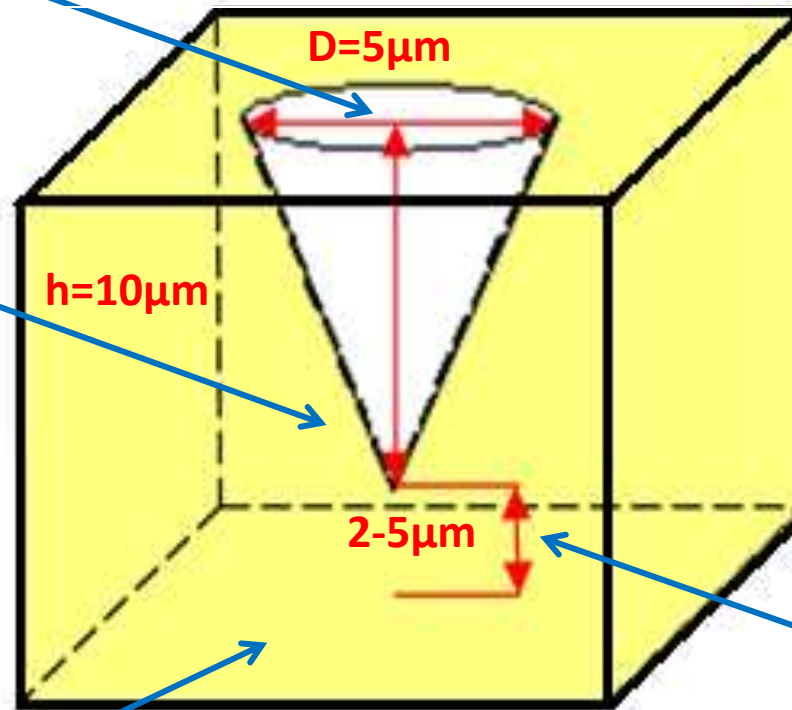


Science & Technology
Facilities Council

Design

Opening diameter ~ focal limit Laser system. (Astra = $2\mu\text{m}$ full width half maximum)

30° opening angle



Array of targets for high repetition rate, $500\mu\text{m}$ spacing to avoid neighbour damage

Small exit distance allows ion acceleration

Polished rear surface $<1\mu\text{m}$ Ra

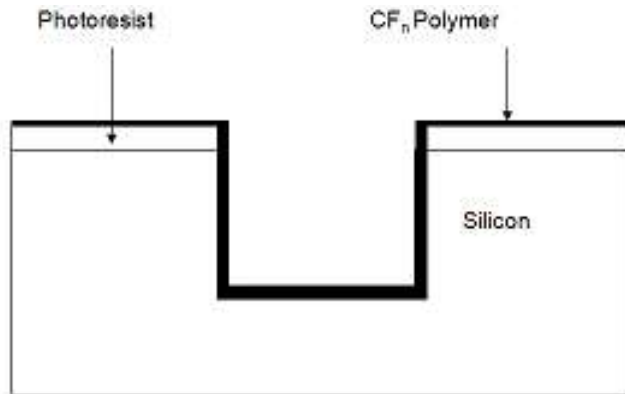


Science & Technology
Facilities Council

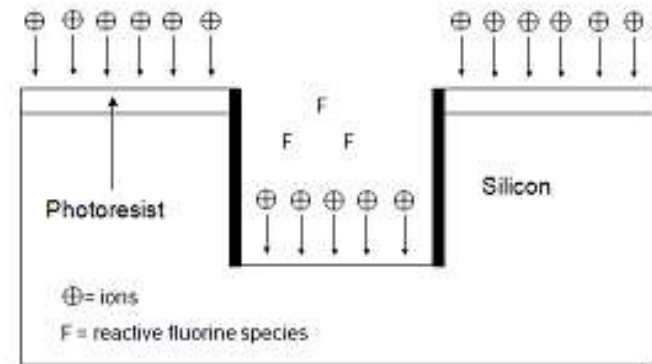
Production of cone shape

Deep Reactive Ion Etching of Silicon substrates:

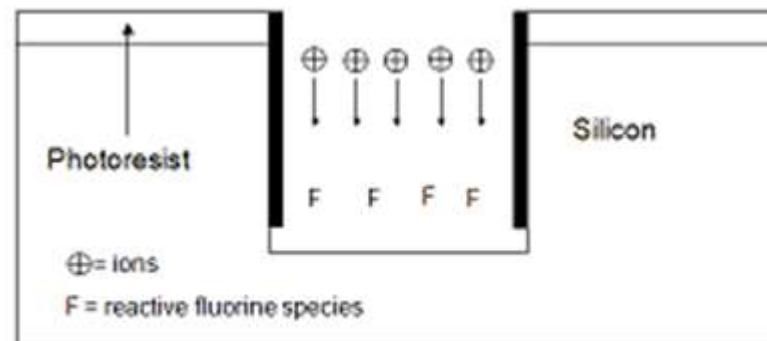
A ratio of the etching gas SF_6 to a sidewall passivation polymer C_4F_8 determines the extent of the etch.



a) A thin polymer layer is deposited on the wafer by the decomposition of C_4F_8 gas in the plasma.



b) The passivation layer is removed by ion bombardment only from the horizontal surfaces.



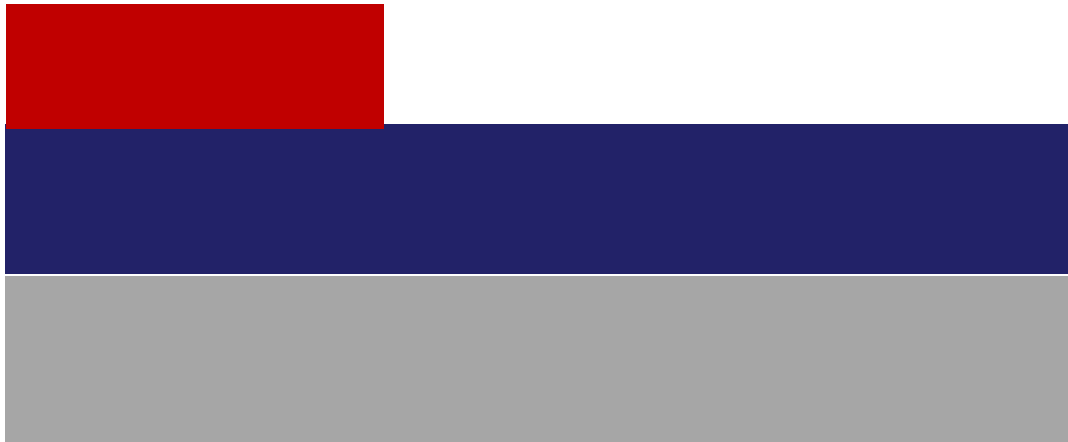
c) Silicon is etched by the fluorine species.



Science & Technology
Facilities Council

Cone Creation

Step 1: Mask silicon area with photoresist



Photoresist mask

Silicon

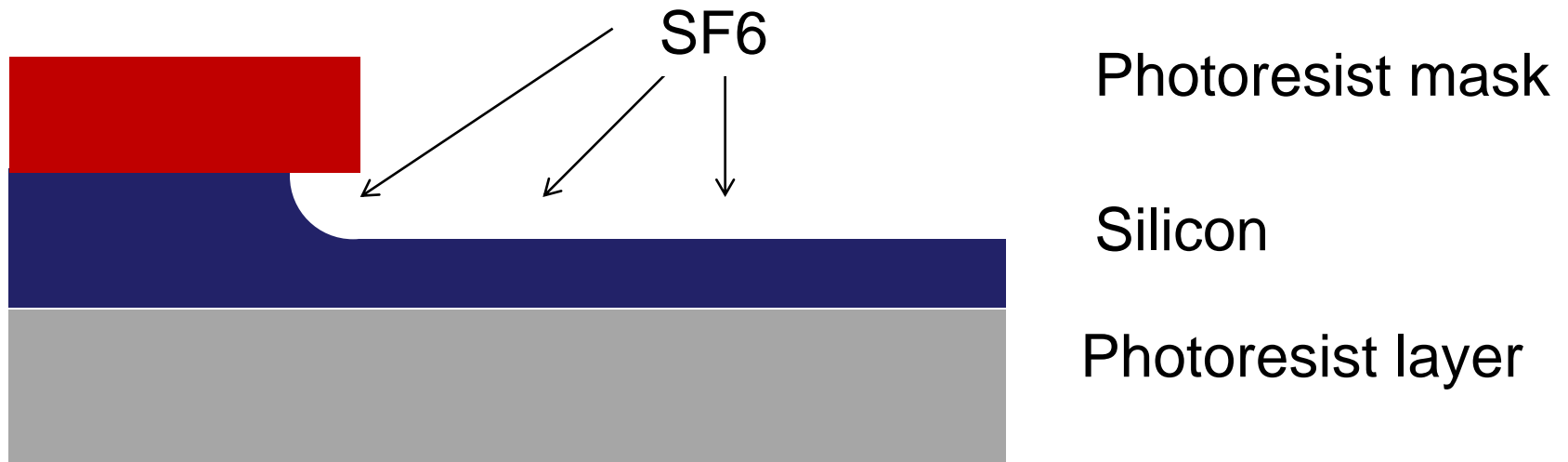
Photoresist layer



Science & Technology
Facilities Council

Cone Creation

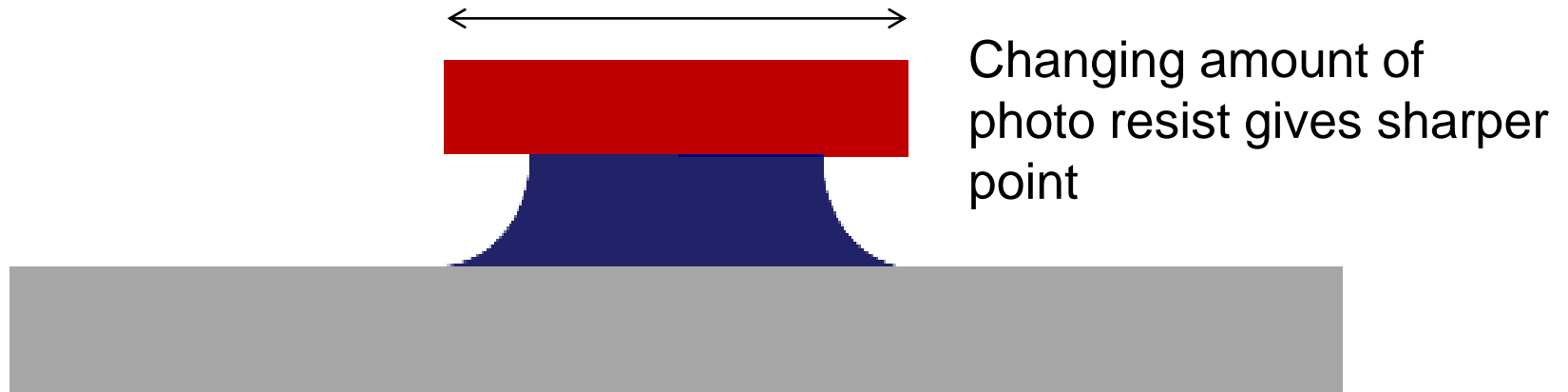
Step 2: SF₆ ions attack silicon. Extent of attack dependant on SF₆/C₄F₈ ratio



Science & Technology
Facilities Council

Cone Creation

**Step 3: Etch simultaneously on the other side.
Continue to reach desired shape**



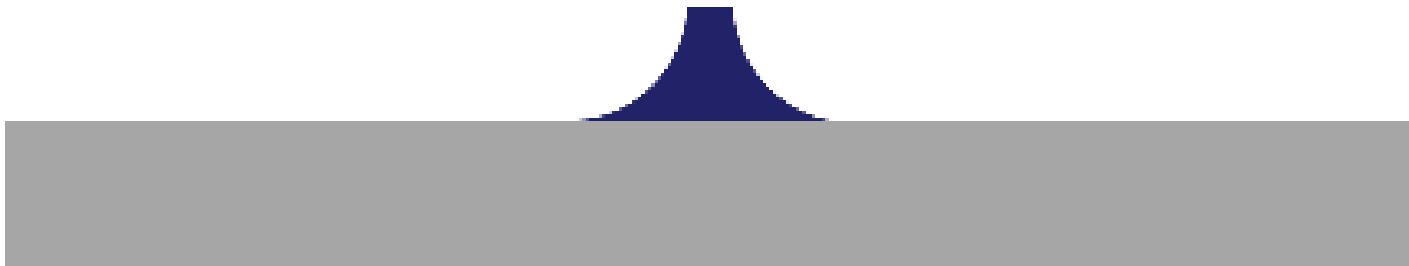
Photoresist mask made into to repeated pattern allowing dozens of cones to be mass produced.



Science & Technology
Facilities Council

Cone Creation

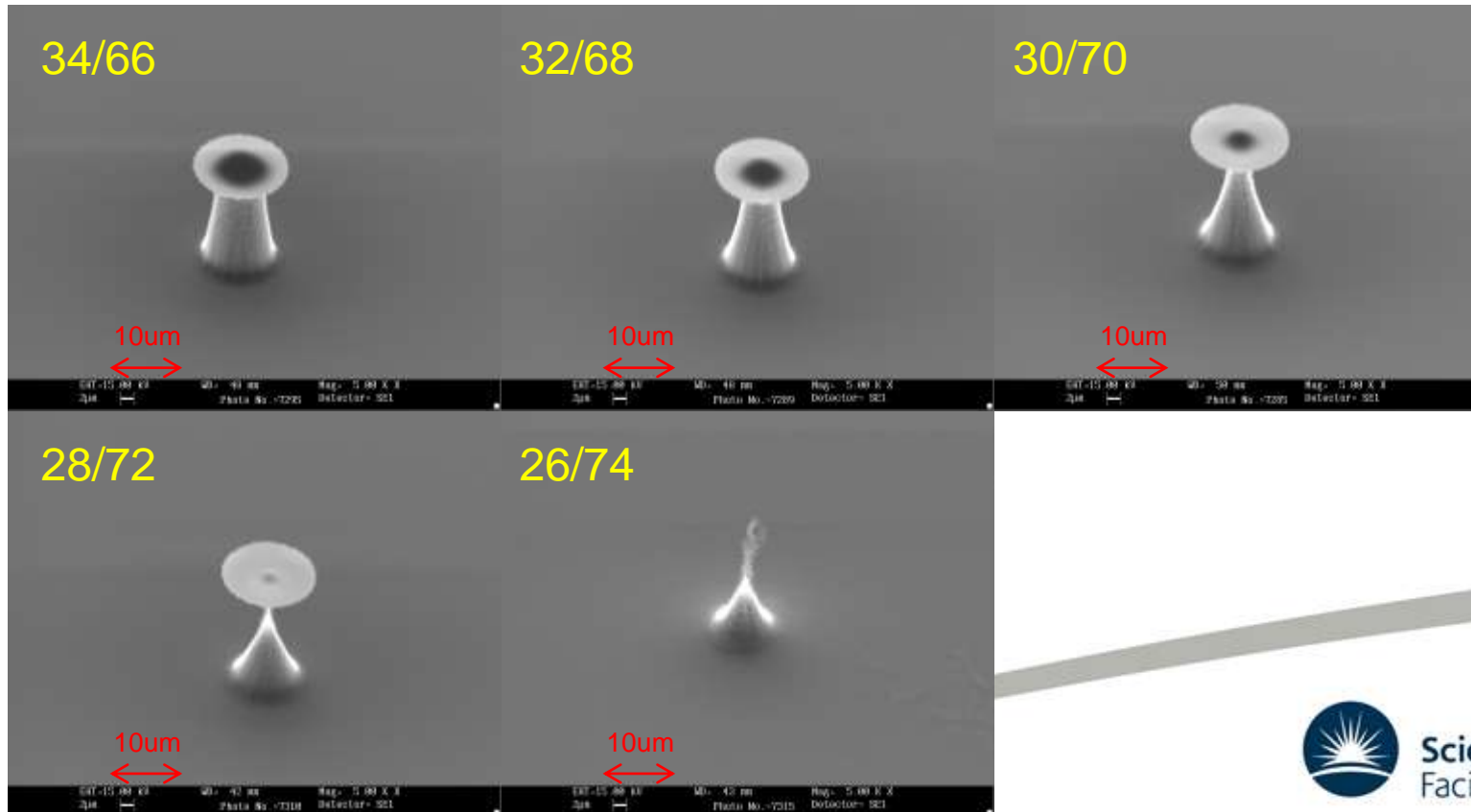
Step 4: Remove photoresist using solvent



Science & Technology
Facilities Council

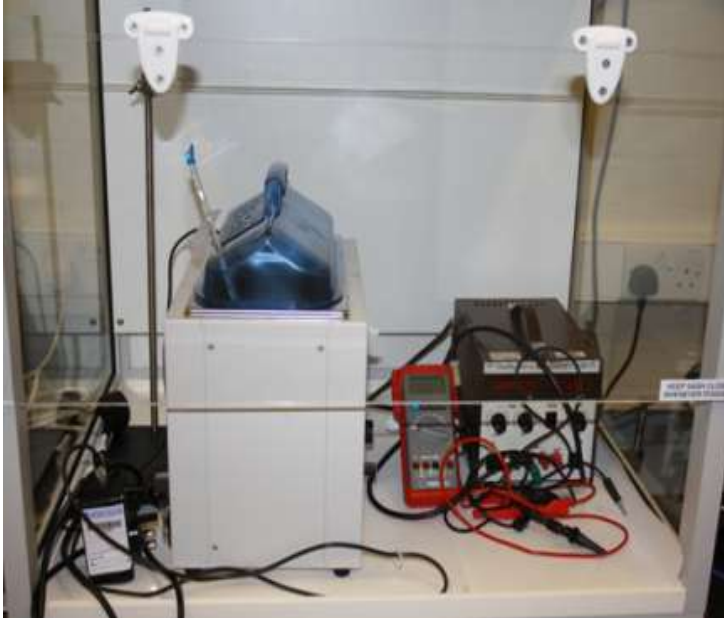
Characterization

- Micro-cones flash coated with gold. Plasma Deposition
- Scanning Electron Microscope for dimension analysis
- Gas Ratio of **Passivation/Etch**
- Increase in relative amount of etching gas to passivation gas gives differing shapes



Electroplating

- Deposition of thick metal layers (up to $30\mu\text{m}$) allows the coating of complex intricate forms
- The deposition of a metallic coating onto an object is achieved by putting a negative charge on the object to be coated and immersing it into a solution which contains a salt of the metal to be deposited. The object to be plated is made the cathode of an electrolytic cell

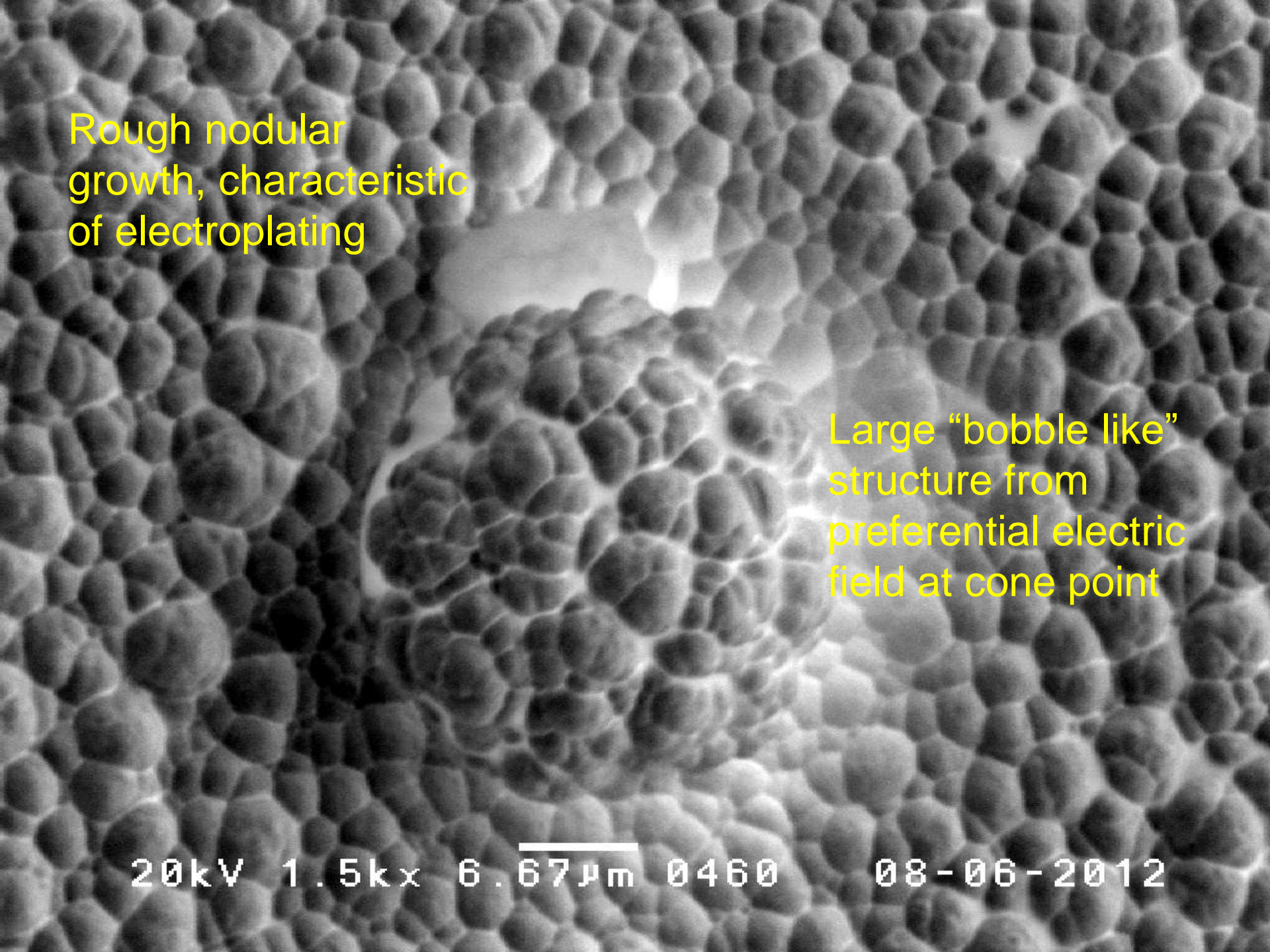


Negative
Cathode

Ammonium
Gold Sulphite
Solution



Science & Technology
Facilities Council

A scanning electron micrograph (SEM) showing a surface with a rough, nodular texture. The surface is covered with numerous small, rounded nodules of varying sizes, creating a bumpy appearance. A larger, more prominent nodular structure is visible in the center-right area.

Rough nodular
growth, characteristic
of electroplating

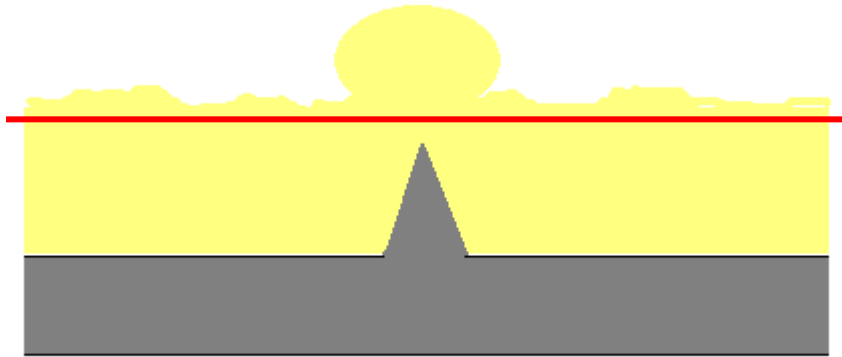
Large “bobble like”
structure from
preferential electric
field at cone point

20kV 1.5kx 6.67µm 0460

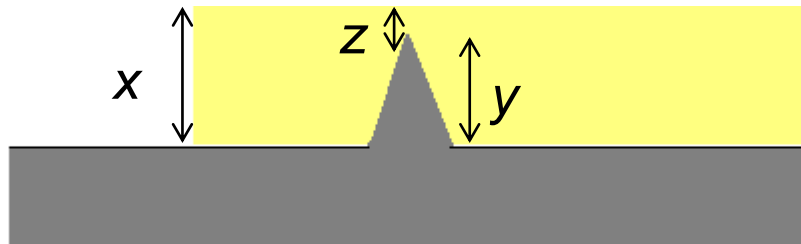
08-06-2012

Precision Machining

- Need to remove nodular structure and leave a polished exit surface



- High precision machining tool strips rough surface layer
- Leaves polished flat surface $<1\mu\text{m Ra}$



- x dimension known from step height measurement
- y dimension known from SEM
- Therefore z characterized with accuracy equal to that of the x and y measurements

Final Stage: Etch Silicon with Potassium Hydroxide!



Science & Technology
Facilities Council

Conclusion

- Concept: Improve Laser interaction efficiency by cone-indent geometry

Order of magnitude ~ Focal spot

- Create cone mould by DRIE of Silicon. Ratio of Passivation and etching gas important
- Characterization at mould stage

- Electroplate to above cone height
- Precision Machine rear surface form. Etch Silicon



Thank you!

Dave Neely – *Concept*

Eleanor Barber – *DRIE*

Sam Serra - *Electroplating*

Matt Beardsley – *Precision Machining*

Chris Spindloe – *Supervision*

QUESTIONS?



Science & Technology
Facilities Council

References

- [1] *Fabrication and Experimental Delivery of Targets for High Power Laser Systems*

C.Spindloe – Target Fabrication CLF

- [2] **Micron & nano scale targets for high power laser experiments.**

A.Malik - MNTC

